PERMEANT ION AND SUBUNIT DEPENDENCE OF EXTERNAL Mg^{2+} BLOCK OF NMDA RECEPTORS

by

Anqi Qian

BA, Concordia University, 1995

Submitted to the Graduate Faculty of

Arts and Sciences in partial fulfillment

of the requirements for the degree of

Doctor of Philosophy

University of Pittsburgh

2003

UNIVERSITY OF PITTSBURGH

FACULTY OF ARTS AND SCIENCES

This dissertation was presented

by

Anqi Qian

It was defended on

October 23, 2003

and approved by

Elias Aizenman, Ph. D.

Peter F. Drain, Ph.D.

Stephen D. Meriney, Ph.D.

Lonnie P. Wollmuth, Ph.D.

David C. Wood, Ph.D.

Jon W. Johnson, Ph.D.

Dissertation Director

PERMEANT ION AND SUBUNIT DEPENDENCE OF EXTERNAL Mg^{2+} BLOCK OF NMDA RECEPTORS

Anqi Qian, PhD

University of Pittsburgh, 2003

Advisor: Dr. Jon W. Johnson

N-methyl-D-aspartate (NMDA) receptors are broadly involved in the CNS physiological and pathological processes. The voltage-dependent block by external Mg^{2+} is a signature characteristic of the NMDA receptors and is partly responsible for the many important roles NMDA receptors play. The work included in this Dissertation was designed to advance our understanding of the mechanism of Mg^{2+} block of NMDA receptors by exploring the permeant ion and subunit dependence of this process. Whole-cell and outside-out patch recordings from primary cultures of rat cortical neurons or heterologous mammalian cell lines were performed in combination with kinetic modeling.

I report that Mg^{2+} inhibition of whole-cell NMDA currents in cortical neurons, which express NMDA receptors with NR2A or NR2B NR2 subunits, is very sensitive to ionic conditions. This phenomenon can be explained by a kinetic model which incorporates external permeant ion binding sites within the pore. Permeant ions binding to these sites prevents Mg^{2+} blocking or unblocking the channel.

The general mechanisms of Mg^{2+} channel block of NR1/2D receptors is fundamentally similar to that of cortical receptors. However, Mg^{2+} block of NR1/2D receptors is much weaker than cortical receptors, mostly due to faster Mg^{2+} unblocking. Permeant ions also greatly affect Mg^{2+} block of NR1/2D receptors. The results can be explained by a kinetic model that incorporates two

external and one internal permeant ion binding sites in the channel of NMDA receptors. When these sites are occupied by permeant ions, Mg^{2+} blocking or unblocking is affected.

Thus, the research included in this Dissertation has deepened our understanding of the mechanism of Mg^{2+}_{o} block . The work also provides insights into NMDA receptor structure and gating.

PREFACE

Many people have helped me along the path of the work included in this dissertation. Drs. M. Bartell and R. Kirchenberg of Concordia University, IL, encouraged my interest in scientific research. Dr. E. A. Schwartz of the University of Chicago showed me the delight, as well as the turmoil, of the life of a scientist.

I am most indebted to Dr. Jon W. Johnson, my thesis adviser, for his energetic and steadfast mentorship. My thesis committee, Drs. Elias Aizenman, Peter F. Drain, Stephen D. Meriney, Lonnie P. Wollmuth, and David C. Wood, guided me with their insights and critical support through the course of this disseratation. Members of the Johnson lab and the neuroscience community at the University of Pittsburgh also greatly facilitated my graduate work.

My family and friends, in particular my husband, John G. Robertson, have provided me with an abundance of love and distraction so that life is always savory.

TABLE OF CONTENTS

LIST OF TABLES

LIST OF FIGURES

I. INTRODUCTION

A. OVERVIEW

N-methyl-D-aspartate (NMDA) receptors, members of the ionotropic glutamate receptor superfamily, are widely distributed in the central nervous system (CNS) (Monaghan & Cotman, 1985). Since their identification pharmacologically in the early 1980s, these receptors have fascinated many researchers with their broad involvement in CNS processes and intricate biophysical properties.

Two decades of extensive research has revealed that NMDA receptors play versatile roles in vertebrate CNS. NMDA receptors are expressed very early during development and contribute to the establishment of neuronal patterning by participating in forming neuronal connection and activity-dependent synaptic pruning (Cline *et al.*, 1990; Iwasato *et al.*, 2000; Kakizawa *et al.*, 2000; Ramoa *et al.*, 2001; Erisir & Harris, 2003). In adult vertebrates, NMDA receptors are key players in activity-dependent long term modulation of synaptic strength (Bliss & Collingridge, 1993; Feldman *et al.*, 1999; Lisman & McIntyre, 2001) and some forms of learning and memory (Maren, 1999; Tang *et al.*, 1999; Nakazawa *et al.*, 2002).

NMDA receptors are also implicated, directly or indirectly, in many pathological states of the brain. These range from acute ischemia-induced cell death to neurodegenerative disorders such as Alzheimer's disease (Meldrum, 1992; Mohn *et al.*, 1999; Chapman, 2000; Cull-Candy *et al.*, 2001; Tsai & Coyle, 2002; Zeron *et al.*, 2002). Hence, regulation of NMDA receptors is crucial for normal functioning of the CNS.

B. MOLECULAR PROPERTIES OF NMDA RECEPTORS

1. Subunits and splice variants

Three NMDA receptor subunit families have been identified, namely NR1, NR2, and NR3 (Moriyoshi *et al.*, 1991; Ikeda *et al.*, 1992; Kutsuwada *et al.*, 1992; Meguro *et al.*, 1992; Monyer *et al.*, 1992; Yamazaki *et al.*, 1992; Ishii *et al.*, 1993; Ciabarra *et al.*, 1995; Sucher *et al.*, 1995; *Das et al.*, 1998; Chatterton *et al.*, 2002). The NR1 subunit type has one gene product, with eight splice variants. The NR2 subunit type has four gene products, NR2A-D. NR1 and NR2 are both required to form a functional NMDA receptor. The NR3 subunit type has two gene products, NR3A and NR3B. Although the NR3 subunit can modify receptor characteristics (Das *et al.*, 1998; Chatterton *et al.*, 2002), I will not further discuss their importance since the presence of NR3 subunit is not obligatory for a functional receptor.

The expression of NR2 subunits follows distinct developmental patterns. For example, in rat brain, NR2B subunits are present prenatally, throughout development and also in adult animals; NR2A subunits are only found postnatally; NR2D subunits, sometimes referred to as the "embryonic subunit", first appear prenatally, then start to disappear around P7 (Monyer *et al.*, 1994). The

regional expression of NR2 subunits is tightly controlled as well. Even within a single brain structure, neuron specific expression of NR2 subunits has been reported. For example, in the hippocampus, NR2A and 2B subunits are expressed in pyramidal cells while NR2C and 2D subunits are expressed in interneurons (Monyer *et al.*, 1994). Different NR2 subunits do not share the same subcellular distribution pattern either. For example, in Golgi cells of the cerebellum, NR2A subunits are expressed both synaptically and extrasynaptically while NR2D subunits are expressed exclusively at extrasynaptic sites (Brickley *et al.*, 2003). The temporal and regional distributions of NR2 subunits probably reflect different roles for NMDA receptor-mediated signaling at different developmental stages or brain structures; NMDA receptors with different NR2 subunits have distinct biophysical and signaling properties (see below).

2. Modulation of NMDA receptors

NMDA receptors are subject to modulation by many substances, including sulfhydryl reagents, polyamines, histamine, protons, steroids, protein kinases, arachidonic acid, ethanol, divalent cation species, and various synthetic organic compounds (see Review by Dingledine *et al.*, 1999). Nearly every drug action displays NR2 subunit specificity.

The mechanisms of drug action are diverse. Some substances exert their actions as pharmacological agents; others may regulate NMDA receptors by covalent modification of protein structure. Modulatory substances sometimes have multiple modes of actions. Endogenous Mg^{2+} is a particularly interesting example. It can act as a voltage-dependent channel blocker from both sides of the membrane (Mayer *et al.*, 1984; Nowak *et al.*, 1984; Ascher & Nowak, 1988; Johnson &

Ascher, 1990; Li-Smerin & Johnson, 1996). Surprisingly, Mg^{2+} can also potentiate NMDA receptor activity by increasing the affinity of glycine for the NMDA receptor (Wang & MacDonald, 1995), and through a glycine-independent mechanism (Paoletti *et al.*, 1995).

3. Stoichiometry

The stoichiometry of NMDA receptors, although not definitively known, is likely a tetrameric protein complex containing two NR1 subunits and two NR2 subunits (Clements & Westbrook, 1991; Behe *et al.*, 1995; Laube *et al.*, 1998; Schorge & Colquhoun, 2003). The fact that non-NMDA glutamate receptors appear to be tetrameric structures (Rosenmund *et al.*, 1998; Stephenson, 2001; Bowie & Lange, 2002; Sun *et al.*, 2002) also lends support for a tetrameric assembly for NMDA receptors. However, there is also evidence supporting a pentameric structure for NMDA receptors (Premkumar & Auerbach, 1997).

Biochemical and biophysical experiments in neurons have found evidence for coassembly of different NR2 subunits within the same receptor (referred to as triheteromers – NR1 subunit and two distinct NR2 subunits) (Sheng *et al.*, 1994; Chazot & Stephenson, 1997; Dunah *et al.*, 1998; Tovar & Westbrook, 1999; Cathala *et al.*, 2000; Brickley *et al.*, 2003). Triheteromeric NMDA receptors bring forth greater functional heterogeneity, since NMDA receptors with two types of NR2 subunits exhibit characteristics distinct from those with only one or the other type of NR2 subunit (Wafford *et al.*, 1993; Brimecombe *et al.*, 1997; Cheffings & Colquhoun, 2000; Brickley *et al.*, 2003).

4. Subunit topology and modular design

The primary amino acid sequence is organized in the same way in both NR1 and NR2 subunits: extracellular amino terminal (N - terminus), followed by M1, M2, M3, and M4 regions, and ending with intracellular carboxyl terminal (C - terminus). The membrane topology of NR1 or NR2 subunits is shown in Figure 1. There are three transmembrane regions, M1, M3 and M4. M2 forms a reentrant loop, reminiscent of the P-loop in voltage-gated channels (MacKinnon, 1995). The N - terminus contains the amino terminal domain ("ATD", which includes the first 400 amino acids) and S1; S2 is located between M3 and M4. S1 and S2 form a complex, the S1S2 complex, which is involved in ligand binding.

a. Ligand-binding domain

The S1S2 complex, the ligand-binding region, shares sequence homology with the bacterial periplasmic leucine-arginine-ornithine-binding protein (LAOBP). Activation of NMDA receptors requires the binding of both glutamate and glycine. The glycine binding site is formed by the S1S2 complex on the NR1 subunit (Kuryatov *et al.*, 1994; Hirai *et al.*, 1996; Wood *et al.*, 1997; Furukawa & Gouaux, 2003) and the glutamate binding site by S1S2 on the NR2 subunit (Laube *et al.*, 1997; Anson *et al.*, 1998; Lummis *et al.*, 2002). Site-directed mutagenesis studies identified amino acids in S1S2 that are potentially involved in ligand binding (Kuryatov *et al.*, 1994; Hirai *et al.*, 1996; Laube *et al.*, 1997; Wood *et al.*, 1997; Anson *et al.*, 1998; Lummis *et al.*, 2002). Early molecular models of NMDA receptor ligand-binding sites were based on structures of LAOBP, for which high resolution structures based on crystallographic data were available (Oh *et al.*, 1993; Oh *et al.*, 1994).

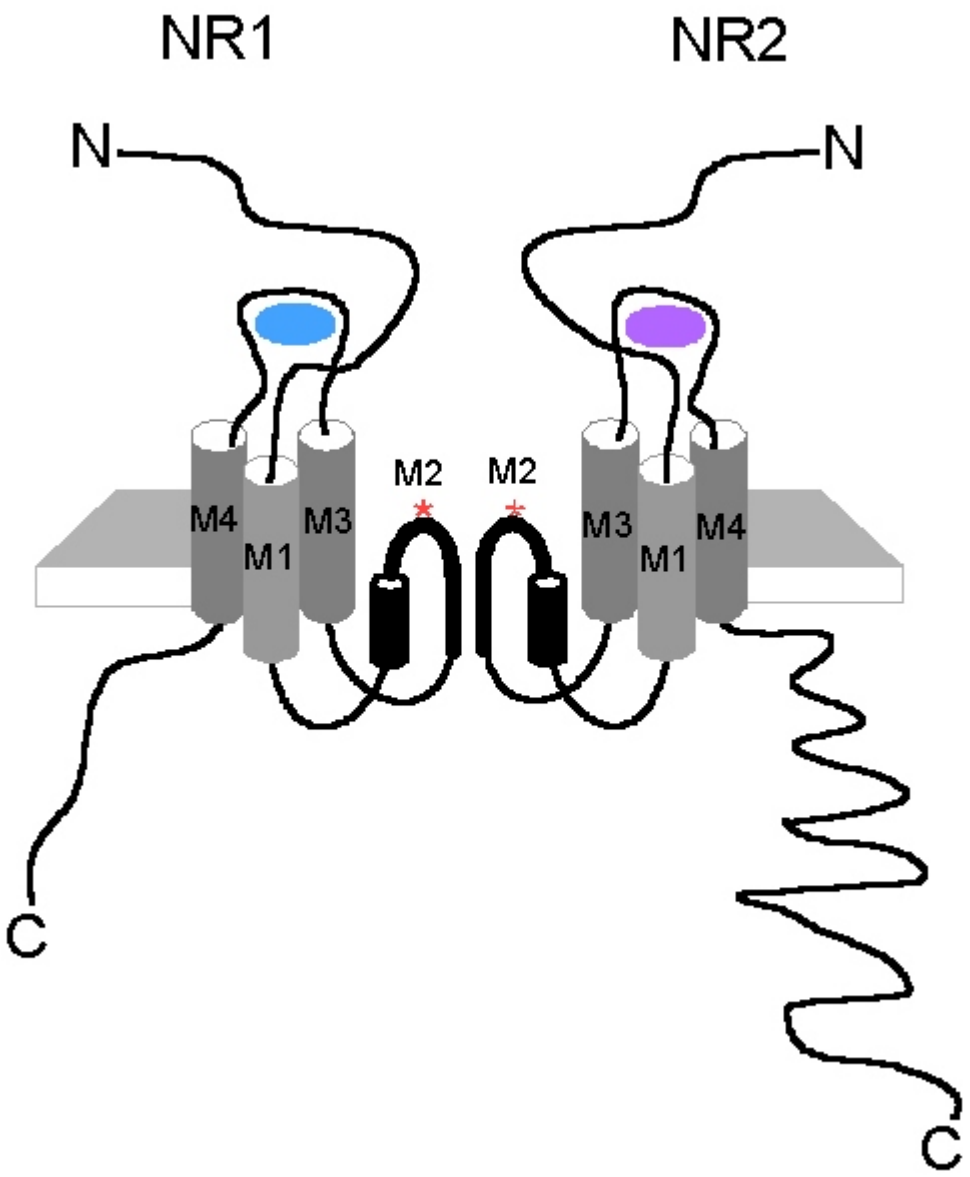

Figure 1 Topology of NMDA receptor subunit. An NMDA receptor subunit inserted in the cell membrane is shown. M1, M3 and M4 traverse the membrane; M2 is a reentrant loop which has a α-helical portion (shown in cylinder) and an extended region (shown in line). Asterisk denotes the *N*–site. Portions of N - terminus domain and the linker between M3 and M4 form the ligand binding site. NMDA receptor subunits, especially NR2, have long intracellular C - terminus regions. The three dimensional structure of the NMDA receptor is not known.

Recently, high resolution structures became available for the S1S2 complex of NR1 subunit based on X-ray crystallography study (Furukawa & Gouaux, 2003). The structure shows that S1 and S2 form a clam shell-like structure with agonist or competitive antagonist nested between the two halves of the clam shell. The two halves are closed with an agonist bound but more open when an antagonist is present (Furukawa & Gouaux, 2003). The authors proposed that initial ligand binding promotes the closure of the clam shell. This model was also proposed for non-NMDA glutamate receptors (Armstrong *et al.*, 1998; Armstrong & Gouaux, 2000; Sun *et al.*, 2002). It is likely that glutamate binding at the S1S2 complex of NR2 subunit triggers similar movements in the ligand-binding region.

b. Channel region

The channel region of the NMDA receptor has been probed using the substituted cysteine accessibility method (SCAM). With this method, amino acids of interest are mutated one by one to cysteine and water-soluble methanethiosulfonate (MTS) reagents are applied. If the cysteine residue is exposed to the aqueous pore, as amino acids lining the channel region would be, MTS reagents can react with the residue and covalently modify the sulfhydryl group of the cysteine. Persistent change in channel behavior can be interpreted as accessibility of the cysteine and its covalent modification by the MTS reagent. Results from SCAM experiments demonstrate that the M2 region contributes to the formation of the intracellular vestibule (Kuner *et al.*, 1996), while the extracellular vestibule is formed by the segments N-terminal to M1, C-terminal to M3, and N–terminal to M4 regions (Beck *et al.*, 1999; Sobolevsky *et al.*, 2002b).

A conserved amino acid residue in glutamate receptors, the *Q/R/N* site in the M2 loop, is occupied by one of three amino acids, glutamate (Q), arginine (R), or asparagine (N). In NMDA receptors, the selectivity filter, the narrowest point of the channel, is formed by *N*–site in NR1 subunits and the asparagine next to *N*–site in NR2 subunits. This conclusion was based on experiments testing the sensitivity of pore diameter to mutations of residues near the *N*–sites in both subunits, as probed by measuring permeability of organic cations of varying sizes (Wollmuth *et al.*, 1996). Results from SCAM experiments are also consistent with this conclusion (Kuner *et al.*, 1996). Interestingly, these sites are also important for high Ca^{2+} permeability and Mg^{2+}_{o} block (Burnashev *et al.*, 1992; Wollmuth *et al.*, 1998a), two hallmark properties of NMDA receptors.

c. Intracellular region

NMDA receptors have long intracellular C - termini, especially in NR2 subunits. For example, over 40% of the amino acids in NR2A subunits are within the C-terminal domain. C-terminals are functionally important: mutant mice with large C-terminal deletions have severe developmental and behavioral deficits (for example, see Sprengel *et al.*, 1998).

The C-terminal region is involved in NMDA receptor biogenesis and subcellular targeting (Ehlers *et al.*, 1995; Standley *et al.*, 2000; Roche *et al.*, 2001; Scott *et al.*, 2001). The C-terminal region is also involved in linking intracellular signaling pathways to NMDA receptors by harboring (1)kinase phosphorylation sites (Kohr & Seeburg, 1996; Tingley *et al.*, 1997); (2) binding domains for cytoskeletal proteins (Ehlers *et al.*, 1998; Lin *et al.*, 1998); (3) interaction sites for actin-binding proteins (Wyszynski *et al.*, 1997; Lei *et al.*, 2001); and (4) binding motifs for many signaling

molecules (Ehlers *et al.*, 1996; Kim *et al.*, 1996; Lau *et al.*, 1996; Muller *et al.*, 1996; Niethammer *et al.*, 1996).

5. Homology between NMDA receptors and voltage-gated K^+ channels

Research on NMDA receptors has been greatly facilitated by progress made in the voltage gated K^+ channel field. Glutamate receptors, including NMDA receptors, are more similar to voltage-gated K^+ channels than to other ligand-gated channel families. Glutamate receptors share sequence homology with K^+ channels in the channel region (Wood *et al.*, 1995; Panchenko *et al.*, 2001). Systematic site-directed mutagenesis of amino acids in the channel region (Panchenko *et al.*, 2001) and SCAM experiments (Sobolevsky *et al.*, 2003) confirm that the three-dimensional arrangement of the amino acid residues are also likely to be similar in glutamate receptors and K^+ channels. Identification of a prokaryotic glutamate receptor, GluR0, further supports the close link between glutamate receptors and K^+ channels, since GluR0 is related in sequence and functions to both families (Chen *et al.*, 1999).

C. BIOPHYSICAL PROPERTIES OF NMDA RECEPTORS

1. Gating of NMDA receptors

NMDA receptor activation requires the binding of both glutamate and glycine. Aspartate and serine may also act as agonists at the respective glutamate and glycine sites (Patneau & Mayer, 1990; Schell *et al.*, 1995) under physiological conditions. The full activation of NMDA receptors probably requires binding of two glutamates and two glycines per receptor (Clements & Westbrook, 1991). The kinetics of NMDA receptor activation and deactivation are slow compared to other non-NMDA

glutamate receptors and depend on the NR2 subunit present (Monyer *et al.*, 1992; Vicini *et al.*, 1998; Wyllie *et al.*, 1998). The time constants of NR1/2D receptor deactivation after glutamate application is over 1 second (Vicini *et al.*, 1998; Wyllie *et al.*, 1998). The slow deactivation kinetics of NR1/2D receptors is striking: at the synapse, the duration of receptor activation is about three orders of magnitude longer than the duration of glutamate present in the synaptic cleft.

There are three distinct forms of NMDA receptor desensitization: glycine-dependent desensitization, glycine-independent desensitization, and calcium-dependent inactivation. All three forms of desensitization demonstrate NR2 subunit dependence. Glycine-dependent desensitization appears to be the result of negative allosteric interaction between glutamate and glycine binding to the receptor (Mayer *et al.*, 1989; Vyklicky *et al.*, 1990; Regalado *et al.*, 2001). The glycine-independent desensitization involves the ATD and the small segment preceding M1 (Krupp *et al.*, 1998; Villarroel *et al.*, 1998), two regions adjacent to the ligand-binding S1 region. Interestingly, the ATD of NMDA receptors has been identified as the locus for modulation by a number of other substances (Low *et al.*, 2000; Zheng *et al.*, 2001). Calcium-dependent inactivation is not strictly a form of desensitization, since it does not require receptor activation. The inactivation is likely to be mediated by calcium dependent binding of calmodulin to a site in the C-terminal of NR1 subunit and the subsequent dissociation of the NMDA receptor from cytoskeletal elements (Ehlers *et al.*, 1996; Zhang *et al.*, 1998; Krupp *et al.*, 1999).

The mechanism of NMDA receptor gating is unknown. However, rapid progress made in other ligand-gated channel fields has suggested some tantalizing models. In Glu2 AMPA receptors

(Figure 2) (Armstrong *et al.*, 1998; Armstrong & Gouaux, 2000; Sun *et al.*, 2002), D1 and D2 domains are involved in ligand binding. D1, which is made mostly of S1, dimerizes with neighboring D1 of a different subunit to form a stable interface. D2, made mostly of S2, is presumably linked to the channel portion of the receptor. Ligand binding induces movement of D2 towards D1, pulling the linked channel open. A model based on similar principles was proposed for gating of Ca^{2+}-activated MthK channels (Jiang *et al.*, 2002a), although the specifics, for example, the formation of a stable interface, are different from GluR2 receptors.

Several regions of NMDA receptors have been implicated in channel gating, notably, the ATD and the C-terminal portion of M3. The ATD is one of the main molecular constituents for receptor desensitization and is the interaction site for several modulators that affect gating (Krupp *et al.*, 1998; Villarroel *et al.*, 1998; Dingledine *et al.*, 1999; Fayyazuddin *et al.*, 2000; Low *et al.*, 2000; Paoletti *et al.*, 2000; Zheng *et al.*, 2001). The C-terminal portion of M3 has eight amino acids that are conserved among all ionotropic glutamate receptors. Site-directed mutagenesis and SCAM experiments suggest that this portion of M3 is involved in channel gating as well (Kohda *et al.*, 2000; Jones *et al.*, 2002; Kashiwagi *et al.*, 2002). Additionally, *N*–site may also be involved in channel gating, as suggested by mutagenesis work (Schneggenburger & Ascher, 1997).

2. Ion channel characteristics

The pore diameter of NMDA receptor was estimated to be approximately 5 Å, judged by the permeability of organic molecules of known dimensions (Villarroel *et al.*, 1995; Zarei & Dani, 1995). The channels of NMDA receptor are not selective among monovalent cations: it is nearly

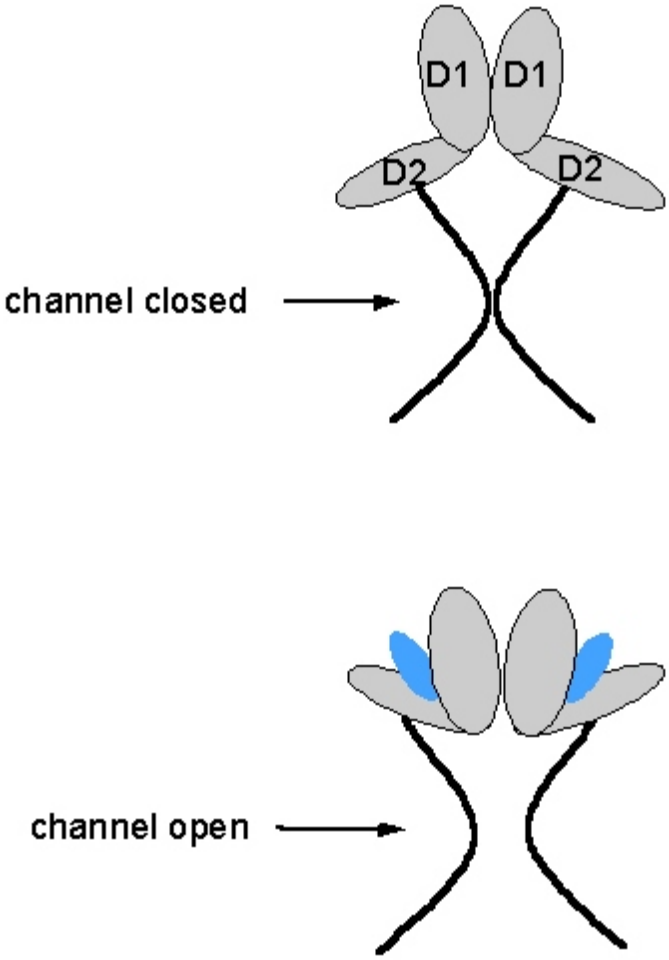

Figure 2 Model of channel gating of GluR2 receptor. The ligand binding domains of two NMDA receptors subunits are shown. D1 of neighboring subunits dimerize with each other to form a stable interface. D1 and D2 have an open conformation in the absence of ligand (top). Ligand-binding causes D2 to move towards D1 (bottom) and this movement pulls the channel open.

equally permeable to Na^+, K^+ and Cs^+ ions (Tsuzuki *et al.*, 1994). An interesting and important feature of NMDA receptor is its high permeability to Ca^{2+} (MacDermott *et al.*, 1986), which can act as an intracellular signaling molecule. The permeability ratio of Ca^{2+} to monovalent ions is over 5 (Ascher & Nowak, 1988; Iino *et al.*, 1990; Jahr & Stevens, 1993). Under physiological conditions, Ca^{2+} carries about 6-18% of the total current through NMDA receptors even though its concentration is much lower than $[Na^+]$ or $[K^+]$ (Schneggenburger *et al.*, 1993; Burnashev *et al.*, 1995; Schneggenburger, 1996). NMDA receptors are also permeable to other divalent ions such as Ba^{2+} and Sr^{2+} (Iino *et al.*, 1990).

An important question regarding the ion channel is whether it can accommodate more than one ion at a time. Multi-ion pores provide mechanisms for channels to be both selective and of high conductance: a high affinity binding site for particular ions ensures selectivity; neighboring ion binding sites facilitate ion flux. Facilitation of ion flux could be achieved by either electrostatic repulsion between binding ions, or by lowering the energy barrier for an ion to hop to the next binding site (for examples, Hess & Tsien, 1984; Dang & McCleskey, 1998). Multi-ion pores may also display complex interactions between permeant ion and blocker (for examples, Neyton & Miller, 1988b, a; Jiang & MacKinnon, 2000). Under monovalent ion conditions, the NMDA receptor behaves more consistently with a single-ion pore (Zarei & Dani, 1994). However, when divalent ions are present, the channel of NMDA receptor can simultaneously hold more than one ion (Antonov *et al.*, 1998; Wollmuth & Sakmann, 1998; Antonov & Johnson, 1999; Zhu & Auerbach, 2001a, b).

Many molecules can block the channel of NMDA receptors. Studies of the actions by these molecules have yielded rich information regarding the structure and gating of NMDA receptors. This topic will be discussed in detail in the next two sections.

D. EXTERNAL Mg^{2+} BLOCK OF NMDA RECEPTORS

Voltage-dependent external Mg^{2+} (Mg^{2+}_o) block of the channel of NMDA receptors is an unusual property which, along with high Ca^{2+} permeability, is essential for the wide range of physiological roles NMDA receptors play. Under physiological conditions, at resting potential, NMDA receptors allow little ion flux even with neurotransmitters bound, due to the strong inhibition by Mg^{2+}_o. Ions can flow readily through the channels of NMDA receptors only when the membrane is depolarized and, as a result, Mg^{2+}_o is released from the channel. Hence, NMDA receptors can detect the coincident presynaptic release of neurotransmitters and postsynaptic depolarization.

Mg^{2+}_o block is also arguably one of the most interesting biophysical properties of NMDA receptors. Investigation of Mg^{2+}_o block has yielded a wealth of information with respect to mechanism of drug action, channel structure and the gating process (Mayer *et al.*, 1984; Nowak *et al.*, 1984; Mayer & Westbrook, 1987; Ascher & Nowak, 1988; Jahr & Stevens, 1990a, b; Burnashev *et al.*, 1992; Mori *et al.*, 1992; Ruppersberg *et al.*, 1994; Kuner & Schoepfer, 1996; Kupper *et al.*, 1996; Sharma & Stevens, 1996a, b; Wollmuth *et al.*, 1998a; Antonov & Johnson, 1999; Sobolevsky & Yelshansky, 2000; Zhu & Auerbach, 2001a, b; Johnson & Qian, 2002; Qian *et al.*, 2002).

1. Overview of Mg^{2+}_o block

At the whole-cell level, in the presence of physiological Mg^{2+}_o concentrations, the slope of the I-V curve of NMDA activated current is reasonably linear at positive voltages, but at negative voltages the I-V curve shows a region with negative slope (Mayer *et al.*, 1984; Nowak *et al.*, 1984; Ascher & Nowak, 1988). Under resting conditions, Mg^{2+}_o inhibits the majority of the NMDA receptor-mediated current flow. Therefore, Mg^{2+}_o effectively regulates the number of ions, including Ca^{2+}, that traverse the NMDA receptors. The characterization of Mg^{2+}_o block at the single-channel level has been limited to receptors with NR2A or NR2B subunits. For these receptors, addition of Mg^{2+}_o causes the channel openings to be interrupted by brief closures ("channel flicker"). Each single "channel flicker" presumably reveals one Mg^{2+}_o blocking and unblocking event.

2. Modulation of Mg^{2+}_o block

While all NMDA receptors are subject to Mg^{2+}_o block, the degree of inhibition by Mg^{2+}_o is highly variable. For example, Mg^{2+}_o inhibition of NMDA currents is highly dependent on brain region (for example, Momiyama *et al.*, 1996) or the developmental stage (Kato and Yoshimura, 1993; Nabekura *et al.*, 1994). NMDA receptors in immature brain structures in general are not as susceptible to Mg^{2+}_o inhibition (but see Kleckner & Dingledine, 1991). It is very likely that the spatial and temporal regulation of NR2 subunit expression is responsible for this variability, as Mg^{2+}_o inhibition is dependent on the NR2 subunits.(Monyer *et al.*, 1994; Kuner & Schoepfer, 1996).

The amount of Mg^{2+}_o inhibition can also be altered during pathological states such as nerve injury, inflammation or chemical ischemia (Hori & Carpenter, 1994; Zhang *et al.*, 1996; Furukawa

et al., 2000; Guo & Huang, 2001; Aizenman *et al.*, 2000). In some cases, alteration in Mg^{2+}_o inhibition was found to be correlated with protein kinase C modulation (PKC) (Zhang *et al.*, 1996; Guo & Huang, 2001); PKC has been reported to reduce Mg^{2+}_o inhibition (Chen & Huang, 1992; but see Wagner & Leonard, 1996). Another way to modulate Mg^{2+}_o inhibition is by changing permeant ion concentrations. Permeant ions not only have powerful influence on the degree of Mg^{2+}_o inhibition, they also shape the voltage dependence of Mg^{2+}_o inhibition (Ruppersberg *et al.*, 1994; Zarei & Dani, 1995; Antonov & Johnson, 1999; Zhu & Auerbach, 2001a, b; Qian *et al.*, 2002). It is known that changes in permeant ion concentrations may occur during pathological states (Grisar, 1984; Lux *et al.*, 1986; Kager *et al.*, 2000). It is therefore possible that changes in permeant ion concentrations are responsible for altered Mg^{2+}_o inhibition during some diseased states.

3. Molecular basis of Mg^{2+}_o block

The molecular constituents of the NMDA receptors that influence Mg^{2+}_o inhibition are being identified using site-directed mutagenesis techniques. Dramatic changes occur when the *N* site of the NR2 subunit is mutated (Burnashev *et al.*, 1992; Mori *et al.*, 1992; Sharma & Stevens, 1996b): an asparagine to glutamine substitution caused the Mg^{2+}_o IC_{50} to increase by as much as over 20-fold. In addition, residues adjacent to *N*–site of NR2 subunits are also crucial for Mg^{2+}_o inhibition (Kupper *et al.*, 1996; Wollmuth *et al.*, 1998a). Other amino acids may also be involved in Mg^{2+}_o block, such as tryptophan at position 607 of NR2B subunit (Williams *et al.*, 1998) and the *N*–site on NR1 subunit (Burnashev *et al.*, 1992; Mori *et al.*, 1992; Sakurada *et al.*, 1993; Premkumar & Auerbach, 1996; Wollmuth *et al.*, 1998a).

Amino acids near the *N*–site are completely conserved among all NR2 subunits. Kuner and Schoepfer (1996) have presented convincing evidence that multiple other regions of the NR2 subunits also influence Mg^{2+}_o inhibition. These regions include segments of pre M1 regions, the linker between M2 and M3, the region near M4 . These segments likely line the external and internal vestibules of the channel (Kuner *et al.*, 1996; Beck *et al.*, 1999). It is interesting that structural elements affecting Mg^{2+}_o inhibition are distributed in such a diffuse manner.

4. Mechanism of Mg^{2+}_o block

The kinetics of Mg^{2+}_o block is amenable to detailed single-channel analysis. The kinetics are fast relative to the channel activation and deactivation and can thus be identified and studied; at the same time, the block action is slow enough that the blocking and unblocking events can be resolved by the recording system (Hille, 2001). Single-channel analysis of Mg^{2+}_o block revealed that while Mg^{2+}_o blocks as an open channel blocker (Ascher & Nowak, 1988; Jahr & Stevens, 1990a), its action deviates from that of a classic "sequential blocker", which does not allow channel closure during block (Armstrong, 1971; Adams, 1977; Neher & Steinbach, 1978). Instead, Mg^{2+}_o block does not appear to prevent channel closure.

The traditional explanation for the voltage-dependence of Mg^{2+}_o inhibition is that Mg^{2+}_o obstructs current flow by binding to a site within the open channel of NMDA receptors and subsequently unbinding to the external site. The binding site is within the voltage field. The affinity of Mg^{2+}_o inhibition is higher at hyperpolarized voltages because Mg^{2+}_o blocking is sped up with hyperpolarization while its unblocking is slowed down with hyperpolarization.

The Woodhull model (Woodhull, 1973), often used to explain the voltage-dependence of channel block, predicts that the percentage of voltage-field Mg^{2+}_o has to cross to reach its binding site from the outside is about 90%. This is surprisingly steep since Johnson and Ascher (1990) reported that the intracellular Mg^{2+} blocking site is about 35% into the voltage field from the inside. It implies that the paths for Mg^{2+} from inside and outside to their respective binding sites overlap one another. This is not very likely since it requires that Mg^{2+} from either side ignores the first Mg^{2+} binding site it reaches when entering the channel. Data from mutation studies (Kupper *et al.*, 1996; Wollmuth *et al.*, 1998b, a) indeed provided evidence that the binding sites for internal and external Mg^{2+} are separate, and that the latter is positioned more externally.

The Woodhull model makes a fundamental assumption that there is no interaction between the blocker and permeant ions so that the voltage-dependence of block arises solely from the electrical field that the blocker passes through. This assumption is violated in the case of Mg^{2+}_o block of NMDA receptor. Permeant ions can interact with Mg^{2+}_o block (Ruppersberg *et al.*, 1994; Zarei & Dani, 1995). The detailed mechanism of permeant ion and Mg^{2+}_o interactions was provided by recent studies in cortical neurons (Antonov & Johnson, 1999) and in an expression system (Zhu & Auerbach, 2001a, b), where NMDA receptors with NR2A or NR2B were studied.

The study by Antonov and Johnson (1999) is particularly relevant to the experiments described in this Dissertation. Antonov and Johnson studied the interaction of Mg^{2+}_o with monovalent permeant cations during block of NMDA-activated channels. Specifically, they looked

at how external sodium (Na^+_o) and internal cesium (Cs^+_i) affect the blocking and unblocking rates of Mg^{2+}_o block using single-channel recording techniques. Based on the results, a model (Figure 3) that describes the interaction between Na^+_o or Cs^+_i and Mg^{2+}_o block of NMDA receptors was proposed: (1) There are two binding sites for permeant monovalent ions at the mouth of the external vestibule of the receptor. Na^+_o can bind to one or both of these sites while Cs^+_i can occupy only one of the sites. (2) When either site is occupied by Na^+_o or Cs^+_i, Mg^{2+}_o cannot enter to block the pore. (3) When Mg^{2+}_o is within the pore, Na^+_o can occupy the external site(s) and prevent Mg^{2+}_o from exiting to the external solution until Na^+_o dissociates from the binding site. (4) The majority of the time, Mg^{2+}_o exits the external side of the membrane but sometimes, especially at extremely hyperpolarized voltages, Mg^{2+}_o does go through the pore and exits to the internal side. This model provides a mechanism by which we can explain the high voltage-dependence of Mg^{2+}_o block of NMDA receptors: the interaction between Mg^{2+}_o and permeant ions enhances the voltage-dependence of Mg^{2+}_o block.

E. CHANNEL BLOCKERS AND CHANNEL STRUCTURE

Classic work on voltage-gated ion channels have used blockers to probe the structure of channel. The questions addressed using channel blockers include the nature of the channel pore, permeant ion and blocker sites within the channel, and the position of the gate. The validity of this experimental approach has been established: conclusions drawn from work using channel blockers (Armstrong, 1966; Neyton & Miller, 1988b, a) have been confirmed by crystal structure of

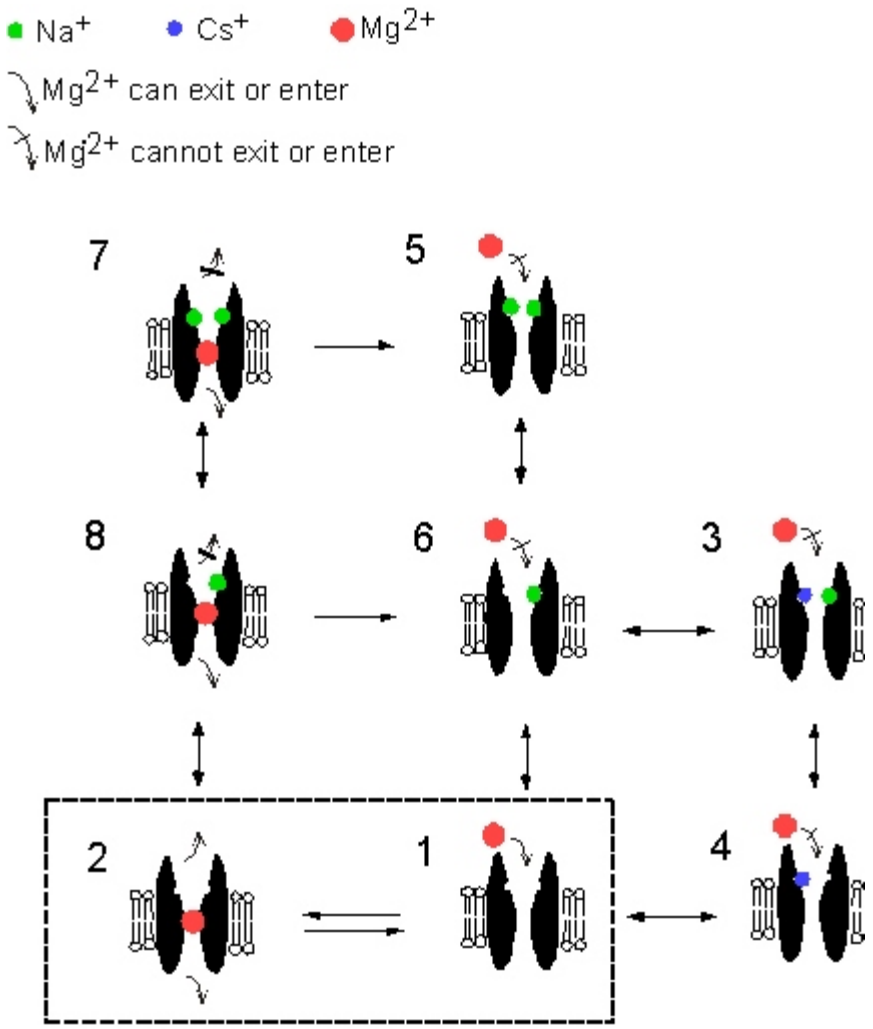

Figure 3 Model of Mg^{2+}_o block of cortical NMDA receptors. The model based on single-channel measurement of Mg^{2+}_o block (Antonov & Johnson, 1999) is schematized here. States 1 and 2 illustrate Mg^{2+}_o block and unblock of the open channel of the NMDA receptor when Na^+_o or Cs^+_i are not bound. States 3-6 illustrate states in which Na^+_o and/ or Cs^+_i occupy the external ion sites and prevent Mg^{2+}_o from entering the channel. States 7-8 illustrate that occupancy by Na^+_o of the external ion site(s) prevents bound Mg^{2+}_o from exiting to the external solution, although permeation to the internal solution is still permitted.

bacterial K^+ channels (Jiang & MacKinnon, 2000; Zhou *et al.*, 2001). The method of using blockers to probe channel structures has been readily applied to NMDA receptors, for which direct structural information is scarce. The information obtained sheds light on the dimension of the channel pore as well as conformational changes associated with channel gating.

1. Dimension of the channel of NMDA receptor

Molecules of different size have been used to survey the structure of the NMDA receptor. The diameter of the selectivity filter is about 5 Å (Zarei & Dani, 1995; Wollmuth *et al.*, 1996). The external vestibule, probably larger than the internal one (Zarei & Dani, 1995), can accommodate blockers as large as 8 Å wide (Sobolevsky *et al.*, 2002a). The voltage field encompasses about 23Å along the pore axis (Subramaniam *et al.*, 1994), while the length of the pore could be at least 29Å, judging by the locations of the permeant ion binding sites (Antonov *et al.*, 1998). The selectivity filter resides about two-thirds of the way from the outside between the external and internal permeant ion binding sites; the selectivity filter senses about 50% of voltage drop (Antonov *et al.*, 1998). Interestingly, evidence suggests that at least portions of the external vestibule of NMDA receptor are hydrophobic in nature, since blocker affinity increases with the length of the carbon chain (Subramaniam *et al.*, 1994).

2. Conformational changes associated with gating

One of the most fundamental questions about an ion channel is the location and the nature of the channel gate, which is the point where small permeant ions cannot pass if the gate is closed. It is distinct from any other restrictions which impede the movements of larger molecules such as

channel blockers. In principle, the gate region need not be located at a point; a section of the pore can form the gate.

Many molecules can block the channel of NMDA receptor from the extracellular side, and subsequently the channel can close and trap the molecules in the channel. These molecules are referred to as the "trapping blockers" (Johnson & Qian, 2002). This is very similar to the internal blocker interaction with the voltage-gated K channel (Armstrong, 1966; Yellen, 1998; del Camino & Yellen, 2001; Jiang *et al.*, 2002b), which was found to have a gate located between the blocker binding site and the internal solution. The characteristics of external trapping blockers in NMDA receptors suggest that the external part of the channel moves during gating. Although consistent with an external gate, this is not conclusive evidence for an external gate since (1) location where blockers cannot pass through may not be the true gate for smaller permeant ions; (2) trapping can in principle occur by collapsing the channel over a distance and the channel simply squeezing the blocker in place. If trapping occurs by collapsing of the channel, the gate could be elsewhere. The fact that many blockers of different dimension and mechanism can affect gating (Johnson & Qian, 2002) suggests that channel conformational changes induced by gating movements may be fairly extensive.

Large conformation changes during gating were confirmed by SCAM (Sobolevsky *et al.*, 2002a): gating-dependent accessibility changes were observed for cysteine substituted residues lining the external vestibule. Surprisingly, the cysteine residues along the external vestibule could be modified by MTS reagents even when the channel was closed, arguing strongly that the gate is located deep in the channel, near the selectivity filter, or even deeper. Location of channel gate at

the selectivity filter has been reported for other ion channels (Yellen, 1998; Flynn *et al.*, 2001; Bruening-Wright *et al.*, 2002).

Although a deep gate position based on SCAM study is convincing, other researchers have made different observations. Antonov and Johnson (1999) showed that the larger blocker IEM-1857 prevents gate closure, while smaller IEM-1754 prevents gate closure when binding at a shallow site but does not prevent gate closure once it moves to a deeper site. Sobolevsky showed that while larger tetrapentylammonium prevents channel closure, smaller tetraethylammonium does not (Sobolevsky *et al.*, 1999). These data suggest that gating-associated conformation changes are greater towards the external part of the channel but smaller deeper into the channel; larger molecules, which presumably cannot readily access the deep portion of the channel, have the greatest effects on gating by preventing gate closure.

Mg^{2+}_{o} block does not appear to affect gating (Qian *et al.*, 2002), suggesting that the conformational changes associated with gating are not substantial around the Mg^{2+}_{o} binding site. Since the Mg^{2+}_{o} binding site is very near the selectivity filter (Burnashev *et al.*, 1992; Mori *et al.*, 1992; Kupper *et al.*, 1996; Sharma & Stevens, 1996b; Wollmuth *et al.*, 1998a), the gate could be either towards the external side, or deeper than the selectivity filter. A deeper location of the gate would mean that during gating, there are movements at the external vestibule as well as the gate that nevertheless leave a center region of the channel relatively immobile.

In summary, studies of blocker interaction with the pore of the NMDA receptor have generated a wealth of information regarding the structural and mechanistic aspects of channel function. Although all previous data cannot yet be understood in a unified way, intriguing and useful models have been suggested and our understanding of these issues thereby have advanced.

F. GOALS OF THE DISSERTATION STUDY

NMDA receptors are key components of vertebrate CNS circuitry. The voltage-dependent block by Mg^{2+}_o is an essential feature of NMDA receptor function and presumably, along with high Ca^{2+} permeability, underlies the many important roles NMDA receptors play. Many studies have suggested that Mg^{2+}_o block itself is under regulation during physiological conditions, providing a mechanism to dynamically control NMDA receptor-mediated activities. The central objective of this Dissertation was to enhance our understanding of the mechanism of Mg^{2+}_o block of NMDA receptors by exploring the permeant ion and subunit dependency of this process. This was achieved by investigating the following three topics:

1. The effects of permeant ions on Mg^{2+}_o inhibition of cortical NMDA currents.

Mg^{2+}_o inhibition of cortical NMDA receptor-mediated currents under various ionic conditions was examined in whole-cell experiments. The results suggest that Mg^{2+}_o inhibition of whole-cell NMDA currents is very sensitive to ionic conditions. This phenomenon can be explained by a kinetic model which incorporates external permeant ion binding sites within the pore. This part of the research is presented in Chapter II. Note that a portion of this work has been published (Qian *et al.*, 2002).

2. The characteristics of Mg^{2+}_o block in NR1/2D receptors.

Whole-cell and outside-out patch recording techniques were used to investigate Mg^{2+}_o inhibition of NR1/2D currents and the microscopic kinetics of Mg^{2+}_o block. The results suggest that the general mechanisms of Mg^{2+}_o channel block of NR1/2D receptors is fundamentally similar to that of cortical receptors which are likely to be NR1/2A or NR1/2B receptors. However, Mg^{2+}_o block of NR1/2D receptors is much weaker than cortical receptors, mostly due to faster Mg^{2+}_o unblocking. This part of the research is presented in Chapter III.

3. Effects of permeant ions on Mg^{2+}_o block of NR1/2D receptors.

Whole-cell and outside-out patch recordings were used to investigate the effects of permeant ions on Mg^{2+}_o block of NR1/2D receptors. The results, which demonstrate the powerful effects of permeant ions on Mg^{2+}_o block, can be explained by a kinetic model that incorporates two external and one internal permeant ion binding sites. This part of the research is presented in Chapter IV.

II. MODULATION BY PERMEANT IONS OF Mg^{2+} INHIBITION OF NMDA-ACTIVATED CURRENTS IN RAT CORTICAL NEURONS

A. SUMMARY

Whole-cell NMDA-activated currents were recorded from cultured rat cortical neurons. I report here a powerful effect of changing permeant ion concentrations on the voltage-dependent inhibition by Mg^{2+}_o of these currents. Internal Cs^+ (Cs^+_i) affected Mg^{2+}_o inhibition of the NMDA-activated currents in a voltage-dependent manner. A decrease in $[Cs^+]_i$ from 125 mM to 8 mM reduced Mg^{2+}_o IC_{50} by 1.4 fold at -105 mV and by 11.5 fold at -15 mV. A decrease in external Na^+ (Na^+_o) concentration also reduced Mg^{2+}_o IC_{50}. This effect was voltage-independent. A decrease in $[Na^+]_o$ from 140 mM to 70 mM reduced Mg^{2+}_o IC_{50} by 1.4 fold at -105 mV and by 1.6 fold at -15 mV. These data are consistent with a model in which Na^+_o and Cs^+_i modulate Mg^{2+}_o inhibition of NMDA-activated currents by occupying external permeant ion binding sites. Varying external Ca^{2+} (Ca^{2+}_o) concentrations from 0.1 mM to 1 mM did not affect Mg^{2+}_o inhibition, even though changing $[Ca^{2+}]_o$ over the same range strongly influenced the magnitude of NMDA-currents in the absence of Mg^{2+}_o. However, increasing $[Ca^{2+}]_o$ to higher concentrations (2 - 20 mM) greatly increased Mg^{2+}_o IC_{50}; this effect was stronger at hyperpolarized voltages. The Mg^{2+}_o IC_{50} values reported here are similar to Mg^{2+}_o K_D values calculated from previous single-channel measurements of Mg^{2+}_o blocking kinetics. This similarity implies that Mg^{2+}_o does not affect gating while blocking the channel.

B. INTRODUCTION

NMDA receptors are critically involved in physiological processes of both the developing and mature vertebrate CNS, including neuronal patterning formation (Iwasato *et al.*, 2000) and learning and memory (Bliss & Collingridge, 1993; Tang *et al.*, 1999). NMDA receptors are also implicated, directly or indirectly, in disease states ranging from acute ischemia-induced cell death to neurodegenerative disorders (Meldrum, 1992). Hence, regulation of the NMDA receptors is crucial for proper functioning of the CNS.

Many substances modulate NMDA receptor function (McBain & Mayer, 1994; Dingledine *et al.*, 1999). Mg^{2+} is a particularly important modulator, and exhibits a number of modes of actions. It can act as a voltage-dependent channel blocker from both the external (Mayer *et al.*, 1984; Nowak *et al.*, 1984; Ascher & Nowak, 1988) and internal (Johnson & Ascher, 1990; Li-Smerin & Johnson, 1996) sides of the membrane. Mg^{2+} can potentiate NMDA receptor activity by increasing the affinity of glycine for the NMDA receptor (Wang & MacDonald, 1995) or through a glycine-independent mechanism (Paoletti *et al.*, 1995). Under certain conditions, Mg^{2+} also permeates the channel of NMDA receptors (Mayer & Westbrook, 1987; Stout *et al.*, 1996; Antonov & Johnson, 1999; Zhu & Auerbach, 2001a, b).

The open-channel block of channels of NMDA receptors by Mg^{2+}_o has been heavily investigated. The widely accepted mechanism of Mg^{2+}_o block involves Mg^{2+}_o binding to a discrete site within the open channel of NMDA receptors, obstructing current flow, and then unbinding to

the external solution under most circumstances. The binding site is thought to be deep in the channel of the NMDA receptor, within the region where the transmembrane voltage drop occurs. As a result, the affinity of Mg^{2+}_o for the binding site changes as a function of membrane voltage. At hyperpolarized membrane voltages, the probability of Mg^{2+}_o occupying the site is higher, hence the block is more pronounced.

While Mg^{2+}_o occupies the pore, it may influence channel gating transitions. There are many ways in which a blocker can interact with gating. Sequential blockers, examples of which are thought to include 9-aminoacridine (Costa & Albuquerque, 1994; Benveniste & Mayer, 1995), IEM-1857 (Antonov & Johnson, 1996), and tetrapentylammonium (Sobolevsky *et al.*, 1999), have the extreme effect of preventing the channel gate from closing during block. Other channel blockers allow the gate to close and can be subsequently "trapped" in the channel when the agonist is removed. Examples of such blockers of the NMDA receptor are MK-801 (Huettner & Bean, 1988), memantine (Blanpied *et al.*, 1997; Chen & Lipton, 1997), and ketamine (MacDonald *et al.*, 1987). The trapped blocker may also perturb gating parameters by affecting binding of agonists or gating transitions (Blanpied *et al.*, 1997; Sobolevsky *et al.*, 1999). The action of Mg^{2+}_o on gating is not yet clear. Several pieces of evidence suggest that there is little or no effect of block by Mg^{2+}_o on channel gating: (1) single-channel burst analysis of Mg^{2+}_o block indicated a clear departure from predictions for a sequential blocker (Nowak *et al.*, 1984); (2) the channel of the NMDA receptor can close from the Mg^{2+}_o blocked state (Jahr & Stevens, 1990a; Sobolevsky & Yelshansky, 2000); (3) Mg^{2+}_o does not prevent NMDA or glycine dissociation (Benveniste & Mayer, 1995; Sobolevsky & Yelshansky, 2000). However, a reduction in the burst duration and a decrease in the channel opening frequency

may indicate that channel closure is accelerated during block by Mg^{2+}_o (Nowak *et al.*, 1984; Ascher & Nowak, 1988).

Several molecular constituents of the channel of NMDA receptors have been identified that influence Mg^{2+}_o block. Notably, the *N*-site, located at the tip of the M2 region, and its neighboring asparagine of NR2 subunits are most likely the key residues that coordinate Mg^{2+}_o during block (Burnashev *et al.*, 1992; Mori *et al.*, 1992; Kupper *et al.*, 1996; Wollmuth *et al.*, 1998a). Kuner & Schoepfer (1996) found that Mg^{2+}_o block is also influenced by multiple other regions of the receptor, which probably form the external and internal vestibules and the pore (Kuner *et al.*, 1996; Beck *et al.*, 1999) and thus are unlikely all to contribute to the Mg^{2+} binding site. This diffuse distribution of structural elements responsible for Mg^{2+}_o block appears inconsistent with the idea that Mg^{2+}_o blocks at a discrete site within the channel. This discrepancy echos the long-existing puzzle of how Mg^{2+}_o block acquires its unusually strong voltage-dependence.

An explanation for this puzzle was provided by recent single-channel studies (Antonov & Johnson, 1999; Zhu & Auerbach, 2001a, b) which demonstrated that permeant monovalent ions have a powerful effect on the kinetics of channel block and unblock by Mg^{2+}_o. These studies suggest that voltage-dependent binding of permeant monovalent ions to the external channel vestibule NMDA receptors accentuates the voltage-dependence of Mg^{2+}_o block.

In the work presented here I investigated the effect of permeant ions on Mg^{2+}_o inhibition of whole-cell NMDA-activated currents. There are three goals. First, I characterized the relevance of

the interaction between monovalent permeant ion and Mg^{2+}_o to current inhibition. The results demonstrated that the equilibrium constant of Mg^{2+}_o inhibition of macroscopic currents was dramatically regulated by the ionic environment of a neuron. Second, I compared the whole-cell data with predictions of the previous proposed model based on single-channel measurements (Antonov & Johnson, 1999; Zhu & Auerbach, 2001a, b). This comparison tested whether the model, which was derived from kinetic measurements made in low $[Mg^{2+}]_o$s, is adequate to explain Mg^{2+}_o inhibition of macroscopic currents at higher, more physiologically relevant $[Mg^{2+}]_o$. The good agreement between whole-cell measurements of IC_{50} and single-channel measurements of K_D also implied that Mg^{2+}_o block has no effect on channel gating. Third, I studied the effect of Ca^{2+}_o on Mg^{2+}_o block at the whole-cell level. Ca^{2+}_o is a highly permeant ion whose interaction with Mg^{2+}_o has never been carefully addressed. The results show that at $[Ca^{2+}]_o$s higher than 2 mM, Ca^{2+}_o also influences the voltage-dependent Mg^{2+}_o block.

C. METHODS

1. Cell Culture

Primary cultures of cortical neurones were prepared as described in Li-Smerin & Johnson (1996). The procedure was approved by the Institutional Animal Care and Use Committee at the University of Pittsburgh. Briefly, 16-day pregnant Sprague-Dawley rats were sacrificed by CO_2 inhalation. Brains from the embryos were removed and cerebral cortices were harvested. The cortical cells were dissociated enzymatically and plated at a density of $2x10^5$ - $2.5x10^5$ cells per ml onto 35 mm plastic petri dishes that contained glass coverslips, which either had been coated with poly-L-lysine or contained a glial cell feeder layer. Cells were used from 10 to 42 days after plating.

2. Solutions

Solutions were delivered through a five- or seven-barrel fast perfusion system, similar to the one described in Blanpied *et al.* (1997). Solution changes were accomplished by movements of barrels. Each barrel was connected to a gravity-fed reservoir of solution. At the output of the reservoir, a solenoid valve was used to turn solution flow on or off. The speed of flow was adjusted by varying the height of the reservoirs to ensure rapid and complete change of solution following movement of the barrels. With this system, a 98 to 99% complete solution exchange typically occurs within 120 ms (Blanpied *et al.*, 1997).

Solutions were prepared daily from frozen stocks. For external solutions, 0.2 μM tetrodotoxin was added. Currents were activated by 10 μM NMDA + 30 μM glycine (identified on figures as "NMDA"). 1 μM strychnine was also included to prevent activation of the strychnine-sensitive glycine receptor. Mg^{2+} concentrations from 1 μM to 3 mM were added to external solutions. To determine whether the contaminating [Mg^{2+}] was great enough to affect significantly the final [Mg^{2+}] of external solutions, [Mg^{2+}] was measured using an atomic absorption spectrophotometer (Perkin-Elmer 2380). The contaminating [Mg^{2+}] in control external solution + 10 μM NMDA + 30 μM glycine was too low to be measured accurately, but it must be less than 0.31 μM. Based on this low maximal level of contaminating Mg^{2+}, I did not use Mg^{2+} buffers (which in some cases may yield inaccurate final free [Mg^{2+}]; (Li-Smerin *et al.*, 2001)) or make corrections to Mg^{2+} concentrations. The abbreviations and contents of external bath solutions are (in mM): "140 Na^{+}_{o}" solution, 140 NaCl, 1 $CaCl_2$, 2.8 KCl, and 10 HEPES; "70 Na^{+}_{o}" solution, 70 NaCl, 140

sucrose, 0.5 $CaCl_2$, 2.8 KCl, and 10 HEPES. The pH of external solutions was adjusted to between 7.1 and 7.2 using NaOH. In experiments in which $[Ca^{2+}]_o$ was changed to 0.2, 0.5, or 2 mM (in the 140 Na^+_o solution) or to 0.1 mM (in the 70 Na^+_o solution), no other changes in solute concentration were made. When $[Ca^{2+}]_o$ was raised to 5 or 20 mM (in the 70 Na^+_o solution), the sucrose concentration was reduced to 125 or 80 mM, respectively.

Cs^+ was used as the principal intracellular permeant cation because it inhibits K^+ conductances in neurons, but is about as permeant through the channel of NMDA receptors as Na^+ and K^+ (Tsuzuki *et al.*, 1994). The abbreviations and contents of internal solutions are (in mM): "125 Cs^+_i" solution, 125 CsCl, 10 EGTA and 10 HEPES; "8 Cs^+_i" solution, 8 CsCl, 117 *N*-methyl-D-glucamine (NMDG), 10 EGTA and 10 HEPES. The pH of internal solutions was adjusted to between 7.1 and 7.2 using CsOH or HCl.

NMDG was used to adjust the osmolality of internal solutions because it maintained ionic strength while neither blocking nor permeating the channel (Villarroel *et al.*, 1995). Sucrose was used for external solutions because no ionic substitute for Na^+ could be found that did not either block or permeate the channel from the external solution at the necessary concentrations (Antonov *et al.*, 1998). The junction potentials between the pipette and bath solution were measured and found to be 5 mV for 140 Na^+_o / 125 Cs^+_i solution, -3 mV for 140 Na^+_o / 8 Cs^+_i solution, and -7 mV for 70 Na^+_o / 8 Cs^+_i solution. All holding potentials were corrected for junction potentials. Ultra pure salts were used when available. Tetrodotoxin was purchased from Alomone Labs (Jerusalem, Israel); all other chemicals were from Sigma Chemical Co. (St. Louis, USA).

3. Whole-cell Recordings and Analysis

Whole-cell patch-clamp recordings were performed at room temperature according to standard methods (Hamill *et al.*, 1981). Pipettes (resistance of 2-5 MΩ) were pulled from borosilicate thin-walled glass with filaments (Warner Instrument Corp.). Access resistance was compensated 60-80%. Currents were recorded with an Axopatch-1D or -200 amplifier, low-pass filtered at 10 kHz, digitized at 44 kHz with a Neuro-Corder and stored on video tape for later analysis. A continuous printout of the current trace on a chart recorder was used to monitor the quality of the recording and for later analysis. There was a wait of at least 5 minutes between breaking into the whole-cell configuration and the start of the recording, allowing for adequate exchange of the cytoplasm with the pipette solution. NMDA-activated currents in the absence and presence of Mg^{2+}_o were used to estimate Mg^{2+}_o IC_{50} from -105 mV to -15 mV at 10 mV increment. During each measurement, agonists were applied to obtain the steady state current in the absence of Mg^{2+}_o ($I_{control}$); one or several different $[Mg^{2+}]_o$s were applied in the presence of agonists to obtain current in the presence of Mg^{2+}_o (I_{Mg}); Mg^{2+}_o application was followed by a second measurement of $I_{control}$. Recordings were discarded if the amplitudes of the first and second steady state $I_{control}$ differed by more than 12%.

The steady state whole-cell current amplitudes were measured either directly from the chart recorder output or using pCLAMP 6 (Axon Instrument). Similar results were obtained with either approach. Normalized current in the presence of Mg^{2+}_o at each voltage was calculated as a ratio of I_{Mg} to $I_{control}$ (represented in %).

Millimolar Mg^{2+}_o can potentiate NMDA responses in a glycine- and voltage-independent manner (Paoletti *et al.*, 1995). To accurately measure inhibition of NMDA-activated current by Mg^{2+}_o, $I_{Mg} / I_{control}$ was corrected for Mg^{2+}_o potentiation. I tested the potentiation only when $[Mg^{2+}]_o$ was 1 mM or higher because initial experiments indicated that 300 μM Mg^{2+}_o (the next highest $[Mg^{2+}]_o$ to 1 mM) showed negligible potentiation. Potentiation by Mg^{2+}_o was quantified by measuring $I_{Mg} / I_{control}$ at +35 or +55 mV. Then, $I_{Mg} / I_{control}$ measured at negative voltages was corrected for Mg^{2+}_o potentiation using the equation:

$$\text{corrected fractional current (\%)} = 100\% * I_{Mg} / (I_{control} * A)$$

where A is the value of $I_{Mg} / I_{control}$ measured at + 35 or +55 mV in the same cell. Figure 4A shows a recording where potentiation by 1 mM Mg^{2+}_o was observed. At +55 mV, $I_{Mg} / I_{control}$ was 116%; at -25 mV, $I_{Mg} / I_{control}$ was 48% in the presence of 1 mM Mg^{2+}_o, with the corrected $I_{Mg} / I_{control}$ being 42%. Mg^{2+}_o potentiation interfered with accurate measurements of IC_{50}, as shown in Figure 4B where corrected and uncorrected IC_{50} values are compared from -15 mV to -45 mV.

The IC_{50} of Mg^{2+}_o at each voltage was obtained by fitting $I_{Mg} / I_{control}$ at various Mg^{2+}_o concentrations using the following equation:

$$I_{Mg} / I_{control} (\%) = 100\% / [1+ ([Mg^{2+}]_o / IC_{50})^{n_H}]$$

IC_{50} and n_H (Hill coefficient) were free parameters in fitting. Curve fitting was performed using Origin 3.0 or 4.0 (Microcal Software, Northampton, MA). All data points were used in fitting to

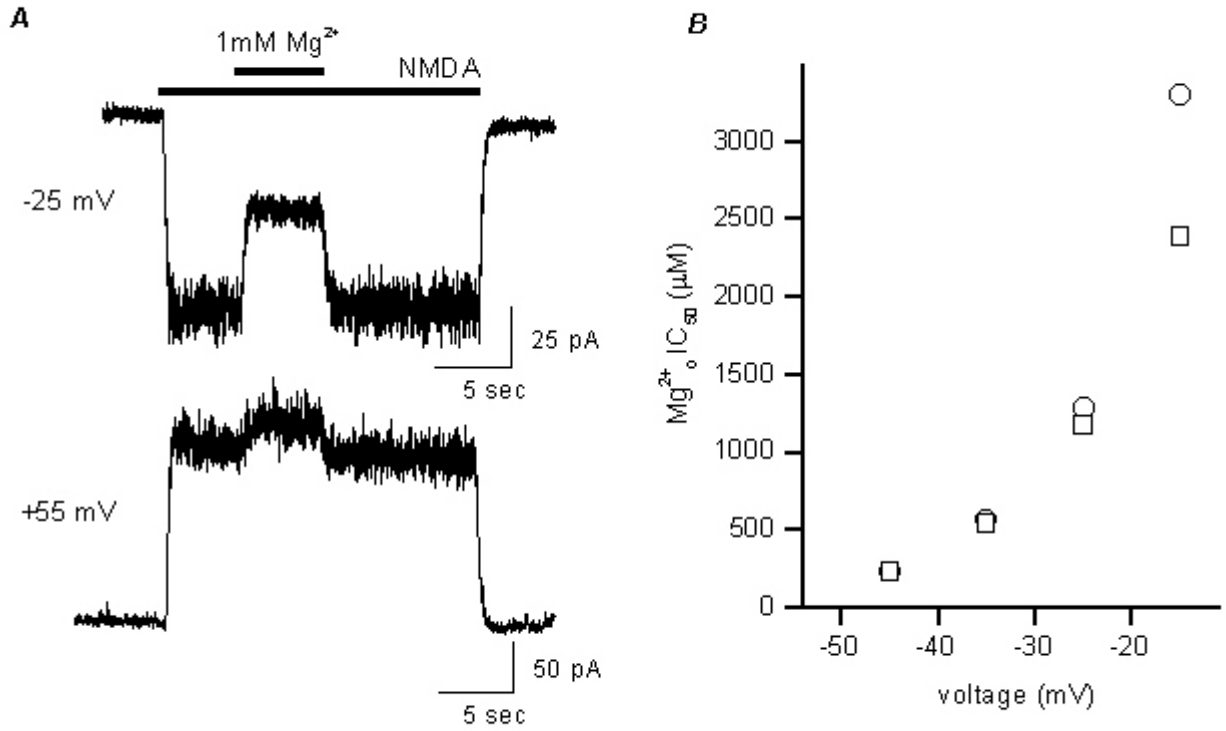

Figure 4 Correction for potentiation by Mg^{2+}_o. A. Example of a cell in which the NMDA-activated current was potentiated by Mg^{2+}_o. Bars above the traces indicate times of agonist and Mg^{2+}_o application. At -25 mV, the inward current was inhibited by 1 mM Mg^{2+}_o; at +55 mV, 1 mM Mg^{2+}_o potentiated the outward current. B. Calculated Mg^{2+}_o IC_{50} values before (○) and after (□) correction for Mg^{2+}_o potentiation are plotted here for comparison. At depolarized voltages, where Mg^{2+}_o IC_{50} reaches the millimolar range, Mg^{2+}_o potentiation leads to overestimation of IC_{50} values and exaggeration of the voltage dependence of Mg^{2+}_o inhibition.

obtain the IC_{50}, although the means were plotted for clarity in Figures 5B and 6B. Each IC_{50} value was based on $I_{Mg} / I_{control}$ measurements at 3-8 different $[Mg^{2+}]_o$s from 20 to 112 measurements. Data are expressed as mean ± s.e.m. Student's *t* test was used for statistical comparisons.

D. RESULTS

1. Effect of internal permeant ions on Mg^{2+}_o inhibition of NMDA-activated currents

I first investigated the effect of changing $[Cs^+]_i$ on Mg^{2+}_o inhibition of NMDA-activated whole-cell currents. I compared Mg^{2+}_o inhibition of NMDA-activated currents in two sets of solutions, 140 Na^+_o / 125 Cs^+_i and 140 Na^+_o / 8 Cs^+_i solutions. Figure 5A shows current traces recorded at -95 mV (left) and -55 mV (right) for 125 Cs^+_i (upper traces) and 8 Cs^+_i (lower traces). At -95 mV, the two traces (with 125 and 8 Cs^+_i) exhibited similar values of $I_{Mg} / I_{control}$ at each $[Mg^{2+}]_o$. At -55 mV, Mg^{2+}_o inhibited NMDA-activated currents more effectively with 8 Cs^+_i.

To further quantify Mg^{2+}_o inhibition of NMDA-activated current with the 125 and 8 Cs^+_i solutions, concentration-inhibition curves were constructed at each voltage tested. The IC_{50} of Mg^{2+}_o at each voltage was obtained by curve fitting of $I_{Mg} / I_{control}$ at various $[Mg^{2+}]_o$s as described in Methods. Examples of concentration-inhibition curves are shown in Figure 5B. These examples demonstrate a general trend: IC_{50} was lower with 8 Cs^+_i than 125 Cs^+_i at each voltage, suggesting that Cs^+_i reduces Mg^{2+}_o inhibition of the NMDA receptor-mediated currents. In addition, this effect of changing $[Cs^+]_i$ was voltage-dependent, since at -95 mV Cs^+_i had a much weaker effect on Mg^{2+}_o IC_{50} than at -45 mV.

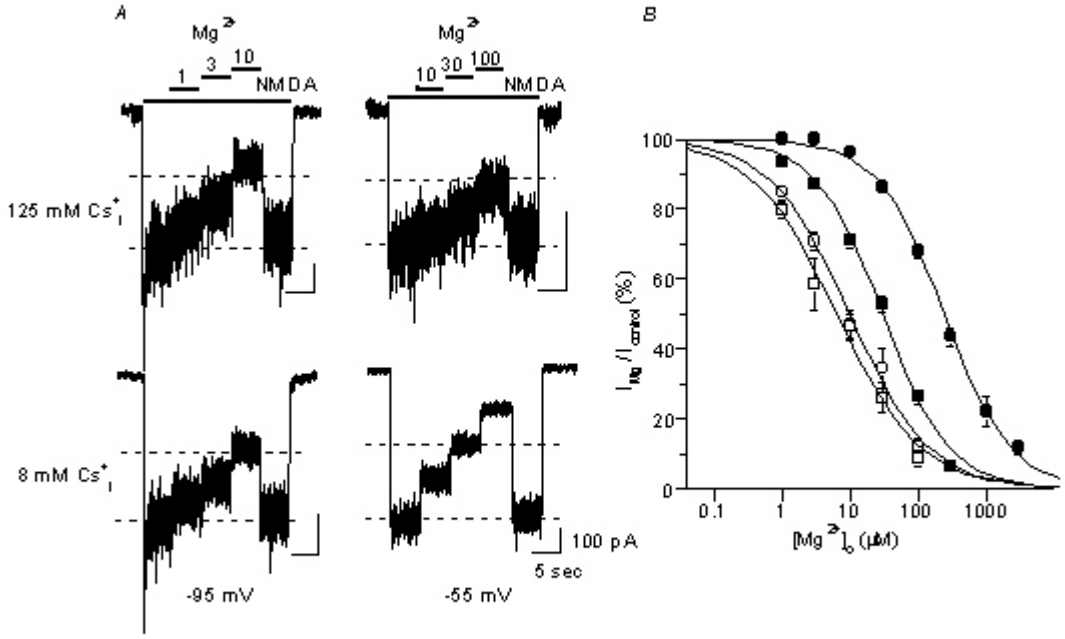

Figure 5 Effect of Cs^+_i on inhibition by Mg^{2+}_o of NMDA-activated current. A. Whole-cell NMDA-activated currents were inhibited by the indicated $[Mg^{2+}]_o$s (in μM). The $[Mg^{2+}]_o$s used were the same for upper and lower current traces. Bars above the traces show times of application of each solution. Each of the four current traces is from a different cell. At -95 mV (left), the values of $I_{Mg} / I_{control}$ were 80%, 69% and 38% for 125 Cs^+_i (upper) and 85%, 71% and 47% for 8 Cs^+_i (lower) in 1 μM, 3 μM and 10 μM Mg^{2+}_o, respectively. At -55 mV (right), the values of $I_{Mg} / I_{control}$ were 91%, 77% and 59% for 125 Cs^+_i (upper) and 73%, 50% and 27% for 8 Cs^+_i (lower) in 10 μM, 30 μM and 100 μM Mg^{2+}_o, respectively. The dash lines indicate 50% and 100% of $I_{control}$ to assist visual comparison among traces. B. Examples of concentration-inhibition curves are shown. The symbol, solution, voltage, and IC_{50} for each trace are: ○, 140 Na^+_o / 125 Cs^+_i, -95 mV, 9.79 μM; □, 140 Na^+_o / 8 Cs^+_i, -95 mV, 6.46 μM; ●, 140 Na^+_o / 125 Cs^+_i, -45 mV, 232 μM; ■, 140 Na^+_o / 8 Cs^+_i, -45 mV, 30.8 μM.

2. Effect of external permeant monovalent ion on Mg^{2+}_o inhibition of NMDA-activated currents

I next investigated how changing $[Na^+]_o$ affects Mg^{2+}_o inhibition of NMDA receptors. To minimize potential competition between Na^+_o and Cs^+_i (Antonov & Johnson, 1999), low $[Cs^+]_i$ was used in this series of experiments. Mg^{2+}_o inhibition of NMDA-activated currents was quantified with 70 Na^+_o / 8 Cs^+_i and with 140 Na^+_o / 8 Cs^+_i solutions. Figure 6A shows sample traces recorded at -95 mV (left) and -35 mV (right) with 140 Na^+_o (upper traces) and 70 Na^+_o (lower traces). At each voltage, increasing $[Na^+]_o$ reduced inhibition by Mg^{2+}_o. Voltage-dependence of the effect of changing $[Na^+]_o$ on Mg^{2+}_o inhibition of NMDA-activated currents was not apparent.

Concentration-inhibition curves were constructed at each voltage tested with the 140 and the 70 Na^+_o solutions. Examples of these curves are shown in Figure 6B. The IC_{50} of Mg^{2+}_o was lower when $[Na^+]_o$ was reduced, indicating that Mg^{2+}_o block becomes more pronounced in low $[Na^+]_o$. The shift of concentration-inhibition curves was comparable at both voltages.

3. Comparison of the effects of internal and external permeant monovalent ions on Mg^{2+}_o inhibition of NMDA-activated currents

Mg^{2+}_o IC_{50} values measured as described above are listed in Table 1 and plotted in Figure 7 for all three solution combinations. The data demonstrate that changing permeant monovalent ion concentrations has a profound effect on the Mg^{2+}_o IC_{50}. For example, at -15 mV, a decrease in permeant ion concentrations resulted in reduction of Mg^{2+}_o IC_{50} from 2390 μM (in 140 Na^+_o / 125

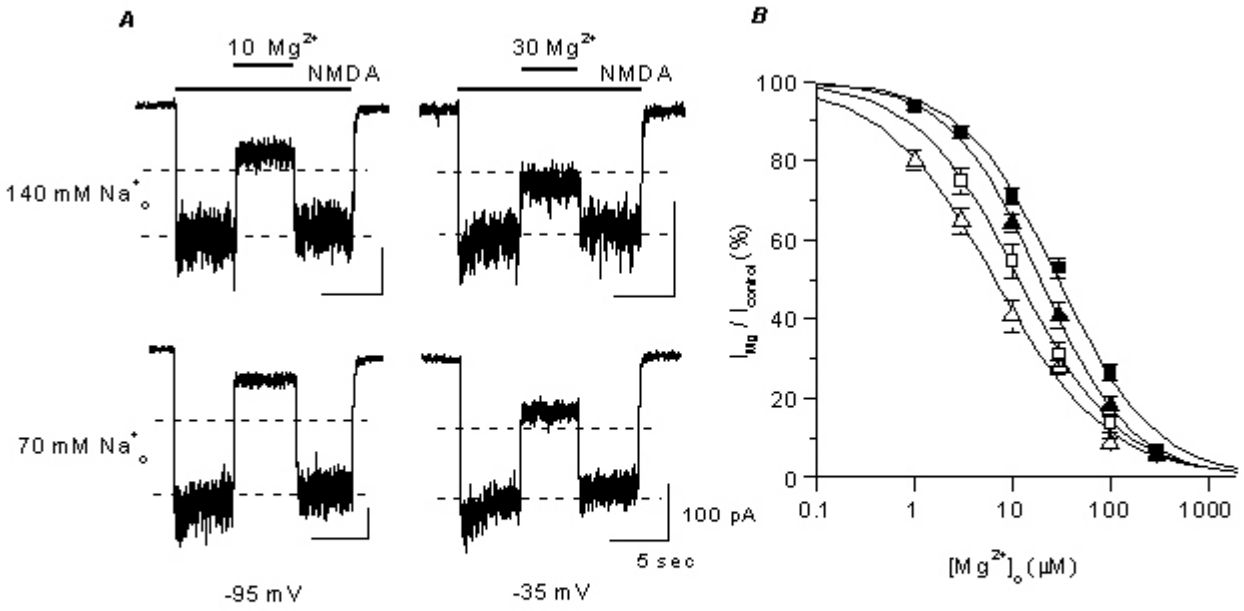

Figure 6 Effect of Na^+_o on inhibition of NMDA-activated currents. A. Whole-cell NMDA-activated currents were inhibited by the indicated $[Mg^{2+}]_o$s (in μM). The upper traces are from two different cells and the lower traces are from a third cell. At -95 mV (left), the values of $I_{Mg} / I_{control}$ were 36% for 140 Na^+_o (upper) and 19 % for 70 Na^+_o (lower). At -35 mV (right), the values of $I_{Mg} / I_{control}$ were 60% for 140 Na^+_o (upper) and 38% for 70 Na^+_o (lower). Dash lines, 50% and 100% of $I_{control}$. B. Examples of concentration-inhibition curves are shown. The symbol, solution, voltage, and IC_{50} for each trace are: △, 70 Na^+_o / 8 Cs^+_i, -85 mV, 3.72 μM; □, 140 Na^+_o / 8 Cs^+_i, -85 mV, 6.55 μM; ▲, 70 Na^+_o / 8 Cs^+_i, -45 mV, 19.4 μM; ■, 140 Na^+_o / 8 Cs^+_i, -45 mV, 30.8 μM.

Table 1 Measured Mg^{2+}_o IC_{50} values in rat cortical neurons

Voltage (mV)	Mg^{2+}_o IC_{50} (μM) 140 Na^+_o / 125 Cs^+_i	Mg^{2+}_o IC_{50} (μM) 140 Na^+_o / 8 Cs^+_i	Mg^{2+}_o IC_{50} (μM) 70 Na^+_o / 8 Cs^+_i
-15	2390	208	132
-25	1180	70.3	63.2
-35	541	56.3	35.8
-45	232	30.8	19.4
-55	116	24.9	12.3
-65	55.5	12.1	7.06
-75	41.5	12.1	5.89
-85	17.2	6.55	3.72
-95	9.79	6.46	2.98
-105	4.60	3.43	2.36

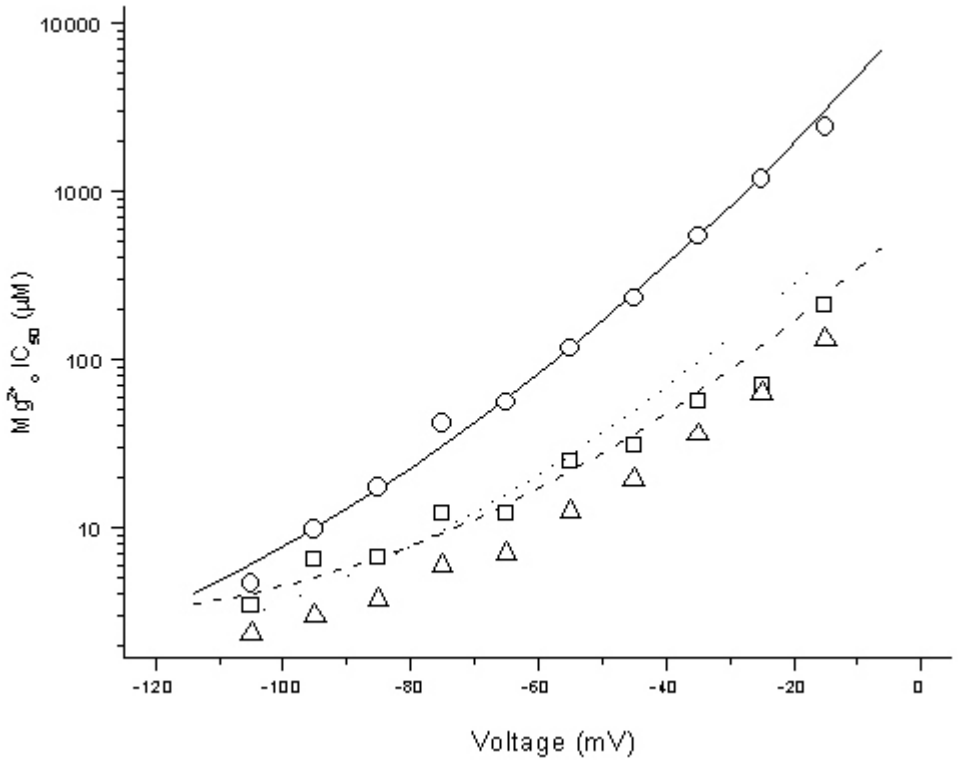

Figure 7 Voltage and permeant monovalent ion concentration dependence of Mg^{2+}_o IC_{50}. IC_{50} values (symbols) measured as shown in Figures 5 and 6, and quantitative predictions of Mg^{2+}_o K_D values (lines) made with the model of Johnson & Antonov (1999; see Figure 3), are plotted as follows: 140 Na^+_o / 125 Cs^+_i, ○ and — ; 140 Na^+_o / 8 Cs^+_i, □ and - - -; 70 Na^+_o / 8 Cs^+_i, ▵ and ·····. The following equations were used to calculate the predictions of the model (V_m is voltage; all predictions are made with no free parameters):

K_D (apparent dissociation constant for Mg^{2+}_o) = $k_{-,\,app}$ / $k_{+,\,app}$

$k_{-,\,app}$ (apparent Mg^{2+}_o unbinding rate) = $k_{-,\,o}$ / $[(1+ [Na^+]_o / K_{Na})]^2$ + $k_{-,\,i}$

$k_{+,\,app}$ (apparent Mg^{2+}_o binding rate) = k_+ /$[(1 + [Na^+]_o / K_{Na})*(1 + [Na^+]_o /K_{Na} + [Cs^+]_i /K_{Cs})]$

$k_{-,\,o}$ (intrinsic Mg^{2+}_o unbinding rate to external solution) = $1.10 \cdot 10^5$ s^{-1} $\exp(V_m/52.7$ mV)

$k_{-,\,i}$ (intrinsic Mg^{2+}_o unbinding rate to internal solution) = 61.8 s^{-1} $\exp(-V_m/50.0$ mV)

k_+ (intrinsic Mg^{2+}_o binding rate) = $1.10 \cdot 10^9$ $M^{-1}s^{-1}$ $\exp(-V_m/55.0$ mV)

K_{Na} ($[Na^+]$ at which each external site half occupied by Na^+) = 34.4 mM

K_{Cs} ($[Cs^+]$ at which external site half occupied by Cs^+) = 0.279 mM $\exp(-V_m/21.0$ mV)

Cs^+_i), to 208 μM (in 140 Na^+_o / 8 Cs^+_i), and further to 132 μM (in 70 Na^+_o / 8 Cs^+_i). The large variation in Mg^{2+}_o IC_{50} values in different solutions gradually diminished with hyperpolarization such that at -105 mV, the same decrease in permeant ion concentrations resulted in reduction of Mg^{2+}_o IC_{50} from 4.60 μM (in 140 Na^+_o / 125 Cs^+_i), to 3.43 μM (in 140 Na^+_o / 8 Cs^+_i), and further to 2.36 μM (in 70 Na^+_o / 8 Cs^+_i). Changing permeant ion concentrations not only affected the magnitude of Mg^{2+}_o inhibition, it also altered the voltage-dependence of Mg^{2+}_o inhibition, which was shallower in 140 Na^+_o /8 Cs^+_i and 70 Na^+_o / 8 Cs^+_i than in 140 Na^+_o / 125 Cs^+_i. The lines plotted in Figure 4 are quantitative prediction of the kinetic model of Antonov & Johnson (1999). In this model, binding of permeant monovalent ions to sites in the external vestibule of the channel of NMDA receptor prevents Mg^{2+}_o block and unblock the channel (see DISCUSSION).

The effects on Mg^{2+}_o IC_{50} of changing $[Cs^+]_i$ and of changing $[Na^+]_o$ exhibit a striking difference in voltage dependence. To illustrate this difference, the ratio of Mg^{2+}_o IC_{50} values measured in normal and low concentrations of each permeant monovalent ion is plotted as a function of voltage in Figure 8 (see legend). Decreasing either $[Cs^+]_i$ or $[Na^+]_o$ reduced the Mg^{2+}_o IC_{50}, since all the ratios are greater than 1. At -105 mV, the effects of changing $[Cs^+]_i$ and $[Na^+]_o$ were comparable, as the ratios were both 1.4. With depolarization, the effect of changing $[Cs^+]_i$ on Mg^{2+}_o IC_{50} became more pronounced. At -15 mV, decreasing $[Cs^+]_i$ caused a 11.5 fold reduction in Mg^{2+}_o IC_{50} value while decreasing $[Na^+]_o$ resulted in a 1.6 fold reduction in Mg^{2+}_o IC_{50} value.

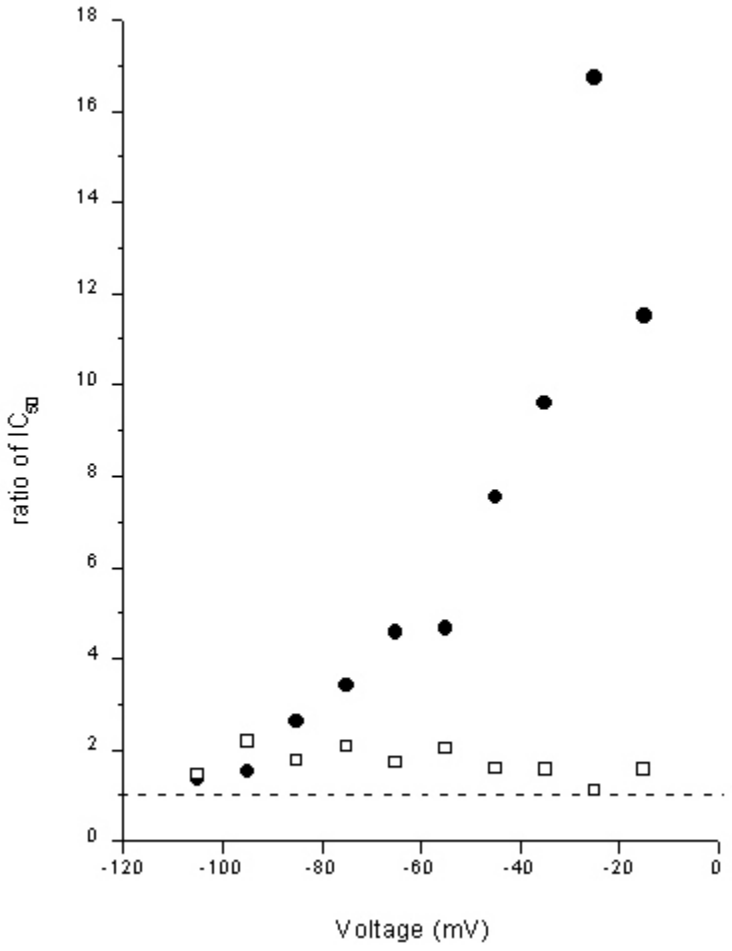

Figure 8 Comparison of voltage-dependence of permeant ion effects on Mg^{2+}_o IC_{50}. Ratios of IC_{50} values measured in normal and low permeant ion concentrations are plotted as a function of voltage. ●, IC_{50} (in 140 Na^+_o / 125 Cs^+_i) / IC_{50} (in 140 Na^+_o / 8 Cs^+_i); □, IC_{50} (in 140 Na^+_o / 8 Cs^+_i) / IC_{50} (in 70 Na^+_o / 8 Cs^+_i). The dash line marks a ratio of 1. The ratio for a change in $[Cs^+]_i$ increases with depolarization, while the ratio for a change in $[Na^+]_o$ shows no apparent voltage-dependence.

4. Effect of $[Ca^{2+}]_o$ on Mg^{2+}_o inhibition of NMDA-activated currents

In the whole-cell experiments described so far, external solutions contained a $[Ca^{2+}]_o$ of 1 mM when 140 mM Na^+_o was used and 0.5 mM when 70 mM Na^+_o was used. Because the channel of NMDA receptors is highly permeable to Ca^{2+}_o (MacDermott *et al.*, 1986; Mayer & Westbrook, 1987; Ascher & Nowak, 1988; Burnashev *et al.*, 1995), even these low $[Ca^{2+}]_o$s might have interfered with our measurements of the effects of Na^+_o and Cs^+_i on Mg^{2+}_o inhibition. Therefore, I next examined the effects on Mg^{2+}_o inhibition of variations of $[Ca^{2+}]_o$ around 1 mM.

Representative current traces recorded in several $[Ca^{2+}]_o$s are shown in Figure 9A. The left panel shows current traces recorded in the same cell in 140 Na^+_o / 125 Cs^+_i at -65 mV, in normal $[Ca^{2+}]_o$ (top, 1 mM Ca^{2+}_o) and in low $[Ca^{2+}]_o$ (bottom, 0.2 mM Ca^{2+}_o). The right panel shows an example recorded in a second cell in 70 Na^+_o / 8 Cs^+_i at -45 mV, in normal $[Ca^{2+}]_o$ (top, 0.5 mM Ca^{2+}_o) and in low $[Ca^{2+}]_o$ (bottom, 0.1 mM Ca^{2+}_o). Within each trace, the $[Ca^{2+}]_o$ was the same in each solution (external solutions without agonists or Mg^{2+}_o, with only agonists, and with agonists and Mg^{2+}_o). When $[Ca^{2+}]_o$ was decreased five-fold, the steady state $I_{control}$ became larger, as expected (Mayer & Westbrook, 1987; Ascher & Nowak, 1988), while inhibition by(Mg^{2+}o) reflected by I_{Mg} / $I_{control}$) was not noticeably affected.

Figure 9 Effect of low $[Ca^{2+}]_o$ on NMDA-activated current and its inhibition by $Mg^{2+}{}_o$. A. Sample traces are from recordings in the $[Ca^{2+}]_o$s indicated below each trace. The effect of $Ca^{2+}{}_o$ is shown for experiments done with 140 $Na^+{}_o$ /125$Cs^+{}_i$ at -65 mV (left two traces) and with 70 $Na^+{}_o$ /8 $Cs^+{}_i$ at -45 (right two traces). Top traces are in normal $[Ca^{2+}]_o$s and bottom traces are in 5-fold reduced $[Ca^{2+}]_o$s. $[Mg^{2+}]_o$ was in μM. To assist visual data comparison, dashed lines are plotted at the value of I_{Mg} / $I_{control}$ measured in normal $[Ca^{2+}]_o$: 34.5 % in 140 $Na^+{}_o$ / 125 $Cs^+{}_i$ (left, top) and 36.8% in 70 $Na^+{}_o$ / 8 $Cs^+{}_i$ (right, top) in . The measured values of I_{Mg} / $I_{control}$ in low $[Ca^{2+}]_o$s are 35.1% in 140 $Na^+{}_o$ / 125 $Cs^+{}_i$ (left, bottom) and 36.6% in 70 $Na^+{}_o$ / 8 $Cs^+{}_i$ (right, bottom). B. $I_{control}$ (○) and I_{Mg} / $I_{control}$ (□) were measured in various $[Ca^{2+}]_o$s; all data were normalized to values in normal $[Ca^{2+}]_o$ from the same cell (top, 1 mM $Ca^{2+}{}_o$; bottom, 0.5 mM $Ca^{2+}{}_o$) and were plotted as a function of $[Ca^{2+}]_o$ for 140 $Na^+{}_o$ /125$Cs^+{}_i$ (top) and for 70 $Na^+{}_o$ /8 $Cs^+{}_i$ (bottom). $I_{control}$ depended on $[Ca^{2+}]_o$, but I_{Mg} / $I_{control}$ was not affected by lowering $[Ca^{2+}]_o$, except for a small decrease in inhibition by $Mg^{2+}{}_o$ at 2 mM $Ca^{2+}{}_o$. Plotted data are pooled from recordings performed at -45 mV and -65 mV in 140 $Na^+{}_o$/125 $Cs^+{}_i$ and at -45, -65 and -95 mV in 70 $Na^+{}_o$/8 $Cs^+{}_i$. At least three cells were used under each $Ca^{2+}{}_o$, $Cs^+{}_i$, $Na^+{}_o$ and voltage condition.

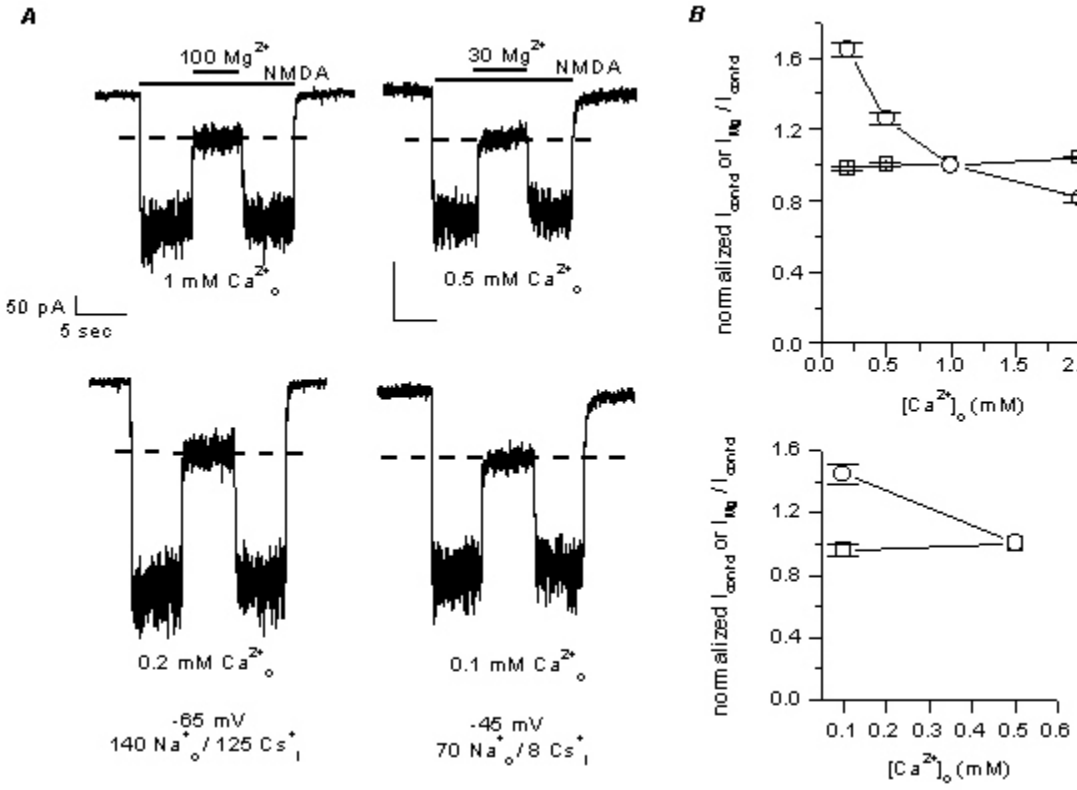
A
100 Mg2+
NMDA
30 Mg2+
NMDA
1 mM Ca2+o
0.5 mM Ca2+o
50 pA
5 sec
0.2 mM Ca2+o
0.1 mM Ca2+o
-65 mV
140 Na+o / 125 Cs+i
-45 mV
70 Na+o / 8 Cs+i
B
normalized Icontrol or INg / Icontrol
[Ca2+]o (mM)
normalized Icontrol or INg / Icontrol
[Ca2+]o (mM)

$I_{control}$ and I_{Mg} / $I_{control}$ measured at various $[Ca^{2+}]_o$s were normalized to values measured in normal $[Ca^{2+}]_o$ within the same cell. The mean normalized values are plotted as a function of $[Ca^{2+}]_o$ in Figure 9B. The majority of the experiments were performed at -45 mV or -65 mV; for experiments in 70 Na^+_o /8 Cs^+_i, recordings were also done at -95 mV to rule out a voltage-dependent effect of changing $[Ca^{2+}]_o$ on I_{Mg} / $I_{control}$ measurements. None of the normalized I_{Mg} / $I_{control}$ at any voltage was statistically different from 1 at $[Ca^{2+}]_o$s from 0.1 to1 mM (the p values range from 0.12 to 0.96). Normalized $I_{control}$ values, on the other hand, increased with reduction of $[Ca^{2+}]_o$. Therefore, under the conditions used here, Ca^{2+}_o did not competitively influence the effects of permeant monovalent ions on Mg^{2+}_o inhibition.

I noticed a slight increase in I_{Mg} / $I_{control}$ in 2 mM Ca^{2+}_o compared to normal $[Ca^{2+}]_o$ (ratio of 1.04 ± 0.01, $p < 0.005$). This observation, and the previous work of Mayer & Westbrook (1987) on relief of Mg^{2+}_o inhibition by Ca^{2+}_o, led us to examine the effects of higher $[Ca^{2+}]_o$. I tested whether 5 or 20 mM Ca^{2+}_o affect the Mg^{2+}_o IC_{50} of NMDA-activated currents at -95 mV. I used this hyperpolarized voltage because, if the effect of Ca^{2+}_o is voltage dependent, its effects should be largest at more negative voltages (Mayer & Westbrook, 1987). 70 mM Na^+_o and 8 mM Cs^+_i were used to minimize potential competition from other permeant ions. Figure 10A shows current traces recorded in 5 mM Ca^{2+}_o (left) and 20 mM Ca^{2+}_o (right). Mg^{2+}_o inhibited NMDA-activated currents more effectively in 5 mM than in 20 mM Ca^{2+}_o.

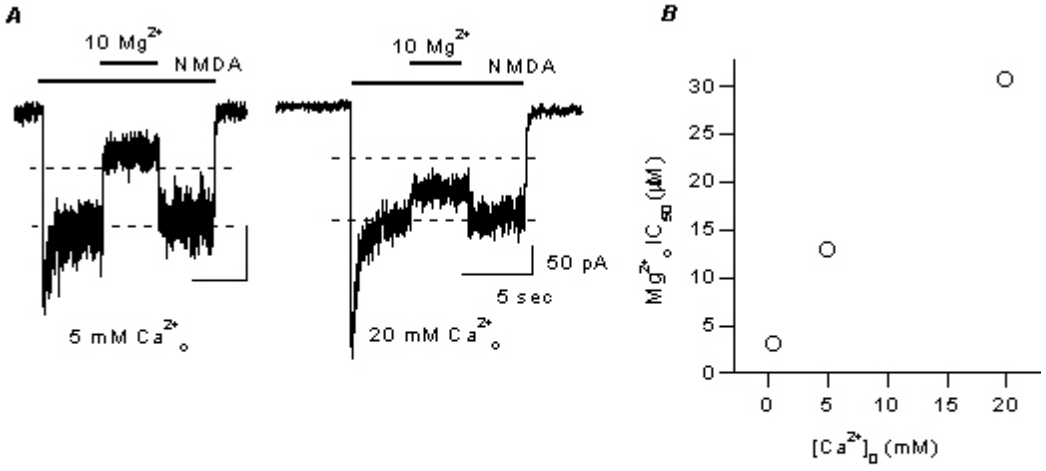

Figure 10 Effect of high $[Ca^{2+}]_o$ on inhibition by Mg^{2+}_o of NMDA-activated current. A. Whole-cell NMDA-activated currents were inhibited by the indicated $[Mg^{2+}]_o$ (in μM) at -95 mV. The traces are from different cells. The values of I_{Mg} / $I_{control}$ were 32% in 5 mM Ca^{2+}_o (left) and 71 % for 20 mM Ca^{2+}_o (right). Dash lines, 50% and 100% of $I_{control}$. B. Whole-cell measurements of Mg^{2+}_o IC_{50} are plotted for three $[Ca^{2+}]_o$s (0.5 mM, 5 mM and 20 mM Ca^{2+}_o). Data for 0.5 mM are replotted from Figure 4. The Mg^{2+}_o IC_{50} values (in μM) are: 2.98, 12.8 and 30.7 in 0.5 mM, 5 mM and 20 mM Ca^{2+}_o.

Figure 10B shows Mg^{2+}_o IC_{50} measured in 0.5, 5 and 20 mM Ca^{2+}_o. Increasing $[Ca^{2+}]_o$ greatly weakened Mg^{2+}_o inhibition. Changing $[Ca^{2+}]_o$ from 0.5 to 5 mM increased the Mg^{2+}_o IC_{50} by 4.3-fold and further increasing $[Ca^{2+}]_o$ to 20 mM increase Mg^{2+}_o IC_{50} by an additional factor of 2.4.

Detailed characterization of the effect of Ca^{2+}_o is shown in Figure 11. Mg^{2+}_o IC_{50} values are measured and plotted again voltage (also see Table 2). Data in 0.5 mM, 5 mM, and 20 mM Ca^{2+}o are shown. Changing $[Ca^{2+}]_o$ from 0.5 to 20 mM had a strong effect on Mg^{2+}_o IC_{50}. In general, increasing $[Ca^{2+}]_o$ reduced Mg^{2+}_o inhibition; the effect of Ca^{2+}o was highly voltage-dependent. At -15mV, changing $[Ca^{2+}]_o$ from 0.5 to 5 mM increased Mg^{2+}_o IC_{50} by 2.5 fold and further increasing $[Ca^{2+}]_o$ had no additional effect. However, at -105 mV, changing $[Ca^{2+}]_o$ from 0.5 to 5 mM increased Mg^{2+}_o IC_{50} by five-fold and further increasing $[Ca^{2+}]_o$ to 20 mM increased Mg^{2+}_o IC_{50} by an additional factor of three. At -95 mV, further hyperpolarization seemed to flatten the voltage-dependence of Mg^{2+}_o inhibition. This effect was more pronounced at higher $[Ca^{2+}]_o$. This may reflect increased Mg^{2+}_o permeation through the channel of the NMDA receptor (Mayer & Westbrook, 1987).

E. DISCUSSION

In this study I investigated the effects of the permeant ions Na^+_o, Cs^+_i, and Ca^{2+}_o on inhibition by Mg^{2+}_o of whole-cell NMDA-activated currents. The main findings are: (1) Mg^{2+}_o inhibition of NMDA-activated currents can be profoundly modulated by changing permeant ion concentrations;

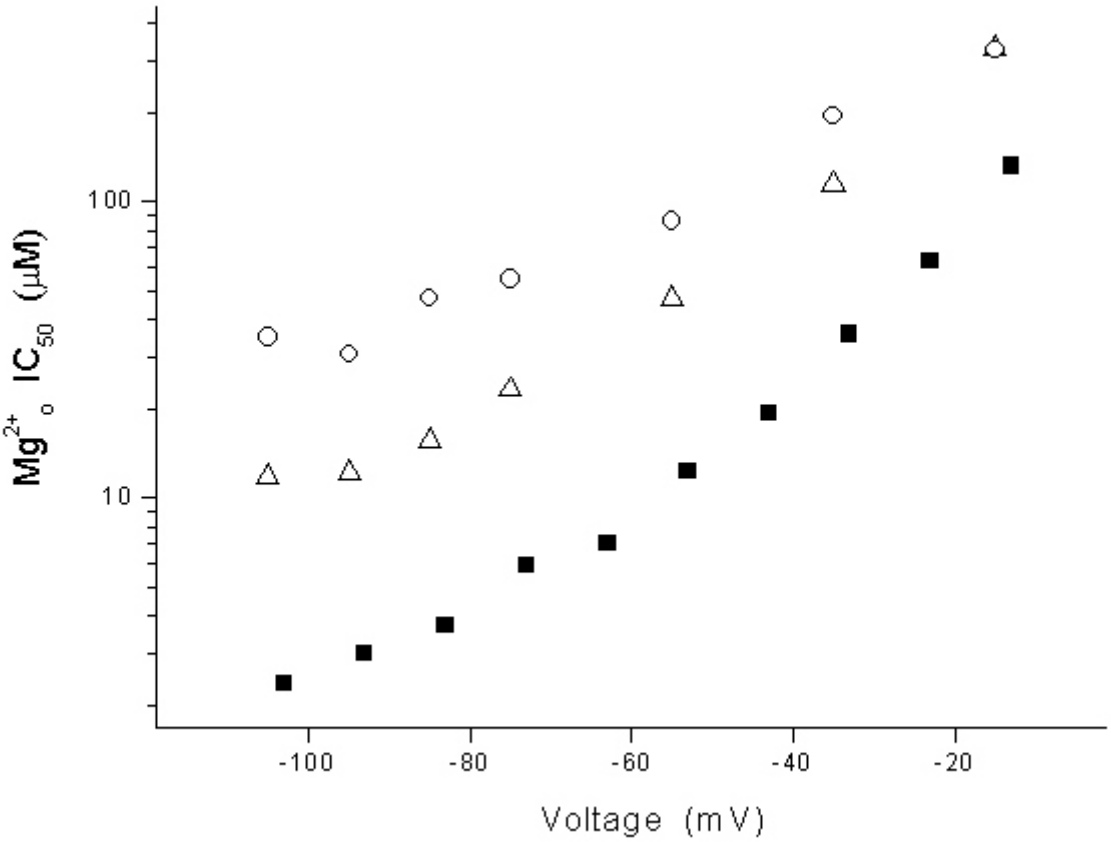

Figure 11 Effect of increasing $[Ca^{2+}]_o$ on Mg^{2+}_o inhibition of NMDA activated currents Whole-cell measurements of voltage-dependence of Mg^{2+}_o IC_{50} are plotted for three $[Ca^{2+}]_o$s: ■, 0.5 mM,; ▵, 5 mM; ○, 20 mM. Increasing $[Ca^{2+}]_o$s reduced Mg^{2+}_o inhibition, and the effect increased with hyperpolarization..

Table 2 Measured Mg^{2+}_o IC_{50} values in different $[Ca^{+}]_o$s

voltage (mV)	in 0.5 mM Ca^{2+}_o (μM)	in 5 mM Ca^{2+}_o (μM)	in 20 mM Ca^{2+}_o (μM)
-15	132	330	326
-25	63.2	--	--
-35	35.8	115	194
-45	19.4	--	--
-55	12.3	47.6	86.2
-65	7.06	--	--
-75	5.89	23.2	54.8
-85	3.72	15.7	47.2
-95	2.98	12.8	30.7
-105	2.36	11.8	34.8

(2) lowering $[Cs^+]_i$ decreased the Mg^{2+}_o IC_{50} in a voltage-dependent manner. At hyperpolarized voltages, the Cs^+_i effect was weak; at depolarized voltages, the Cs^+_i effect was powerful; (3) decreasing $[Na^+]_o$ weakly decreased the Mg^{2+}_o IC_{50} in a voltage-independent manner; (4) In contrast to the permeant monovalent ions, Ca^{2+}_o at concentrations up to those normally present in external solutions (0.5 or 1 mM) had no effect on Mg^{2+}_o inhibition of NMDA-activated currents, while higher $[Ca^{2+}]_o$ appeared to greatly weaken Mg^{2+}_o inhibition.

1. Model of permeant monovalent ion effects on Mg^{2+}_o IC_{50}

Mechanistic interpretation of these results can be aided by a previous model based on single-channel study of the effects of permeant monovalent ions on Mg^{2+}_o blocking kinetics (Antonov & Johnson, 1999). The characteristics of this model (schematized in Figure 3) are: (1) There are two binding sites for permeant monovalent ions in the external vestibule of the NMDA receptor. Na^+_o can bind to one or both of these sites, while Cs^+_i can occupy only one of the sites. (2) When either site is occupied by Na^+_o or Cs^+_i, Mg^{2+}_o cannot enter to block the pore. (3) When Mg^{2+}_o is blocking the pore, Na^+_o can occupy one or both of the external permeant monovalent ion sites and prevent Mg^{2+}_o from exiting to the external solution until Na^+_o dissociates from the binding site. This aspect of the model is reminiscent of the ability of external K^+ to slow Ba^{2+} unblock by binding to the external lock-in site of Ca^{2+}-activated K^+ (Neyton & Miller, 1988b; Jiang & MacKinnon, 2000). (4) Mg^{2+}_o can permeate the channel at a low, voltage-dependent rate. An alternative kinetic model (Zhu & Auerbach, 2001a, b) of permeant monovalent ion effects on Mg^{2+}_o block will be discussed below.

This model described provides an explanation for the high voltage dependence of Mg^{2+}_o inhibition of NMDA receptors. Cs^+_i reduces Mg^{2+}_o inhibition in a voltage-dependent manner by binding at the external permeant monovalent ion site. Since Cs^+_i must cross the entire membrane field to reach its binding site, Cs^+_i binding and its subsequent effect on Mg^{2+}_o inhibition is stronger at depolarized voltages. This voltage-dependent effect of Cs^+_i on Mg^{2+}_o inhibition exaggerates the voltage-dependence of Mg^{2+}_o inhibition due to the blocking site's location in the membrane field (Woodhull, 1973).

2. Effect of Cs^+_i

To determine whether the model shown in Figure 3 can explain the powerful effects of Cs^+_i on Mg^{2+}_o IC_{50}, I compared predicted values of Mg^{2+}_o K_D derived from the model to the IC_{50} values measured here. K_D values were predicted from the model as described in the legend to Figure 7. Predictions were made with all parameters fixed at the values determined from previous single-channel experiments (Antonov & Johnson, 1999). Figure 7 compares the results of whole-cell experiments (symbols) to the model predictions (lines). The agreement was excellent for both 140 Na^+_o / 125 Cs^+_i and 140 Na^+_o / 8 Cs^+_i, supporting the accuracy of the model's description of the effect of Cs^+_i on Mg^{2+}_o inhibition. This agreement between data and model predictions also suggests that the model, which was derived from measurements done in a low $[Mg^{2+}]_o$ range (1 - 100 μM), is adequate to explain the blocking phenomenon at a more physiologically relevant (millimolar) $[Mg^{2+}]_o$ range.

3. Effect of Na^+_o

The effect of changing $[Na^+]_o$ on Mg^{2+}_o inhibition measured in whole-cell experiments and predicted by the model also are compared in Figure 7. Three observations can be made. First, as the model predicts, changing $[Na^+]_o$ did affect Mg^{2+}_o inhibition of NMDA-activated currents. Second, the effect of changing $[Na^+]_o$ was small, which conforms with the model's prediction that the effect of Na^+_o on Mg^{2+}_o unbinding rate (Figure 3, states 7 and 8) should partially compensate for the effect on Mg^{2+}_o binding rate. Third, there were some differences between the model predictions and the whole-cell data. The model predicts that the effect of changing $[Na^+]_o$ on Mg^{2+}_o IC_{50} should be weakly voltage-dependent, but there is no evidence of voltage-dependence based on the whole-cell data. Despite this relatively small discrepancy between the model predictions and the measured Mg^{2+}_o IC_{50} with 70 Na^+_o / 8 Cs^+_i, the whole-cell data are consistent with the basic aspects of the model.

The weak voltage-dependence of the Na^+_o effect predicted by the model stems from Na^+_o and Cs^+_i competition for one of the external permeant monovalent ion sites. At depolarized voltages, the principal effect of increasing $[Na^+]_o$ is to decrease the Mg^{2+}_o unblocking rate to the outside. This is because the probability of Cs^+_i binding is high and hence increasing $[Na^+]_o$ has very little additional effect on the Mg^{2+}_o blocking rate. At hyperpolarized voltages, since Cs^+_i occupies the binding site only infrequently, addition of Na^+_o reduces substantially the blocking as well as the unblocking rates of Mg^{2+}_o.

The reason for the small discrepancy is unclear. One possibility is that under low $[Na^+]_o$ conditions, the channel of NMDA receptor adopts a modified conformation that Mg^{2+}_o blocks with slightly different kinetics. Similarly, a $[K^+]$-dependent change in the conformation of the outer vestibule of K^+ channels that strongly affects block by TEA has been reported (Immke *et al.*, 1999). Consistent with this hypothesis, model predictions describe better the 70 Na^+_o / 8 Cs^+_i data when I use the relevant parameter values reported by Zhu & Auerbach (2001b). Both 140 Na^+_o data sets, however, are better described with the parameter values shown in the Figure 7 legend.

Another possible explanation for the discrepancy with 70 Na^+_o / 8 Cs^+_i is that lowering $[Na^+]_o$ results in a change in the Mg^{2+}_o permeation rate. A previous study suggested that in 0 $[Na^+]_o$, Mg^{2+}_o permeation was greatly accelerated (Stout *et al.*, 1996). Increased Mg^{2+}_o permeation could occur if, in low $[Na^+]_o$, a second Mg^{2+}_o can enter the channel vestibule, destabilize the blocking Mg^{2+}_o, and increase its rate of unblock to the internal solution.

I also attempted to explain our 70 Na^+_o / 8 Cs^+_i data by incorporating into our model an internal permeant ion binding site, similar to the model of Zhu & Auerbach (2001a and b). Their model is based on single-channel studies of the effects of $[Na^+]$ and $[K^+]$ on the kinetics of Mg^{2+}_o block in recombinant NMDA receptors. Although there are many similarities between their model and the model summarized in Figure 3, a prominent difference is that Zhu & Auerbach (2001a) proposed an additional internal ion binding site located 16% into the voltage field from the internal side of the membrane. Occupancy of this site by K^+ was found to increase the unblocking rate of Mg^{2+}_o.

I did not expect that addition of an internal binding site to the model used here would yield better fits to the 70 Na^+_o / 8 Cs^+_i data because: (1) relatively little occupancy of the internal site would be expected at this low $[Cs^+]_i$; (2) the internal site may selectively bind K^+, since Na^+ does not measurably interact with the site (Zhu & Auerbach, 2001a, b). The observation that changes in $[Cs^+]_i$ do not affect Mg^{2+}_o unbinding rate (Antonov & Johnson, 1999) suggests that Cs^+ also may have a low affinity for the site. To test the model with an internal permeant monovalent ion site, I fixed the electrical position of the internal site, and the Mg^{2+}_o unbinding rate with site occupied, to the values specified in Zhu & Auerbach (2001a and b). The Cs^+ affinity for the internal site was left as a free parameter. When the other parameters were fixed at the values reported in Antonov and Johnson (1999; see Figure 7 legend), no significant improvement in fits was observed, despite the addition of a free parameter. When the other parameters were fixed at the values reported in Zhu and Auerbach (2001a and b), an improvement in the fit of the 70 Na^+_o / 8 Cs^+_i data was observed. This improvement, however, also was observed when the Zhu and Auerbach (2001 and b) parameters were used without addition of an internal site, as described above. The fit to the 140 Na^+_o / 8 Cs^+_i data set remained much worse than that shown in Figure 7, despite addition of a free parameter. Thus, the data in Figure 7 do not provide clear support for an internal binding site for Cs^+_i.

It is possible that Cs^+ can bind to an internal site, but does not measurably affect Mg^{2+}_o block or unblock while bound. Previous work with organic channel blockers suggested the presence of an internal Cs^+ binding site located outside the voltage field (Antonov *et al.*, 1998). It is not possible at present to determine whether this internal Cs^+ site is distinct from the internal K^+ site reported by Zhu & Auerbach (2001a).

4. Effect of $[Ca^{2+}]_o$

The powerful influence of Na^+_o and Cs^+_i on Mg^{2+}_o inhibition of NMDA-activated currents suggests the possibility that Ca^{2+}_o may compete with permeant monovalent cations for their external sites, and thereby, affect Mg^{2+}_o inhibition as well. If, under the conditions of these experiments, there was significant binding of Ca^{2+}_o to the external permeant monovalent ion sites, then lowering Ca^{2+}_o should have affected the Mg^{2+}_o IC_{50}. However, I observed that lowering $[Ca^{2+}]_o$ from 1 mM or 0.5 mM to 0.1 mM had no effect on $I_{Mg} / I_{control}$. This observation, in combination with previous single-channel observations (Antonov *et al.*, 1998; Antonov & Johnson, 1999), suggests that Ca^{2+}_o does not compete with Na^+_o or Cs^+_i for their external binding sites under normal (low $[Ca^{2+}]_o$) conditions. NMDA-activated current in 0 Mg^{2+}_o, in contrast, did increase as $[Ca^{2+}]_o$ was reduced. This result is consistent with previous observations (Mayer & Westbrook, 1987; Ascher & Nowak, 1988), and indicates that the site at which Ca^{2+}_o binds with highest affinity during channel permeation is distinct from the external permeant monovalent ion sites. Multiple sites have been identified that are involved in Ca^{2+}_o binding in the channel of NMDA receptors (Ascher & Nowak, 1988; Premkumar & Auerbach, 1996; Sharma & Stevens, 1996a; Wollmuth & Sakmann, 1998; Watanabe *et al.*, 2002).

At high $[Ca^{2+}]_o$, Mg^{2+}_o inhibition was strongly reduced in a voltage- and $[Ca^{2+}]_o$-dependent manner. A concern that may arise with high $[Ca^{2+}]_o$ experiments is that Ca^{2+}_o has multiple effects on the behavior of the NMDA receptor, complicating the interpretations of results. Ca^{2+}_o enhances the affinity of NMDA receptor for the co-agonist glycine (Wang & MacDonald, 1995). This was controlled for by using a saturating concentration of glycine. Ca^{2+}_o-mediates calcium-dependent

inactivation of NMDA receptors (Krupp *et al.*, 1996). It is possible that Mg^{2+}_o affinity changes after calcium-dependent inactivation. However, this is unlikely to explain the results since Krupp *et al.* (1996) had shown that 2 mM Ca^{2+}_o induces maximal calcium-dependent inactivation, while, here when $[Ca^{2+}]_o$ was increased from 5 to 20 mM, an increasing effect of Ca^{2+}_o on Mg^{2+}_o affinity was still observed. Ca^{2+}_o also can decrease Mg^{2+}_o block by activating the protein kinase C pathway (Chen & Huang, 1992). This is unlikely to explain the results here since: (a) recording started at least 5 minutes after breaking into the cell; (b) no ATP was included in the pipette solution; and (c) the effect of PKC on Mg^{2+}_o affinity is voltage-independent. Ca^{2+}_o may also influence the local surface potential and decrease $[Mg^{2+}]_o$ at the entrance of the channel of the NMDA receptor. However, it has been shown (Zarei & Dani, 1994) that increases in the concentration of cations has little effect on surface potential unless the ionic strength of the solution is very low, which was not the case under our experimental conditions.

It is possible that high $[Ca^{2+}]_o$ increases Mg^{2+}_o IC_{50} by binding of Ca^{2+}_o at a previously described binding site in the external portion of the NMDA receptor (Premkumar & Auerbach, 1996; Sharma & Stevens, 1996a; Wollmuth & Sakmann, 1998; Watanabe *et al.*, 2002). This external binding site might overlap with the external permeant monovalent ion sites. High Ca^{2+}_o may increase Mg^{2+}_o IC_{50} by slowing the apparent Mg^{2+}_o binding rate (similar to Na^{+}_o), by binding while Mg^{2+}_o blocks and increasing its permeation rate (as proposed by Mayer & Westbrook, 1987), or by a combination of these effects.

5. Mg^{2+}_o interaction with channel gating

The similarity between Mg^{2+}_o IC_{50} measured in whole-cell experiments and K_D (the ratio of Mg^{2+}_o unblocking and blocking rates) predicted from single-channel experiments also has implications for Mg^{2+}_o interaction with channel gating. IC_{50} and K_D values should differ if channel gating or agonist binding equilibria are modified when Mg^{2+}_o occupies the channel (Johnson & Qian, 2002). For example, if Mg^{2+}_o binding prevents the channel from closing, channel burst duration would be increased by Mg^{2+}_o. As a result, reduction of current flow by Mg^{2+}_o channel block would be partially offset by the lengthening of channel bursts and the macroscopic IC_{50} would be larger than K_D measured from single-channel experiments. The agreement between IC_{50} and K_D values is consistent with the idea that Mg^{2+}_o binding has no effect on the gating of NMDA receptors nor on agonist unbinding. This conclusion also was reached by Sobolevsky & Yelshansky (2000), who proposed that Mg^{2+}_o block does not affect channel desensitization, channel closure or agonist dissociation. They further suggested that Mg^{2+}_o can be trapped in the closed channel. This idea was strongly supported by Amar *et al.* (2001) using an NMDA receptor with a high affinity Zn^{2+} blocking site generated by mutating the *N*-site amino acid to cysteine. The slow unbinding of Zn^{2+} from the mutated receptor permitted a clear demonstration that Zn^{2+} is trapped by closing of the channel. The observation that Mg^{2+}_o blocks without perturbing gating suggests that the selectivity filter, which is very close to the Mg^{2+}_o blocking site (Burnashev *et al.*, 1992; Mori *et al.*, 1992; Wollmuth *et al.*, 1996; Wollmuth *et al.*, 1998a), is relatively insulated from conformational changes associated with gating transitions. The observation that many channel blockers, probably including Mg^{2+}_o, can be trapped points to conformational changes associated with gating in a regions well external to the *N*-site.

6. Physiological or pathological implications

The profound effects of permeant ions on Mg^{2+}_o inhibition may play a role in modulating cellular excitability under physiological or pathological conditions. Ion concentrations fluctuate significantly as a result of neuronal activity. Rose & Konnerth (2001), using two-photon Na^+ imaging, observed an increase of $[Na^+]$ in dendritic spines to 100 mM in response to tetanic stimulation. More extreme fluctuations may result from disease states. Kager *et al.* (2000), for example, predicted an increase of over 50% in the total internal ion concentration during modeled seizure discharge. Based on the results presented here, changes of this magnitude in total internal permeant cation concentration would lead to a substantial decrease in inhibition by Mg^{2+}_o. The result could be a great exacerbation of neuronal damage.

III. CHARACTERIZATION OF Mg^{2+}_o BLOCK IN NR1/2D RECEPTORS

A. SUMMARY

NMDA receptors play vital roles in vertebrate CNS physiology. Understanding the fundamental biophysical processes by which these receptors function is critical to decipher the roles they play. I investigated the effects of Mg^{2+}_o on both whole-cell and single-channel currents recorded from NR1/2D receptors expressed in mammalian heterologous systems.

The main results of this study were: (1) Whole-cell NR1/2D receptor-mediated currents were inhibited by Mg^{2+}_o in a voltage-dependent manner; Mg^{2+}_o inhibition was at least 4-fold weaker in NR1/2D receptor than in NR1/2A receptors at all voltage tested. (2) The duration of NR1/2D receptor single-channel openings is reduced in the presence of Mg^{2+}_o, reflecting block by Mg^{2+}_o. Mg^{2+}_o induced an additional component in the closed-duration distribution, corresponding to the Mg^{2+}_o blocking events. (3) Mg^{2+}_o apparent blocking rate constants ($k_{+,app}$) of NR1/2D receptors are not very different from values of cortical NMDA receptors. Mg^{2+}_o apparent unblocking rate ($k_{-,app}$) of NR1/2D receptors is much faster than cortical receptors. The voltage-dependence of Mg^{2+}_o $k_{+,app}$ is similar between NR1/2D and cortical receptors. The voltage-dependence of $k_{-,app}$ is comparable at voltages positive to -80 mV in the two receptor subtypes; at voltage negative than -80 mV, $k_{-,app}$ appears to increase with hyperpolarization in NR1/2D receptors while $k_{-,app}$ in cortical receptors

appears to be weakly voltage-dependent within the voltage range tested. (4)These results suggest that Mg^{2+}_o inhibits NR1/2D receptor-mediated current less effectively than cortical receptors chiefly because Mg^{2+}_o unbinds much more rapidly from NR1/2D receptors.

B. INTRODUCTION

NMDA receptors, which are members of the ionotropic glutamate receptor family, have been linked to many processes critical for the formation and function of the vertebrate CNS. During development, NMDA receptors are involved in the establishment of neuronal connections (Bear *et al.*, 1990; Cline *et al.*, 1990; Iwasato *et al.*, 2000; Ramoa *et al.*, 2001). In mature vertebrates, NMDA receptors are keys players in long term modification of synaptic strength, which probably underlies some types of learning and memory (Bliss & Collingridge, 1993; Tang *et al.*, 1999). NMDA receptors are also implicated in a number of diseases, including epilepsy and neurodegerative disorders (Chapman, 2000; Cull-Candy *et al.*, 2001; Gardoni *et al.*, 2003; Meldrum, 1992). Therefore, knowledge of the properties of NMDA receptors and their regulation are pertinent to our understanding of CNS functions.

A functional NMDA receptor contains subunits of both NR1 and NR2 subtypes. NR2 has four gene products, NR2A-NR2D. The NR2 subunits follow distinct temporal and regional expression patterns (Akazawa *et al.*, 1994; Monyer *et al.*, 1994). The subcellular distribution of NR2 subunits is not uniform: for example, in mice cerebellar Golgi cells, NR2B subunits are expressed both synaptically and extrasynaptically while NR2D subunits are expressed extrasynaptically (Brickley *et al.*, 2003). NMDA receptors containing different NR2 subunits are distinct in their

biophysical characteristics and their modulation by various substances (Dingledine *et al.*, 1999). Consequently, NMDA receptors exhibit tremendous functional heterogeneity.

This study focuses on NR2D-containing NMDA receptors, which have not been as rigorously studied as the more prevalent NR2A or NR2B-containing NMDA receptors. Earlier works using expression systems or in carefully chosen native preparations have characterized the basic pharmacological and biophysical properties of NR1/2D receptors (Monyer *et al.*, 1994; Momiyama *et al.*, 1996; Wyllie *et al.*, 1996; Wyllie *et al.*, 1998). The channel properties of NR1/2D and NR1/2C receptors are similar, but distinct from the channel properties of NR1/2A or NR1/2B receptors. These properties include single-channel conductance, kinetics (Stern *et al.*, 1992; Momiyama *et al.*, 1996; Wyllie *et al.*, 1996) and sensitivity to external Mg^{2+} block (Monyer *et al.*, 1994; Kuner & Schoepfer, 1996). NR1/2D receptors also have some unique gating properties, including the extremely slow deactivation rate and an unequal probability in transitions between the main and subconductance states (Monyer *et al.*, 1994; Wyllie *et al.*, 1996; Vicini *et al.*, 1998; Wyllie *et al.*, 1998; Misra *et al.*, 2000). Whether these unusual properties have any physiological relevance is unclear. There is evidence suggesting that NR1/2D receptors are involved in stress pathways (Miyamoto *et al.*, 2002), epileptogenesis (Bengzon *et al.*, 1999), and synaptic plasticity (Okabe *et al.*, 1998; Hrabetova *et al.*, 2000). Clearly, a thorough understanding of the properties of these receptors is a first step towards appreciating their functions *in vivo*.

A fundamental property of NMDA receptors is the voltage-dependent block by Mg^{2+}_{o} (Mayer *et al.*, 1984; Nowak *et al.*, 1984; Ascher & Nowak, 1988). It is probably the most physiologically

important mode of regulation of NMDA receptors. Block by Mg^{2+}_o also provides a means to explore the structure and gating of the NMDA receptor. Using channel block to investigate channel structure and gating behavior has a long tradition and has proven extremely useful (see Johnson & Qian, 2002). For these reasons, Mg^{2+}_o block of NMDA receptors have been extensively studied. The majority of work on this subject, however, has been performed on NR1/2A or NR1/2B receptors using expression systems or on native receptors which most likely contain NR2A or NR2B NR2 subunits. Experiments in both neurons and heterologous expression systems have shown that Mg^{2+}_o inhibition of NR1/2D receptor-mediated currents is much weaker than NR1/2A or NR1/2B receptors (Kuner & Schoepfer, 1996; Momiyama *et al.*, 1996; Monyer *et al.*, 1994;). However, the microscopic Mg^{2+}_o blocking kinetics of NR1/2D receptors, to the best of my knowledge, have not been reported. Consequently, the mechanism of Mg^{2+}_o block of NR1/2D receptors has not been firmly established and the single-channel basis for the difference in Mg^{2+}_o block between NR1/2D and NR1/2A or NR1/2B receptors is not known.

The goal of this study was two-fold. First, I investigated the mechanism of Mg^{2+}_o block in NR1/2D receptors. The results are consistent with Mg^{2+}_o acting as an open channel blocker that inhibits current flow by binding to a site within the voltage-field. Second, I explored the origin of the differences in Mg^{2+}_o inhibition between cortical and NR1/2D receptors. The results suggest that weaker inhibition by Mg^{2+}_o in NR1/2D than cortical receptors is the result of a faster Mg^{2+}_o unblocking rate.

C. METHODS

1. Cell Culture

Human embryonic kidney (HEK) 293T cells (ATCC, Manassas, VA, USA) were used for whole-cell experiments and HEK293 cells (ATCC) were used for outside-out patch recordings. The cells were cultured at 37 °C in 5% CO_2 / 95% air. The culture medium for 293T cells was DMEM (Invitrogen Life Technologies, Carlsbad, CA, USA) with 5% fetal bovine serum and 2mM glutamine; the culture medium for HEK293 cells was DMEM with 10% fetal bovine serum, 2 mM glutamine and 1 mM sodium pyruvate. The cells were maintained in 100 mm culture dishes and split twice a week. For experiments, the cells were plated onto glass coverslips treated with poly-D-lysine (0.1 mg/ml) and rat-tail collagen (0.1 mg/ml, BD Biosciences, San Jose, CA, USA) in 35 mm culture dishes at 1 to 4 x 10^5 cells per dish.

2. Transfection

18-48 hours after plating, HEK293 or 293T cells were transiently transfected with cDNAs for NMDA receptor subunits. cDNA for NMDA receptor subunits NR1-1a, NR2A and NR2D were subcloned into mammalian expression vector pcDM8. cDNA for NR1-1a was a gift from S. Nakanishi (Japan) and cDNA for NR2A was a gift from P. Seeburg (Germany). cDNA of enhanced Green Fluorescent Protein (eGFP) (gift from Dr. Mark Fleck, Albany Medical College, NY, USA) was cotransfected as a marker of successfully transfected cells. Nearly every cell positive for eGFP signal had NMDA currents in whole-cell configurations, but this was often not true for outside-out patches.

293T cells were transfected using LipofectAMINE/PLUS reagents (Invitrogen). Briefly, transfection was performed by adding to each dish 1 ml serum free medium containing 1 μg total DNA, 5 μl LipofectAMINE, and 4 μl PLUS. The ratio of cDNA used was 1 eGFP: 3 NR1: 6 NR2 (A or D). Two hundred micromolar DL-APV was added to prevent NMDA receptor mediated-excitotoxicity.

The LipofectAMINE reagents have been reported to weaken the plasma membrane, presumably by incorporation into it, and consequently to be unsuitable for patch experiments (Groot-Kormelink *et al.*, 2002). Therefore, I used a modified calcium phosphate precipitation transfection procedure (Groot-Kormelink *et al.*, 2002). I found this procedure gave more reliable transfection results than the traditional procedure (Chen & Okayama, 1987). The amount of cDNA used per dish was 0.7 μg for eGFP, 0.7 μg NR1-1a and 1.4 μg NR2D. 7-9 hours after addition of DNA, precipitates were washed off with fresh culture medium that contained 200 μM DL-APV.

3. Solutions

Solutions were delivered using an in-house fabricated seven-barrel fast perfusion system (Qian *et al.*, 2002). For whole-cell experiments, a 98 to 99% complete solution exchange typically took less than 120 ms. For single-channel experiments, flow rate was decreased by about 50% to accommodate the delicate patches.

Solutions were prepared daily from frozen stocks. Currents were activated by 10 or 30 μM NMDA + 30 μM glycine. Mg^{2+} concentrations from 1 μM to 10 mM were added to external

solutions. I did not adjust for the change in osmolality as a result of adding Mg^{2+}. I have previously determined the level of contaminating $[Mg^{2+}]_o$ to be negligible (Qian *et al.*, 2002). This was further supported by the absence of voltage-dependence of the main time constant in open-duration histograms in control (0 Mg^{2+} added) experiments; the main time constant of open-duration would decrease with hyperpolarization if appreciable amount of contaminating Mg^{2+} were present. The external solution contained (in mM): 140 NaCl, 1 $CaCl_2$, 2.8 KCl, and 10 HEPES. The contents of internal solutions are (in mM): for whole-cell experiments, 125 CsCl, 10 EGTA and 10 HEPES; for patch recordings, 115 CsF, 10 CsCl, 10 EGTA and 10 HEPES; inclusion of floride ion was conducive for stable patches. Cs^+ is about as permeant through the channel of NMDA receptors as Na^+ and K^+ (Tsuzuki *et al.*, 1994) and was chosen as the principal intracellular permeant cation to facilitate comparison with previous results (Antonov & Johnson, 1999; Qian *et al.*, 2002). The pH of solutions was adjusted to between 7.1 and 7.2 using HCl or the basic form of the major charge carrier. Sucrose and NMDG were used to adjust the osmolality of external and internal solutions, respectively. The junction potentials between the pipette and bath solution were 5 mV in chloride-based internal solution and 9 mV for floride-based internal solution. All holding potentials were corrected for junction potentials. Ultrapure salts were used when available. All chemicals were from Sigma Chemical Co. (St. Louis, MO, USA), except as indicated in the text.

4. Whole-cell Recordings and Analysis

20-72 hours after transfection, electrophysiological experiments were performed. Whole-cell recordings were performed as described in Qian *et al.* (2002). Briefly, currents were recorded at room temperature with an Axopatch 200A or 200B amplifier (Axon Instruments, Foster City, CA,

USA), low-pass filtered at 10 kHz, digitized at 44 kHz with a Neuro-Corder and stored on video tape for off-line analysis. Series resistance was compensated 60-80%. NMDA-activated currents in the absence ($I_{control}$) and presence (I_{Mg}) of multiple $[Mg^{2+}]_o$s were measured from -115 mV to -15 mV at 10 mV increment. The IC_{50} of $Mg^{2+}{}_o$ at each voltage was obtained by fitting $I_{Mg} / I_{control}$ at various $[Mg^{2+}]_o$s using the following equation:

$$I_{Mg} / I_{control} (\%) = 100\% / [1+ ([Mg^{2+}]_o /IC_{50})^{n_H}] \quad (1)$$

IC_{50} and n_H (Hill coefficient) were free parameters during fitting. Curve fitting was performed using Origin 4.0 or 6.0 (Microcal Software, Northampton, MA). All data points were used in fitting of Equation (1), although for clarity only the mean values ± s.e.m. were plotted in Figure 12B. Only one IC_{50} value was obtained at each voltage since all measurements at a single voltage were fit with Equation (1) once; there is no error bar (for example, Figures 13 and 17). Each IC_{50} value was based on $I_{Mg} / I_{control}$ measurements in at least 3 different $[Mg^{2+}]_o$s and at least 3 cells for each $[Mg^{2+}]_o$. Data are expressed as mean ± s.e.m.

5. Single-Channel Recording and Analysis

Outside-out patch recordings were performed at room temperature according to standard methods (Hamill *et al.*, 1981). Pipettes (resistance of 5-8 MΩ) were pulled from borosilicate standard-wall glass with filaments (Warner Instrument Corp., Portland, OR, USA). Pipettes were coated with Sylgard and fire polished. Single-channel currents were recorded using an Axopatch200A or 200B patch-clamp amplifier, low-pass filtered at 10 kHz, digitized at 44 kHz with

a Neuro-Corder and stored on video tape for later analysis. Data were collected at voltages from -105 mV to -45 mV. At each voltage, single-channel currents in each patch were collected in segments: control (0 $Mg^{2+}{}_o$), and in one to three different $[Mg^{2+}]_o$. Data from at least three patches was used at each voltage. It was technically challenging to obtain stable and long-lasting patches from HEK293 cells transfected with cDNAs for the NR1/2D receptors. Cells appeared to be more amenable for obtaining stable patches when HEK293 cells of lower passages number were used (up to higher twenties).

For analysis, each data segment recorded was played back, filtered at 2.5 KHz (-3dB, eight-pole, low-pass bessel filter) and digitally sampled at 25 KHz using pCLAMP 8 Clampex software (Axon Instruments). The effective filter frequency was 2.43 KHz due to cascaded filters. NR1/2D receptor activation is characterized by relatively short open-duration (main open time = 0.67 msec) and frequent subconductance states (see Figure 14A). Single-channel analysis programs which use threshold-crossing techniques, such as PClamp programs from Axon Instrument, are not equipped to analyze single-channel openings with an appreciable amount of subconductance states. I therefore used the DC analysis programs (D. Colquhoun, University College London, UK), which makes use of time-course fitting techniques (Colquhoun & Sigworth, 1995). DC programs fit the time course of single-channel transitions directly, taking into account the characteristics of the recording system. This single-channel analysis method also allows for greater temporal resolution than threshold crossing techniques. For example, at a filter frequency of 2.5 KHz, using threshold crossing method, events shorter than 147 μs (twice the system response time) could not be fitted with confidence; however, time course fitting allows events much shorter than 147 μs to be fitted (see below).

Dwell-time histograms were plotted on square root versus log time scales (Sigworth & Sine, 1987). Dwell-time durations shorter than a cutoff value were omitted from both open and closed-duration distributions and this cutoff value was then subtracted from the time constants of the fit. The dwell-time histograms were then fitted by the maximum likelihood method (Colquhoun & Sigworth, 1995). The cutoff value was 50 μs in most patches (range from 45 -85 μs). The cutoff values was chosen so the false events rate was no higher than 10^{-4} per second and often much lower. I estimated in one patch that less than 0.1% of total events would be false events. This patch had relatively low level of channel openings and therefore gave a conservative upper limit. The cutoff value chosen in this study was reasonable: Wyllie et al. (Wyllie *et al.*, 1996) used 50-70 μs in their work on NR1/2D receptors; much shorter cutoff value has been used in works on other ion channels (for example, Hatton *et al.*, 2003).

Open-duration histograms in the absence or presence of Mg^{2+}_o were fit by one to three exponentials (time constant of the largest exponential, τ_o). Each open event may contain transitions among openings of different amplitude levels. I did not attempt to analyze the main and subconductance levels separately. This was because open events must be long enough (at least twice the filter risetime, 266 μs at 2.5 KHz filter frequency) to reach full amplitude of the conductance level. In NR1/2D receptors, many events would be too short to meet this criteria and it could not be determined with confidence to which conductance level these short events belong.

Closed-duration histograms in the absence of Mg^{2+}_o were adequately fit by the sum of three or four exponentials. There are two general methods to determine the number of exponentials

chosen to fit a distribution: statistical method and method of "reproducibility". The statistical method relies on a statistical test to examine the improvements of fit with an additional exponential component (for example, Horn, 1987). The disadvantage of this method is that statistical significance is not always correlated with functional significance. I chose the number of exponentials to fit closed-duration histograms according to "criterion of reproducibility" (Colquhoun & Sigworth, 1995): initial inspection of closed-time histograms suggested that the distribution could be adequately fitted by four components in control conditions (this was done visually); subsequently, closed-time histograms were fitted by four components; occasionally, the distribution could be fit by three components (the fitting results gave the amplitude of one of the components as less than 0.5%).

In the presence of Mg^{2+}_o, an additional component emerged (time constant, τ_b), corresponding to the blocking events by Mg^{2+}_o. The mean amplitude of τ_b (30%) is significantly larger than the mean amplitude of the neighboring, shorter, time constants (13.6%; $p = 0.004$) or the mean amplitude of the neighboring, longer, time constants (12.4%; $p < 0.001$). Sometimes, the closed-duration histogram was fitted by the same number of exponentials in the absence and presence of Mg^{2+}_o. Even in those cases, the exponential component due to Mg^{2+}_o block could be unambiguously determined: the mean amplitude of τ_b (33.7%) is significantly larger than the neighboring, longer, time constant (17.3%; $p = 0.013$); τ_b was always the shortest time constant, when the same number of exponentials were fit in the absence and present of Mg^{2+}_o.

The true mean duration of the main channel open state must be shorter than τ_o since missed brief closings cause neighboring channel openings to be adjoined during data analysis. The same reasoning applies for overestimation of mean duration of blocked state, due to missed short openings. To minimize errors introduced by missed openings, I chose $[Mg^{2+}]_o$ where τ_o was sufficiently longer than the cutoff values; the shortest τ_o measured was 0.228 ms, which was 4.6 times longer than the cutoff values in that patch. The shortest τ_b measured was 0.2 ms (3.3 times longer than the cutoff value). τ_b values were not dependent on $[Mg^{2+}]_o$ (Figure 15B), suggesting that missed openings did not reach a level to affect τ_b values appreciably. The fact that single-channel derived K_D values (see later) agreed very well with whole-cell measured IC_{50} values (Figure 17) also lends support to the accuracy of our measurements.

The apparent $Mg^{2+}{}_o$ blocking and unblocking rates, $k_{+,app}$ and k_{-app}, were estimated as described in Neher and Steinbach (1978). Previous work (Antonov & Johnson, 1999; Zhu & Auerbach, 2001a, b) have shown that $Mg^{2+}{}_o$ blocking and unblocking rates are affected by permeant ions. Therefore I refer to these as "apparent" rates to distinguish them from the true $Mg^{2+}{}_o$ blocking and unblocking rates in the absence of permeant ion effects. $k_{+,app}$ was estimated from the follow equation by measuring the slope of a linear regression line fit through a plot of $1/\tau_o$ vs. $[Mg^{2+}]_o$ (Figure 14C).

$$1/\tau_{o,Mg} = 1/\tau_{o,control} + k_{+,app} \bullet [Mg^{2+}]_o$$

$k_{-,app}$ was estimated as $1/\tau_b$, assuming that rate of blocked channel closure was low comparing to $k_{-,app}$ (Antonov & Johnson, 1996). The channel closure rate is 1492 s^{-1} while the mean $k_{-,app}$ value ranges from 2380 to 3890 s^{-1}. Data are expressed as mean ± s.e.m.

D. RESULTS

1. Mg^{2+}_o inhibition of NR1/2D receptor-mediated whole-cell currents

Although previous studies have shown, both in native and in heterologous system, that NR1/2D receptors are subject to Mg^{2+}_o inhibition (Monyer *et al.*, 1994; Kuner & Schoepfer, 1996; Momiyama *et al.*, 1996), many mechanistic aspects of Mg^{2+}_o inhibition in NR1/2D receptors remain unknown. I wished first to characterize Mg^{2+}_o inhibition in NR1/2D receptors and to compare the differences in Mg^{2+}_o inhibition between NR1/2A and NR1/2D receptors. Figure 12A shows current traces recorded at -85 mV (left) and -35 mV (right) from NR1/2A (top) and NR1/2D (bottom) receptors. During a continuous agonist application, a single $[Mg^{2+}]_o$ was applied to inhibit currents. Mg^{2+}_o inhibited the currents rapidly in both receptor subtypes. At either voltage, the same $[Mg^{2+}]_o$ inhibited NR1/2A receptor-mediated currents much more effectively than NR1/2D receptor-mediated currents.

I constructed Mg^{2+}_o concentration-inhibition curves to estimate Mg^{2+}_o IC_{50} at -85 and -35 mV. At either voltage, the concentration-inhibition curve for NR1/2D receptors is to the right of the curves for NR1/2A receptors (Figure 12B). These results are consistent with previous reports (Monyer *et al.*, 1994; Kuner & Schoepfer, 1996; Momiyama *et al.*, 1996) that Mg^{2+}_o inhibited NR1/2A receptor-mediated currents much more effectively than NR1/2D receptor-mediated currents.

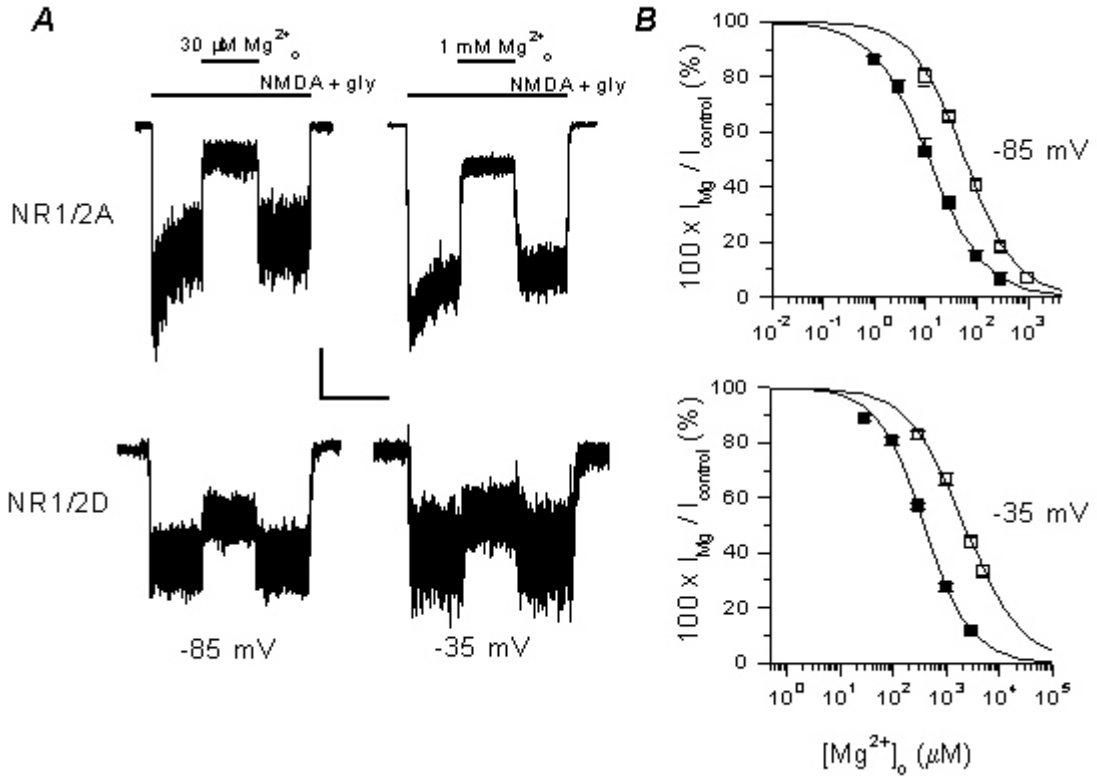

Figure 12 Comparison of Mg^{2+}_o inhibition in NR1/2A and NR1/2D receptors. (A) NMDA receptor-mediated whole-cell currents and their inhibition by Mg^{2+}_o are shown for NR1/2A (upper traces) and NR1/2D (lower traces) receptors. The bars above the current traces show the times of application of the indicated solutions. At -85 mV (left traces), 30 μM Mg^{2+}_o inhibited current by 75% in NR1/2A receptors; the same $[Mg^{2+}]_o$ inhibited current by 29% in NR1/2D receptors. At -35mV (right traces), 1 mM Mg^{2+}_o inhibited current by 73% in NR1/2A receptors; the same $[Mg^{2+}]_o$ inhibited current by 29% in NR1/2D receptors. Scale bar is 5 sec and 100 pA, except for the bottom right trace, which is 20 pA. The traces were from four different cells. (B) Mg^{2+}_o concentration-inhibition curves were plotted for NR1/2A (■) and NR1/2D (□) receptors at -85 mV (top panel) and -35mV (bottom panel). The voltage, receptor type and Mg^{2+}_o IC_{50} values are: -85mV, NR1/2A, 11.8 μM; -85mV, NR1/2D, 60.0 μM; -35mV, NR1/2A, 388 μM; -35mV, NR1/2D, 2.22 mM.

I repeated the procedures shown in Figure 12B and measured Mg^{2+}_o IC_{50} for both NR1/2A and NR1/2D receptor-mediated whole-cell currents from -115mV to -15mV at 10 mV increment (Figure 13). Mg^{2+}_o IC_{50} values are voltage-dependent in both receptor types, suggesting that Mg^{2+}_o blocks both channel types by occupying a site within the voltage field. At each voltage tested, Mg^{2+}_o IC_{50} was at least four-fold higher in NR1/2D than in NR1/2A receptors. The voltage dependence of Mg^{2+}_o IC_{50} is, however, similar in the two receptor types.

Also plotted was Mg^{2+}_o IC_{50} measured from native NMDA receptors (rat cortical cultures) from previous work (Qian *et al.*, 2002). Numerous biochemical and biophysical studies (e.g., Monyer *et al.*, 1994; Zhong *et al.*, 1994; Kirson & Yaari, 1996; Antonov & Johnson, 1999) have demonstrated that in cortical neurons, at the developmental stages we used, the NR2 subunits expressed are nearly exclusively of the NR2A or NR2B subtypes, which exhibit similar Mg^{2+}_o sensitivity (Monyer *et al.*, 1994; Kuner & Schoepfer, 1996). Consistently with these studies, Figure 13 shows that the Mg^{2+}_o IC_{50} measured in NR1/2A receptors expressed in mammalian cells were comparable to values obtained from cortical NMDA receptors, which I will refer to as "cortical receptors". The microscopic Mg^{2+}_o block kinetics have been characterized in detail in cortical receptors (Antonov & Johnson, 1999). I will compare the single-channel Mg^{2+}_o block kinetics between the NR1/2D and cortical receptors in the next section.

2. Mg^{2+}_o block of NR1/2D receptors at the single-channel level

Mg^{2+}_o IC_{50} measurements, although informative regarding the physiological roles of Mg^{2+}_o inhibition, do not reveal the underlying blocking kinetics, since IC_{50} values are related to the ratio

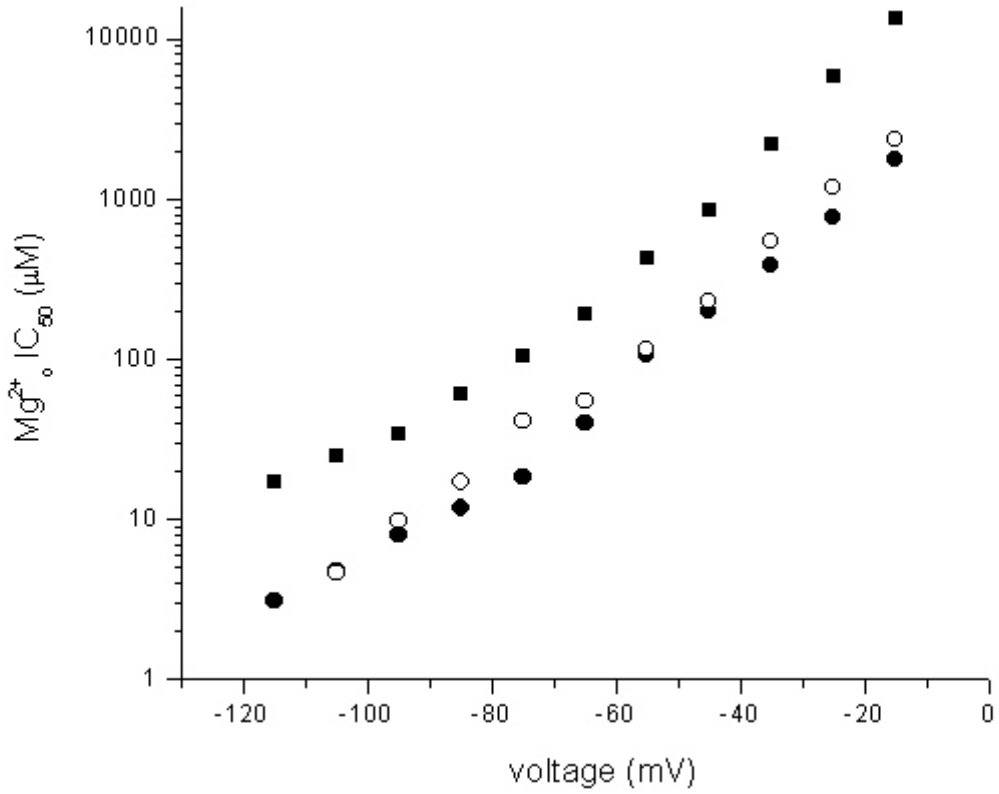

Figure 13 Voltage-dependence of Mg^{2+}_{o} IC_{50} in NR1/2A, NR1/2D, and cortical receptors. Mg^{2+}_{o} IC_{50} values measured from -115mV to -15 mV are plotted for NR1/2A (●) and NR1/2D (■) receptors. Also plotted are Mg^{2+}_{o} IC_{50} values measured from primary cultures of cortical neurons (○), which express NR1. NR2A, and NR2B subunits (Monyer *et al.*, 1994; Zhong *et al.*, 1994; Kirson & Yaari, 1996; Antonov & Johnson, 1999). Data for cortical receptors is replotted from Figure 7.

of Mg^{2+}_o unblocking and blocking rates. I next characterized Mg^{2+}_o block at the single-channel level. Single-channel traces (Figure 14A) show that in the absence of Mg^{2+}_o, NR1/2D channel evens are relatively brief and open to main and subconductance level. Addition of Mg^{2+}_o causes the brief channel openings to appear "flickery"(Figure 14A), consistent with a channel blocker of intermediate kinetics (Hille, 2001).

Dwell-time distributions were used to examine the kinetics of Mg^{2+}_o block. To measure Mg^{2+}_o blocking rates (see METHODS), open duration histogram were constructed (Figure 14B). In this patch at -85mV, 0, 10, 30, and 50 μM $[Mg^{2+}]_o$ were used. In the control condition (0 Mg^{2+}_o), the open-duration histogram was fitted by three exponential components. In the presence of each of the three $[Mg^{2+}]_o$, the histogram was still well fitted by three exponential components. The time constant of the main component, τ_o, declined as $[Mg^{2+}]_o$ increased. I did not further characterize the other two exponential components in different $[Mg^{2+}]_o$s. As expected for a open channel blocker (Neher & Steinbach, 1978), the inverse of τ_o depends linearly on $[Mg^{2+}]_o$ (Figure 14C). $k_{+,app}$ was estimated from the slope of the straight line through the data points.

Closed-time distributions were constructed to study Mg^{2+}_o unblocking rate, $k_{,app}$ (Figure 15A). In this example, the closed-time distributions in control condition could be adequately fitted by four exponential components. In the presence of Mg^{2+}_o, an additional exponential component was needed to adequately fit the closed-time distributions. The time constant of this additional component is τ_b (see METHODS). $k_{-,app}$ was estimated by averaging the inverse of τ_b in 10, 30 and

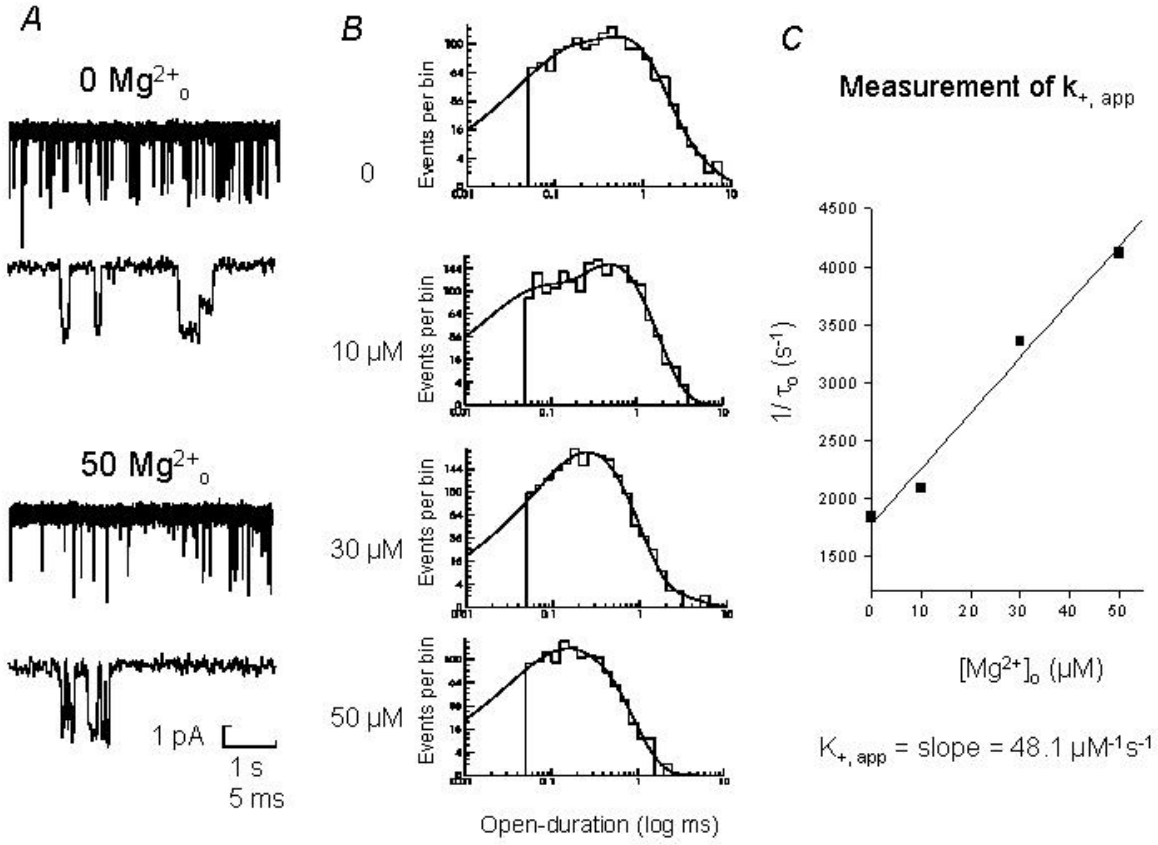

Figure 14 Effect of Mg^{2+}_o on open-duration histograms and measurement of Mg^{2+}_o blocking rates. (A) Single-channel recordings of NR1/NR2D receptor-mediated currents at -85 mV are shown with the indicated $[Mg^{2+}]_o$s at two different time resolution. (B) Open-duration histograms are shown for a patch, same as the one shown in (A), recorded at -85mV in various $[Mg^{2+}]_o$s. The $[Mg^{2+}]_o$, time constant, and relative amplitude of the main component of the four histograms are: 0 Mg^{2+}_o, 0.544 ms, 63.6%; 10 µM Mg^{2+}_o, 0.479 ms, 71.7%; 30 µM Mg^{2+}_o, 0.298 ms, 76.4%; 50 µM Mg^{2+}_o, 0.243 ms, 69.3%. (C) The apparent binding rate constant for Mg^{2+}_o, $k_{+, app}$, was estimated from the slope of a linear regression line fitted to a plot of $1/\tau_o$ vs. $[Mg^{2+}]_o$.

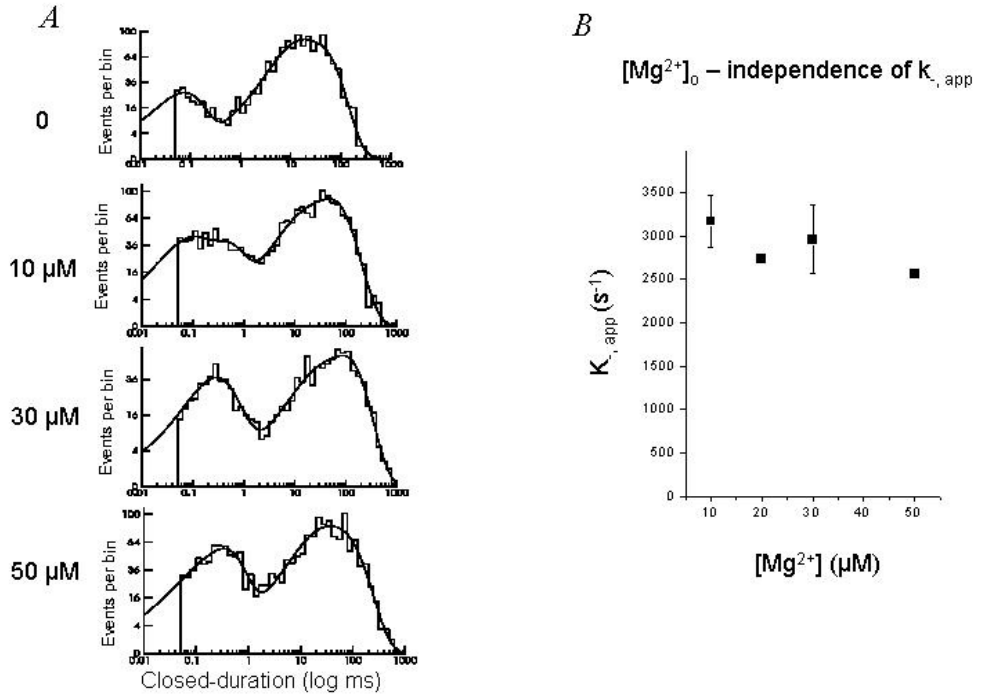

Figure 15 Effect of Mg^{2+}_o on closed-duration histograms of NR1/2D receptors. (A) Examples of closed-duration histograms are shown from the same patch as in Figure 14 in the indicated $[Mg^{2+}]_o$s. In the absence of Mg^{2+}_o, the closed-duration histogram was fitted with four exponential components. In the presence of Mg^{2+}_o, an additional component (τ_b) emerged in each of the histograms. The $[Mg^{2+}]_o$, time constant of τ_b, and amplitude of τ_b are: 10 μM Mg^{2+}_o, 0.372 ms, 19.4%; 30 μM Mg^{2+}_o, 0.255 ms, 23.5%; 50 μM Mg^{2+}_o, 0.330 ms, 31.5%. (B) The apparent unbinding rates for Mg^{2+}_o, $k_{-, app}$, were plotted as a function of $[Mg^{2+}]_o$s at -85 mV. Results are pooled from 5 experiments; n = 2 at 20 and 50 μM. $k_{-,app} = 1 / \tau_b$ (see Methods).

50 μM Mg^{2+}_o. In contrast to $k_{+,app,}$ $k_{-,app}$ is not correlated with $[Mg^{2+}]_o$ at any voltages ($p = 0.27$ at -85 mV; p values range from 0.27 to 0.96).

3. Mechanistic differences between Mg^{2+}_o block of cortical and NR1/2D receptors.

Measurements of Mg^{2+}_o $k_{+,app}$ and $k_{-,app}$ allow me to probe the underlying mechanism of differences between Mg^{2+}_o block of cortical and NR1/2D receptors. Values of $k_{+,app}$ and $k_{-,app}$ for cortical receptors have been published (Antonov & Johnson, 1999) and are replotted in Figure 16 for comparison with NR1/2D receptors. At all voltages tested, $k_{-,app}$ was much faster in NR1/2D than in cortical receptors (Figure 16A). From -40 to -75 mV, the voltage dependence of Mg^{2+}_o $k_{-,app}$ is similar in cortical and NR1/2D receptors; $k_{-,app}$ decreased with hyperpolarization, consistent with an extracellular channel blocker unblocking predominantly to the extracellular side. From -75 to -105 mV, $k_{-,app}$ increased with hyperpolarization in NR1/2D receptors (ANOVA, $p = 0.07$). In cortical receptors, $k_{-,app}$ decreased from -75 to -90 mV; from -90 to -140 mV, $k_{-,app}$ showed very little voltage dependence, presumably reflecting the increase in Mg^{2+}_o permeation (Antonov & Johnson, 1999).

The $k_{+,app}$ of both cortical and NR1/2D receptors decreased with depolarization (Figure 16B), as expected for a extracellular channel blocker. $k_{+,app}$ in both receptors have similar voltage-dependence; $k_{+,app}$ of NR1/2D was slighter lower than the $k_{+,app}$ of cortical receptors at every voltage tested (not statistically significant; paired *t* test).

Therefore, the weaker Mg^{2+}_o inhibition observed in cortical vs. NR1/2D receptors is due almost exclusively to much faster Mg^{2+}_o unblocking.

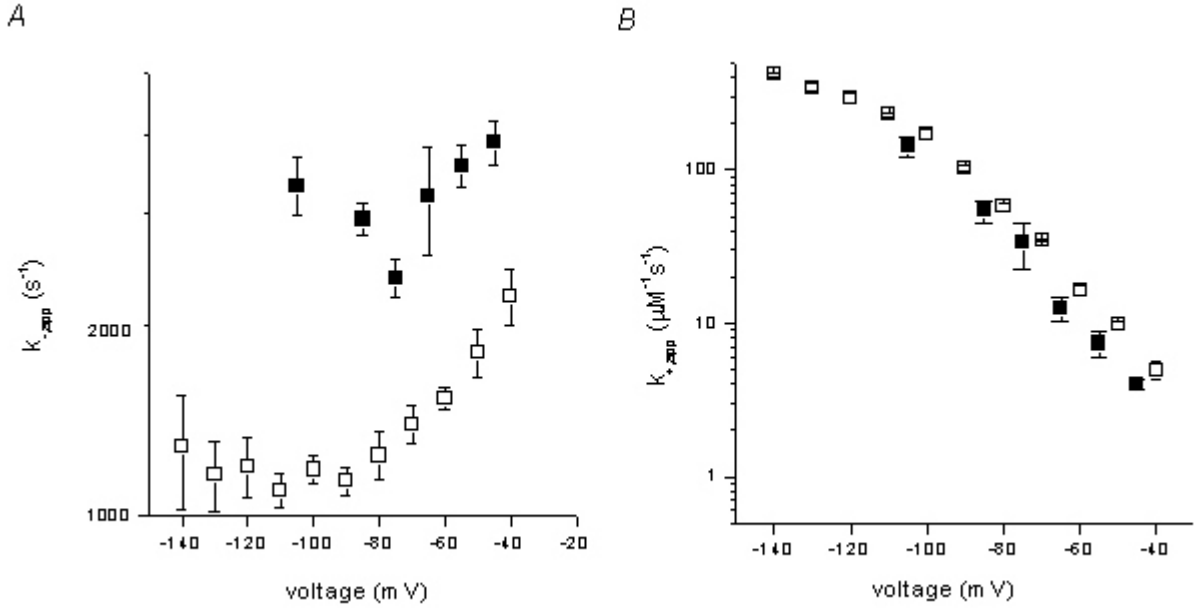

Figure 16 Voltage-dependence of Mg^{2+}_o blocking and unblocking rates in NR1/2D receptors. (A) Voltage-dependent Mg^{2+}_o $k_{-,\,app}$ is plotted for NR1/2D (■). Previous data of $k_{-,\,app}$ from cortical receptors (□) are also plotted for comparison. Data for cortical receptors are average values of $k_{-,\,app}$ in two or more $[Cs^+]_i$s; $k_{-,\,app}$ in cortical receptors are independent of $[Cs^+]_i$ (Antonov & Johnson, 1999). (B) Voltage-dependent $k_{+,\,app}$ is plotted for NR1/2D (■) and for cortical receptors (□) (Antonov & Johnson, 1999).

4. Interaction of Mg^{2+}_o block with gating of NR1/2D receptors.

I examined the relationship between the Mg^{2+}_o IC_{50} values measured from whole-cell experiments (see Figures 12 and 13) and microscopic Mg^{2+}_o K_D measured from single-channel experiment using the relationship $K_D = k_{-,app} / k_{+,app}$ (Qian *et al.*, 2002). At all voltages tested, Mg^{2+}_o IC_{50} values are comparable to K_D values (Figure 17). The similarity between the two data sets at all voltages supports the accuracy of our single-channel measurements. In addition, it suggests that, like cortical receptors (Qian *et al.*, 2002), Mg^{2+}_o block does not affect gating transitions of NR1/2D receptors.

E. DISCUSSION

In this study, the effects of Mg^{2+}_o on whole-cell and single-channel currents of NR1/2D receptors were investigated. The main results were : (1) Whole-cell NR1/2D receptor-mediated currents were inhibited by Mg^{2+}_o in a voltage-dependent manner; Mg^{2+}_o inhibition was more effective at hyperpolarized voltages. (2) Mg^{2+}_o inhibition was weaker in NR1/2D than in NR1/2A receptors but exhibited comparable voltage dependence. (3) Mg^{2+}_o $k_{+, app}$ values and voltage dependence were similar in the two receptor types. (4) Mg^{2+}_o $k_{-, app}$ was much faster in NR1/2D than in cortical receptors. The voltage dependence of $k_{-, app}$ is comparable in NR1/2D and cortical receptors at voltages more positive than -75; at voltages negative than -75 mV, the voltage dependence is different between the two receptors. (5) These data suggest that Mg^{2+}_o inhibits currents less effectively in NR1/2D than in cortical receptors chiefly because of much faster Mg^{2+}_o unbinding rates. (6)The agreement between Mg^{2+}_o IC_{50} and K_D suggests that Mg^{2+}_o block does not affect channel gating of NR1/2D receptors.

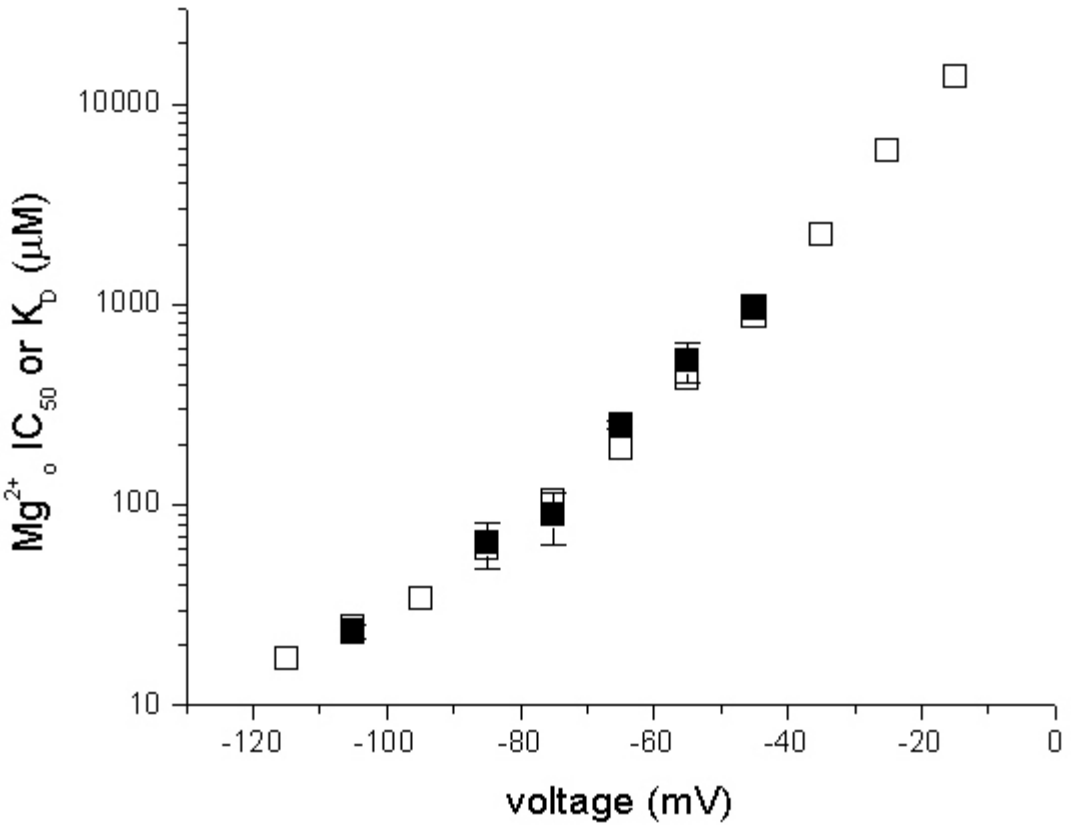

Figure 17 Voltage dependence of Mg^{2+}_o IC_{50} and K_D in NR1/2D receptors. NR1/2D receptors Mg^{2+}_o IC_{50} (□) measured from whole-cell experiments and K_D (■) calculated from single-channel experiments (K_D = $k_{-,\,app}$ / $k_{+,\,app}$) are plotted. Note that there are no error bars associated with Mg^{2+}_o IC_{50} values since at each voltage the IC_{50} value is a single fit to population data (see METHODS). The values of Mg^{2+}_o IC_{50} and K_D are comparable over the voltage range measured.

1. Comparison with previous studies

The subunit dependence of inhibition of whole-cell NMDA currents by Mg^{2+}_o has been studied in *Xenopus laevis* oocytes (Kuner & Schoepfer, 1996). In general, the findings of this study and of Kuner and Schopfer (1996) are similar: both studies reported that voltage-dependent inhibition by Mg^{2+}_o was present in both NR1/2A and NR1/2D receptors and that the inhibition was stronger in NR1/2A receptors. There are, however, some noticeable differences. In our study, the voltage-dependence of Mg^{2+}_o inhibition was comparable in NR1/2D and NR1/2A receptors (Figure 13) while in Kuner and Schoepfer (1996) Mg^{2+}_o IC_{50} values tend to converge at depolarized voltages. The absolute values of Mg^{2+}_o IC_{50} are also much lower in their studies. For example, IC_{50} of NR1/2D receptors at -35 mV is about 403 μM in Kuner and Schoepfer (1996) and 2.22 mM in this study.

We do not know the reasons for these differences. To verify the accuracy of the measurements of whole-cell Mg^{2+}_o IC_{50}, I compared Mg^{2+}_o IC_{50} from two different mammalian systems, 293T cells and rat cortical neurons, and obtained similar IC_{50} values with identical voltage dependence (Figure 13). One possibility is that differences in results of this study and Kuner and Schoepfer (1996) were due to variations in experimental conditions, in particular, the permeant ion concentrations; previous studies (Ruppersberg *et al.*, 1994; Zarei & Dani, 1995; Antonov & Johnson, 1999; Zhu & Auerbach, 2001a, b; Qian *et al.*, 2002) have shown that permeant ion concentrations shape both the affinity and voltage-dependence of Mg^{2+}_o block. The internal ion concentration cannot be adequately controlled in oocytes and can be significantly different from the ion concentration used in this study. Zhu and Auerbach (2001a) showed that internal K^+ can accelerate

Mg^{2+}_o unblocking rate while this effect was not observed when Cs^+ was used as the main internal ion (Antonov & Johnson, 1999). If there is significant K^+ present in oocytes, Mg^{2+}_o unblocking rates would be differently affected from if Cs^+ is present.

Differences in experimental conditions may not explain all the differences in Mg^{2+}_o IC_{50} measured from this study and Kuner and Schoepfer (1996). Kupper *et al.* (1996) used similar experimental conditions as this study and measured Mg^{2+}_o IC_{50} from outside-out patches from oocytes. They reported Mg^{2+}_o IC_{50} values that are at least 2-fold lower than values measured from this study. Even though a previous study (Stern *et al.*, 1994) did not find system-dependent differences in single-channel conductance or dwell-time distributions, I considered the possibility that Mg^{2+}_o block of NMDA receptors expressed in oocytes differs from that of receptors in mammalian expression system. To test this idea, I compared Mg^{2+}_o IC_{50} or fractional block by Mg^{2+}_o from work published from many laboratories under a variety of experimental conditions. In every case I examined, Mg^{2+}_o inhibition was stronger in oocytes than in mammalian systems (Burnashev *et al.*, 1992; Monyer *et al.*, 1992; Kuner & Schoepfer, 1996; Kupper *et al.*, 1996; Wollmuth *et al.*, 1998a). In conclusion, there exist differences in Mg^{2+}_o block of NMDA receptors expressed in mammalian systems and oocytes. The origin for these differences is unclear at this point.

2. Mechanism of Mg^{2+}_o block in NR1/2D receptors

We examined mechanistic aspects of Mg^{2+}_o block in NR1/2D receptors using the dual approaches of whole-cell and single-channel recordings. Whole-cell recording of NR1/2D receptor-mediated currents revealed that, just like NR1/2A receptors, Mg^{2+}_o block was faster than could be

resolved with the perfusion system (Figure 12A). Cursory examination of single-channel recordings (Figure 14A) suggested that addition of Mg^{2+}_o caused flickers in channel openings, a characteristic often present with blockers of intermediate kinetics (Hille, 2001). Measurements of $k_{-, app}$ and $k_{+, app}$ (Figure 14 & 15) confirmed that Mg^{2+}_o block in NR1/2D receptors, as in cortical receptors, is of intermediate kinetics.

Most channel blockers of NMDA receptors are open-channel blockers that can only block the channel after its activation. A practical criterion to determine whether a blocker acts as an open channel is to examine its use-dependence. However, this approach is only useful for blockers with kinetics that are slow compared to channel gating. Blockers such as Mg^{2+}_o in cortical receptors present a difficulty, since their kinetics are fast compared to channel gating, it is ambiguous whether channels need to open prior to blocking. Although Mg^{2+}_o in cortical receptors is consistent with an open channel blocker using other criteria (Nowak *et al.*, 1984; Ascher & Nowak, 1988; Jahr & Stevens, 1990a; Antonov & Johnson, 1999; Sobolevsky & Yelshansky, 2000), it cannot be completely ruled out that Mg^{2+}_o can block a closed NMDA receptors. Although Mg^{2+}_o can clearly inhibits current through an open channel of NR1/2D receptors, it is unclear whether Mg^{2+}_o can block the channel exclusively through the open states. Mg^{2+}_o block of NR1/2D receptors also has relatively fast kinetics.

Channel blockers may interact with channel gating transitions. In general, channel blockers can be grouped depending on their effects on gating transition: (1) A "sequential blockers" prevents the closing of channel. Examples of NMDA receptor channel blocking drugs that have been

proposed to act as sequential blockers include 9-aminoacridine (Costa & Albuquerque, 1994; Benveniste & Mayer, 1995), IEM-1857 (Antonov & Johnson, 1996) and tetrapentylammonium (Sobolevsky *et al.*, 1999). (2) A "trapping blocker" allows channel to close and becomes "trapped". Many trapping blockers also affect gating (for examples, see Johnson & Qian, 2002).

The effect of Mg^{2+}_o block of cortical receptors on channel gating was examined by comparing Mg^{2+}_o IC_{50} from whole-cell experiments and K_D from single-channel experiments (Qian *et al.*, 2002). The relationship between IC_{50} and K_D reveals the interaction between a channel blocker and channel gating: K_D reflects the interaction between blocker and the channel, while IC_{50} measures the effectiveness of a blocker to inhibit whole-cell currents. In the case of a sequential blocker, although it inhibits current during block, it also prolongs channel openings by simply "holding" the channel open for as long as the blocker is there. These two effects, inhibiting current flow and prolonging channel openings, counterbalance each other and hence IC_{50} is much greater than it would be if the blocker only acts through current inhibition. The agreement between IC_{50} and K_D, as is the case in cortical receptors, is consistent with blocker having no effects on gating: it neither prevents nor encourages channel closure. I found in cortical receptors that Mg^{2+}_o IC_{50} and K_D are comparable over a wide voltage range (data not shown), suggesting that Mg^{2+}_o does not interact with gating. This conclusion is also supported by other studies which suggest that (1) Mg^{2+}_o can be trapped (Sobolevsky & Yelshansky, 2000); (2) Mg^{2+}_o does not prevent agonists dissociation (Benveniste & Mayer, 1995; Sobolevsky & Yelshansky, 2000). I also observed an excellent agreement between Mg^{2+}_o IC_{50} and K_D in NR1/2D receptors (Figure 17), suggesting that Mg^{2+}_o block does not interact with gating transition in NR1/2D receptors either.

3. Mechanistic differences of Mg^{2+}_o inhibition between cortical and NR1/2D receptors

It is known that Mg^{2+}_o inhibition is weaker in NR1/2D than in NR1/2A or NR1/2B receptors. The mechanistic basis of this subunit-difference can be addressed in single-channel studies, in which Mg^{2+}_o blocking and unblocking rate constants can be examined separately. Our results show that (1) $k_{+,app}$ in NR1/2D receptors is not very different from cortical receptors; and (2) $k_{-,app}$ values are much faster in NR1/2D than in cortical receptors. Therefore, the weaker Mg^{2+}_o inhibition of NR1/2D receptors is primarily the result of faster unblocking rates. The difference in the voltage dependence between NR1/2D and cortical receptors at voltages negative than -75 mV also suggests that Mg^{2+}_o permeation is more significant in NR1/2D receptors.

IV. PERMEANT ION EFFECTS ON Mg^{2+}_o BLOCK OF NR1/2D RECEPTORS

A. SUMMARY

NMDA receptors are essential participants in vertebrate CNS. I wish to deepen our understanding of the fundamental biophysical processes by which these receptors function. Previous work (Antonov & Johnson, 1999; Zhu & Auerbach, 2001a, b; Qian *et al.*, 2002) has shown that changing permeant ion concentrations has profound effects on Mg^{2+}_o block of NR1/2A or NR1/2B receptors. Here I investigated the effects of changing permeant ion concentration on Mg^{2+}_o block of NR1/2D receptors using whole-cell and single-channel recordings and integration of those data with kinetic modeling. The main findings are: (1) Decreasing $[Cs^+]_i$ reduces Mg^{2+}_o IC_{50} in a voltage-dependent manner: the reduction is greater at depolarized voltages. (2) Decreasing $[Cs^+]_i$ increases Mg^{2+}_o $k_{+,\,app}$ but decreases $k_{-,\,app}$; both effects are stronger at depolarized voltages. (3) Lowering $[Na^+]_o$ modestly increases Mg^{2+}_o IC_{50} at depolarized voltages and decreases Mg^{2+}_o IC_{50} at hyperpolarized voltages. (4) Lowering $[Na^+]_o$ has no apparent effect on Mg^{2+}_o $k_{-,app}$ but increases $k_{+,app}$ in a voltage-independent manner.

The effects of changing $[Cs^+]_i$ and $[Na^+]_o$ on Mg^{2+}_o $k_{+,app}$ and $k_{-,app}$ in NR1/2D receptors could be explained by a kinetic model with two external permeant ion binding sites and an internal Cs^+

binding site: when the external binding site(s) is occupied, Mg^{2+}_o blocking is prevented; when the internal binding site is occupied, Mg^{2+}_o permeation is prevented but its unblocking to the external side is greatly accelerated; during Mg^{2+}_o block, Na^{+}_o binding to the external permeant ion binding sites is negligible.

B. INTRODUCTION

NMDA receptors are widely distributed in the vertebrate CNS and play vital roles in physiological and pathological processes. A thorough knowledge of the properties of these receptors can facilitate the understanding of CNS function.

NMDA receptors are the target of modulation by many substances (Dingledine *et al.*, 1999), among which Mg^{2+}_o block is uniquely important for NMDA receptor function: in order for NMDA receptors to be activated, presynaptic release of glutamate and postsynaptic depolarization (to relieve Mg^{2+}_o block) must fall within a short time window. Investigation of Mg^{2+}_o block has also provided insights into NMDA receptor structure and gating properties (Jahr & Stevens, 1990a; Burnashev *et al.*, 1992; Benveniste & Mayer, 1995; Wollmuth *et al.*, 1998a; Antonov & Johnson, 1999; Sobolevsky & Yelshansky, 2000; Zhu & Auerbach, 2001a, b; Johnson & Qian, 2002; Qian *et al.*, 2002; Qian & Johnson, 2002). Mg^{2+}_o block of NR1/2A or NR1/2B receptors is modulated by permeant ions. Work presented in Chapter II demonstrated the strong influence of internal and external ions on whole-cell current inhibition by Mg^{2+}_o. Single-channel studies (Antonov & Johnson, 1999; Zhu & Auerbach, 2001a, b) revealed the underlying mechanism: permeant ions bind to specific sites within the channel and either prevent or enhance the rates of Mg^{2+}_o movements.

NMDA receptors containing NR2D subunits have important physiological functions (Ikeda *et al.*, 1995; Okabe *et al.*, 1998; Bengzon *et al.*, 1999; Hrabetova *et al.*, 2000; Miyamoto *et al.*, 2002). Even though the properties of Mg^{2+}_o block of NR1/2D receptors have been characterized under normal ionic conditions (Chapter III), it is not known (1) whether permeant ions also affect Mg^{2+}_o block in NR1/2D receptors; (2) whether the permeant ion effects are the same in NR1/2D as in NR1/2A or NR1/2B receptors. I have previously reported (see Chapter III) that the basis for differences in Mg^{2+}_o block between cortical NMDA receptors (likely contains NR2A or NR2B subunits) and NR1/2D receptors is mostly due to much faster Mg^{2+}_o unbinding rates. Here I investigate whether the permeant ion effects play a role in the differences of Mg^{2+}_o block between NR1/2D and NR1/2A receptors.

C. METHODS

1. Cell Culture

The culture methods used in this study are described in section III. C. 1.

2. Transfection

The transfection protocol is described in section III. C. 2.

3. Solutions

Solutions were prepared and applied according to the procedures described in section III. C. 3. In this study I used several solutions to test the effects of Na^+_o and Cs^+_i on Mg^{2+}_o block. The abbreviations and contents of external solutions are (in mM): "140 Na^+_o" solution, 140 NaCl, 1

$CaCl_2$, 2.8 KCl, and 10 HEPES; "70 Na^+_o" solution, 70 NaCl, 140 sucrose, 0.5 $CaCl_2$, 2.8 KCl, and 10 HEPES. The abbreviations and contents of internal solutions are (in mM): "125 Cs^+_i" solution for whole-cell experiments, 125 CsCl, 10 EGTA and 10 HEPES; "125 Cs^+_i" solution for patch recordings, 115 CsF, 10 CsCl, 10 EGTA and 10 HEPES; "8 Cs^+_i " solution for whole-cell experiments, 8 CsCl, 117 NMDG, 10 EGTA and 10 HEPES; "8 Cs^+_i" solution for patch recordings, 8 CsF, 117 NMDG, 10 EGTA and 10 HEPES; "25 Cs^+_i", 25 CsF, 100 NMDG, 10 EGTA and 10 HEPES. Osmolality and pH were adjusted as described in section III. C. 3.

The junction potentials between the pipette and bath solution are: 5 mV for 140 Na^+_o / 125 Cs^+_i (chloride-based); -3 mV for 140 Na^+_o / 8 Cs^+_i (chloride-based); -7 mV for 70 Na^+_o / 8 Cs^+_i; 9 mV for 140 Na^+_o / 125 Cs^+_i (floride-based), -3 mV for 140 Na^+_o / 8 Cs^+_i (floride-based), -7 mV for 70 Na^+_o / 25 Cs^+_i. All membrane potentials reported here were corrected for junction potentials.

4. Whole-cell recording and analysis

Whole-cell recordings and analysis were performed as described in section III. C. 4.

5. Single-channel recording and analysis

Single-channel recording and analysis were performed according to protocols described in III. C. 5.

6. Model fitting and simulations

Kinetic model fitting and predictions were made in SigmaPlot 2001 (SPSS Inc., Chicago, Il, USA). During model fitting, data were weighted by the inverse of data value. Minimization of sum of squared errors was used to achieve optimal fits. Fitting procedures and equations used are described in the Discussion section (IV. D. 5.)

D. RESULTS

1. Effect of changing $[Cs^+]_i$ and $[Na^+]_o$ on Mg^{2+}_o inhibition of whole-cell NMDA currents

I first characterized the effect of changing $[Cs^+]_i$ on Mg^{2+}_o inhibition of whole-cell NMDA currents in NR1/2A and NR1/2D receptors. cDNAs for NMDA receptors were transiently transfected into the 293T expression system. Subsequently, NMDA currents were studied in the absence and presence of added Mg^{2+}_o. In NR1/2A receptors (Figure 18A), at -85 mV, 30 μM Mg^{2+}_o inhibited current by 65% in 140 Na^+_o /125 Cs^+_i and 83% in 140 Na^+_o / 8 Cs^+_i, a 1.3-fold difference; at -35 mV, 30 μM Mg^{2+}_o inhibited current by 10% in 140 Na^+_o /125 Cs^+_i and 43% in 140 Na^+_o / 8 Cs^+_i, a 4.3-fold difference. In NR1/2D receptors (Figure 18B), the effect of changing $[Cs^+]_i$ on Mg^{2+}_o inhibition was generally similar to that in NR1/2A receptors: lowering $[Cs^+]_i$ from 125 mM to 8 mM increased Mg^{2+}_o inhibition by 1.4-fold at -85mV and 4.9-fold at -35 mV.

I then analyzed in detail the voltage dependence of the Cs^+_i effect on Mg^{2+}_o inhibition in NR1/2A and NR1/2D receptors. Concentration-inhibition curves were constructed by measuring Mg^{2+}_o inhibition in several different $[Mg^{2+}]_o$s at each voltage (see Methods). Examples of

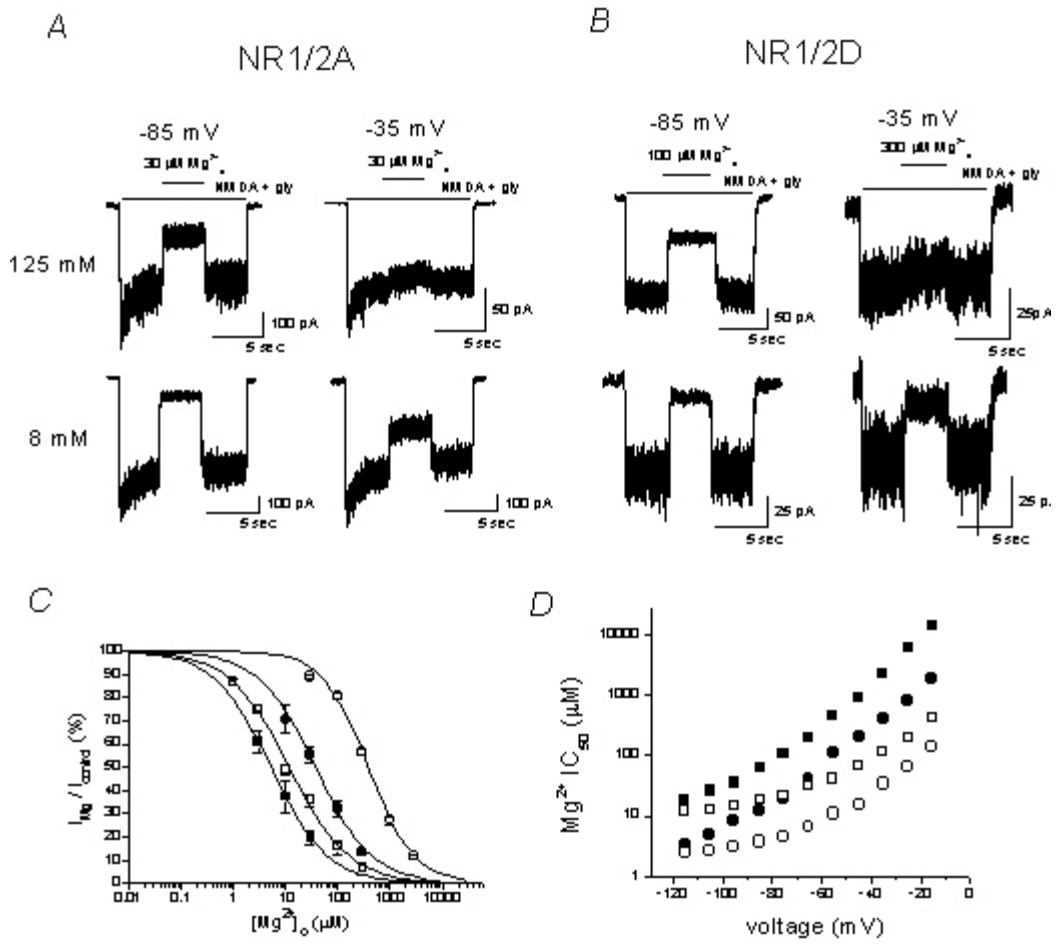

Figure 18. Effect of Cs^+_i on Mg^{2+}_o inhibition of NMDA currents. (A) NR1/2A receptor-mediated currents and their inhibition by Mg^{2+}_o are shown in 140 Na^+_o / 125 Cs^+_i (upper traces) and 140 Na^+_o / 8 Cs^+_i (lower traces). The bars above the current traces indicate the time course of drug application. At both -85 mV and -35 mV, Mg^{2+}_o inhibition was more effective in low than normal $[Cs^+]_i$. (B) In NR1/2D receptors, decreasing $[Cs^+]_i$ also enhanced Mg^{2+}_o inhibition. (C) Examples of concentration-inhibition curves are shown for NR1/2A receptors. The meaning of symbols, $[Cs^+]_i$, voltage and Mg^{2+}_o IC_{50} values are: ■, 8 mM, -85 mV, 5.2 μM; □, 125 mM, -85 mV, 11.8 μM; ●, 8 mM, -35mV, 37.3 μM; ○, 125 mM, -35 mV, 388 μM. (D) Mg^{2+}_o IC_{50} values were plotted as a function of voltage: ■, NR1/2D, 140 Na^+_o / 125 Cs^+_i; ●, NR1/2A, 140 Na^+_o / 125 Cs^+_i; □, NR1/2D, 140 Na^+_o / 8 Cs^+_i; ○, NR1/2A, 140 Na^+_o / 8 Cs^+_i . Data in 140 Na^+_o / 125 Cs^+_i were replotted from Figure 13.

concentration-inhibition curves are shown in Figure 18C for NR1/2A receptors. At each voltage, the concentration-inhibition curves are shifted to the left in low $[Cs^+]_i$, indicating increased Mg^{2+}_o affinity. The shift was greater at -35 mV than at -85 mV. In Figure 18D, I plotted the voltage dependence of the Mg^{2+}_o IC_{50}. It is clear that in each ionic condition, Mg^{2+}_o IC_{50} was lower in NR1/2A than in NR1/2D receptor at any given voltage. For both receptors, in lower $[Cs^+]_i$, not only Mg^{2+}_o IC_{50} decreased, the voltage-dependence of Mg^{2+}_o IC_{50} also became shallower.

The effects of changing $[Na^+]_o$ on Mg^{2+}_o inhibition of whole-cell currents for NR1/2A and NR1/2D receptors were studied next as shown in Figure 19. For these experiments, 8 mm Cs^+_i was used in intracellular solutions to minimize the effect of Cs^+_i on Mg^{2+}_o inhibition. Decreasing $[Na^+]_o$ from 140 mM to 70 mM moderately increased Mg^{2+}_o inhibition of NR1/2A receptors at both -105 and -45 mV (Figure 19A); The same change in $[Na^+]_o$ increased Mg^{2+}_o inhibition of NR1/2D receptors at -105 mV, but decreased Mg^{2+}_o inhibition at -45 mV.

To examine the voltage dependence of the effect of changing $[Na^+]_o$ on Mg^{2+}_o inhibition, Mg^{2+}_o IC_{50} values were measured from concentration-curves similar to those shown in Figure 18C. The results are plotted in Figure 19C. Changing $[Na^+]_o$s affect Mg^{2+}_o IC_{50} modestly in both receptors. The voltage dependence of Na^+_o effect appears to differ between the two receptors: in NR1/2A receptors, decreasing $[Na^+]_o$ reduced Mg^{2+}_o IC_{50} in a voltage-independent manner; in NR1/2D receptors, decreasing $[Na^+]_o$ increase Mg^{2+}_o IC_{50} at voltages more positive than -80 mV while the effect was opposite at voltages more negative than -80 mV.

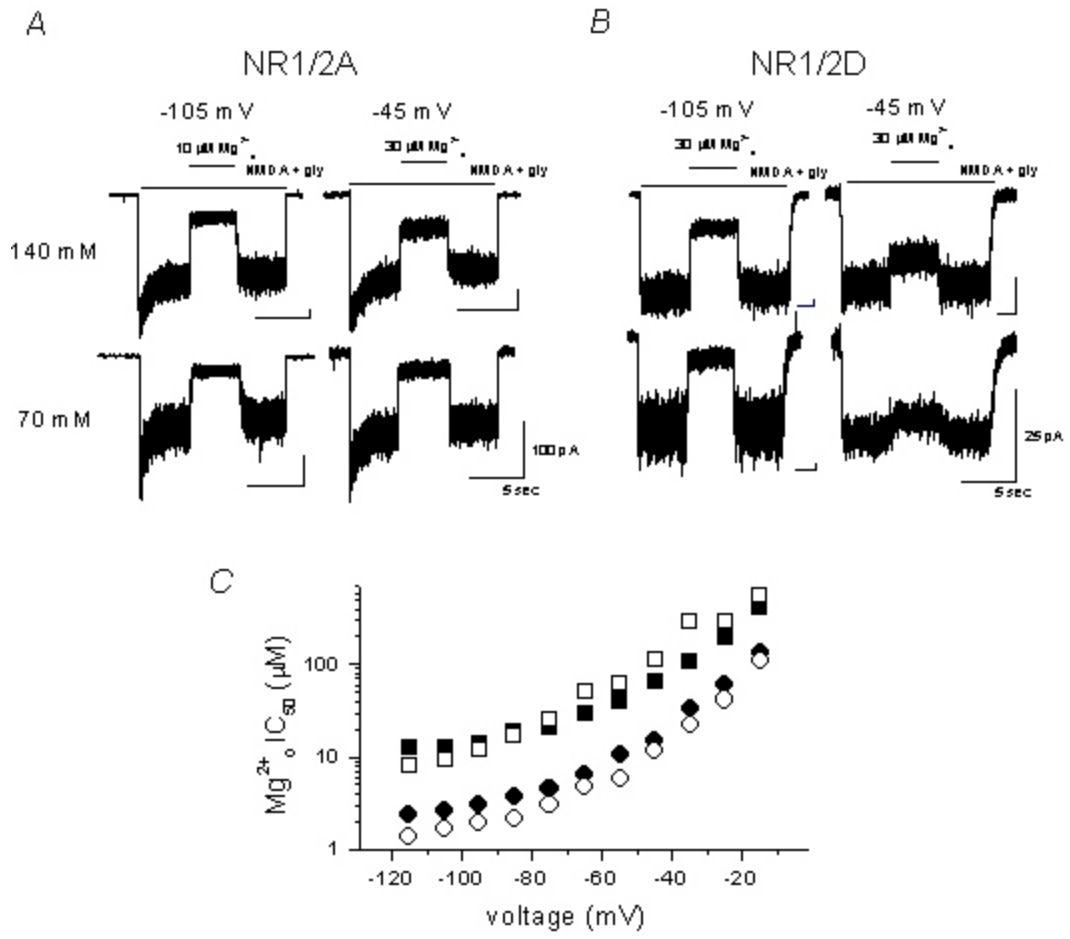

Figure 19. Effect of Na^+_o on Mg^{2+}_o inhibition of NMDA currents. (A) NR1/2A receptor-mediated currents and their inhibition by Mg^{2+}_o are shown in 140 Na^+_o / 8 Cs^+_i (upper traces) and 70 Na^+_o / 8 Cs^+_i (lower traces). At -105 mV (left traces), 10 μM Mg^{2+}_o inhibited current by 72% in 140 Na^+_o / 8 Cs^+_i, and by 79% in 70 Na^+_o / 8 Cs^+_i. At -45 mV (right traces), 30μM Mg^{2+}_o inhibited current by 56% in 140 Na^+_o / 8 Cs^+_i, and by 78% in 70 Na^+_o / 8 Cs^+_i. (B) In NR1/2D receptors, at -105 mV (left traces), 30 μM Mg^{2+}_o inhibited current by 64% in 140 Na^+_o / 8 Cs^+_i, and by 81% in 70 Na^+_o / 8 Cs^+_i. At -45 mV (right traces), 30 μM Mg^{2+}_o inhibited current by 32% in 140 Na^+_o / 8 Cs^+_i, and by 23% in 70 Na^+_o / 8 Cs^+_i. (C) Mg^{2+}_o IC_{50} values, estimated from concentration-inhibition curves, are measured from -115 to -15 mV: ■, NR1/2D, 140 Na^+_o / 8 Cs^+_i; ●, NR1/2A, 140 Na^+_o / 8 Cs^+_i; □, NR1/2D, 70 Na^+_o / 8 Cs^+_i; ○, NR1/2A, 70 Na^+_o / 8 Cs^+_i. Data collected in 140 Na^+_o / 8 Cs^+_i are replotted from Figure 18D.

To illustrate the differential effects of changing permeant ion on Mg^{2+}_o inhibition in NR1/2A and NR1/2D receptors, I studied the ratio of Mg^{2+}_o IC_{50} in normal to low ionic concentrations. To compare the effect of changing $[Cs^+]_i$s on Mg^{2+}_o inhibition in NR1/2A and NR1/2D receptors, the ratios of Mg^{2+}_o IC_{50} measured in 140 Na^+_o / 125 Cs^+_i and140 Na^+_o / 8 Cs^+_i were calculated for the two receptors (Figure 20A). A ratio of 1 in the plot would indicate no effect of $[Cs^+]_i$ on Mg^{2+}_o inhibition. It is clear that the effect of $[Cs^+]_i$ was very different between the two receptors in a voltage-dependent manner. At hyperpolarized voltages, this ratio was comparable for NR1/2D and NR1/2A receptors. In contrast, at depolarized voltages this ratio became much larger for NR1/2D than NR1/2A receptors (32.9 for NR1/2D vs. 13.4 for NR1/2A receptors at -15 mV).

The ratios of Mg^{2+}_o IC_{50} in 140 Na^+_o / 8 Cs^+_i and 70 Na^+_o / 8 Cs^+_i were plotted for both NR1/2A and NR1/2D receptors. Although the effect of changing $[Na^+]_o$ was small in both receptors (compare with Figure 20A), the voltage dependence of changing $[Na^+]_o$ was different between the two receptors: in NR1/2A receptors, the ratio was not correlated with voltage ($p = 0.068$); in NR1/2D receptors, the effect of lowering $[Na^+]_o$ went from reducing Mg^{2+}_o IC_{50} to increasing Mg^{2+}_o IC_{50} as the voltages became more depolarized ($p < 0.01$).

The results presented so far suggest that permeant ions exert powerful effects on the characteristics of Mg^{2+}_o inhibition in NR1/2D, as in NR1/2A receptors. There are also some intriguing differences between the two receptors. To understand the mechanism of these differences, I used single-channel analysis, which allowed me to examine the effect of changing permeant ion concentrations on Mg^{2+}_o blocking and unblocking steps separately.

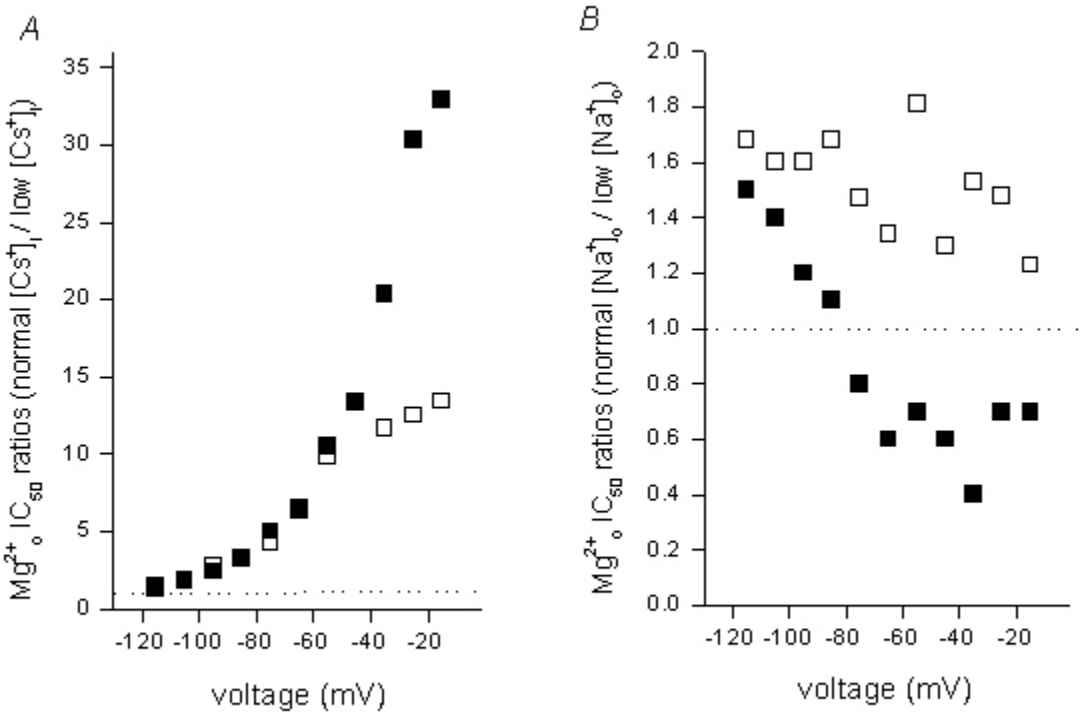

Figure 20. Differential effects of permeant ions on Mg^{2+}_o inhibition in NR1/2A and NR1/2D receptors. (A) Ratios of Mg^{2+}_o IC_{50} in 140 Na^+_o / 125 Cs^+_i and 140 Na^+_o / 8 Cs^+_i are plotted as a function of voltage for both NR1/2A (□) and NR1/2D (■) receptors. The dotted line indicates a ratio of 1. While changing $[Cs^+]_i$ has voltage-dependent effects on both receptors, the effect is stronger on NR1/2D receptors, especially at depolarized voltages. (B) Mg^{2+}_o IC_{50} ratios measured in 140 Na^+_o / 8 Cs^+_i and 70 Na^+_o / 8 Cs^+_i are plotted as a function of voltage for both NR1/2A (□) and NR1/2D (■) receptors. Distinct from the effect of changing $[Cs^+]_i$, changing $[Na^+]_o$ has only weak effects on Mg^{2+}_o IC_{50}. These effects are voltage-independent in NR1/2A receptors and weakly voltage-dependent in NR1/2D receptors.

2. Effect of changing $[Cs^+]_i$ on Mg^{2+}_o blocking and unblocking kinetics

Single-channel NMDA receptor mediated currents in the presence and absence of Mg^{2+}_o were recorded in normal and low $[Cs^+]_i$s (Figure 21). In normal $[Cs^+]_i$ (top), addition of Mg^{2+}_o made the brief channel openings appear flickery. This effect was also observed in low $[Cs^+]_i$ (bottom), but was achieved at much lower $[Mg^{2+}]_o$.

I first measured the voltage dependence of the Mg^{2+}_o blocking rate in two $[Cs^+]_i$s (Figure 22A). I will refer to this rate as the apparent blocking rate, $k_{+,app}$, which is distinct from the true Mg^{2+}_o blocking rate, k_+. Previous results from cortical NMDA receptors (Antonov & Johnson, 1999), in the same ionic solutions, are also shown for comparison. Cortical receptors most likely contain either NR2A or NR2B NR2 subunits. This is supported by previous biochemical and biophysical findings (Monyer *et al.*, 1994; Zhong *et al.*, 1994; Kirson & Yaari, 1996; Antonov & Johnson, 1999). In cortical receptors, lowering $[Cs^+]_i$ increased Mg^{2+}_o $k_{+,app}$; this effect was especially prominent at depolarized voltages. In NR1/2D receptors, I observed similar effects: at -105 mV, lowering $[Cs^+]_i$ from 125 to 8 mM changed $k_{+,app}$ from 144 $\mu M^{-1}s^{-1}$ to 232 $\mu M^{-1}s^{-1}$ (1.6-fold increase); at -45 mV, the same reduction in $[Cs^+]_i$ increased $k_{+,app}$ from 4 $\mu M^{-1}s^{-1}$ to 41.3 $\mu M^{-1}s^{-1}$ (10-fold increase). Under the same experimental conditions (ionic concentrations and voltage), the Mg^{2+}_o $k_{+,app}$ of NR1/2D is always slightly lower than cortical receptors, although the differences are not statistically significant.

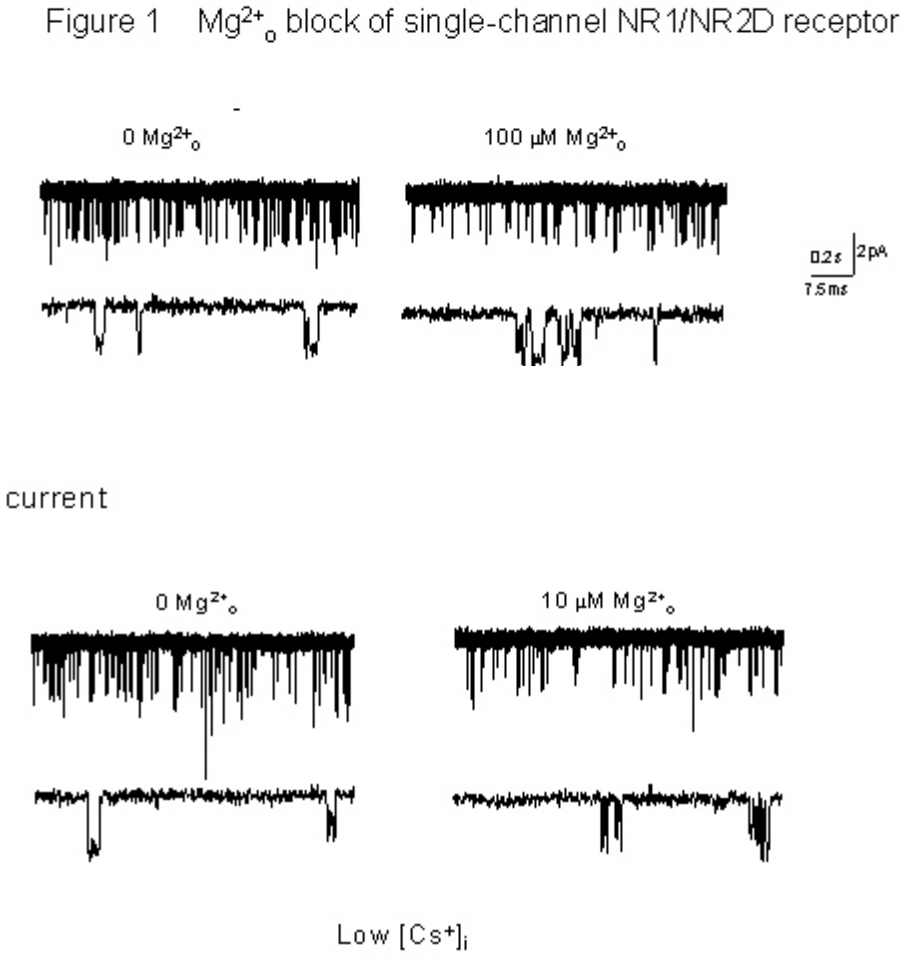

Figure 21. Examples of Mg^{2+}_o induced single-channel "flicker". Examples of NR1/2D receptor single-channel openings in the absence (left) and presence of the indicated concentrations of Mg^{2+}_o (right) are shown in normal $[Cs^+]_i$ (140 Na^+_o / 125 Cs^+_i, upper) and low $[Cs^+]_i$ (140 Na^+_o / 8 Cs^+_i, lower) conditions. Two traces are shown for each condition at different time scales. Including Mg^{2+}_o caused channel "flickers" at lower $[Mg^{2+}]_o$ in low $[Cs^+]_i$ than in normal $[Cs^+]_i$ conditions.

I next examined the effects of changing $[Cs^+]_i$ on the Mg^{2+}_o $k_{-,app}$ in NR1/2D receptors (Figure 22B). The results were compared to cortical receptors from a previous study (Antonov & Johnson, 1999). In cortical receptors, lowering $[Cs^+]_i$ did not affect Mg^{2+}_o $k_{-,app}$ over the wide voltage range tested (Antonov & Johnson, 1999). This is not the case for NR1/2D receptors. Lowering $[Cs^+]_i$ from 125 to 8 mM appeared to decrease $k_{-,app}$ in a voltage-dependent manner: at -45 mV, lowering $[Cs^+]_i$ changed $k_{-,app}$ from 3893 s^{-1} to 2516 s^{-1} ($p<0.05$); at -105 mV, lowering $[Cs^+]_i$ changed $k_{-,app}$ from 3323 s^{-1} to 2798 s^{-1} (not statistically significant). Aside from the differences in Cs^+_i effect, it seems possible that the true k_- rates, Mg^{2+}_o unblocking rate in the absence of permeant ion effects, may be different between the two receptors as well, since in $[Cs^+]_i$ as low as 8 mM, $k_{-,app}$ in cortical and NR1/2D receptors are very different at most voltages (significantly different at voltages negative than -60 mV). The voltage-dependence of $k_{-,app}$ in NR1/2D receptors was essentially flat over the range tested (in 8 mM Cs^+_i).

In summary, Cs^+_i plays a major role in shaping the characteristics of Mg^{2+}_o $k_{+,app}$ and $k_{-,app}$ in NR1/2D receptors. Similar to cortical receptors, lowering $[Cs^+]_i$ caused a voltage-dependent increase in Mg^{2+}_o $k_{+,app}$. Unlike the cortical receptors, lowering $[Cs^+]_i$ caused a decrease in Mg^{2+}_o $k_{-,app}$; this effect was also voltage-dependent. This suggests that Cs^+_i interaction with Mg^{2+}_o of NR1/2D receptors differ fundamentally from cortical receptors.

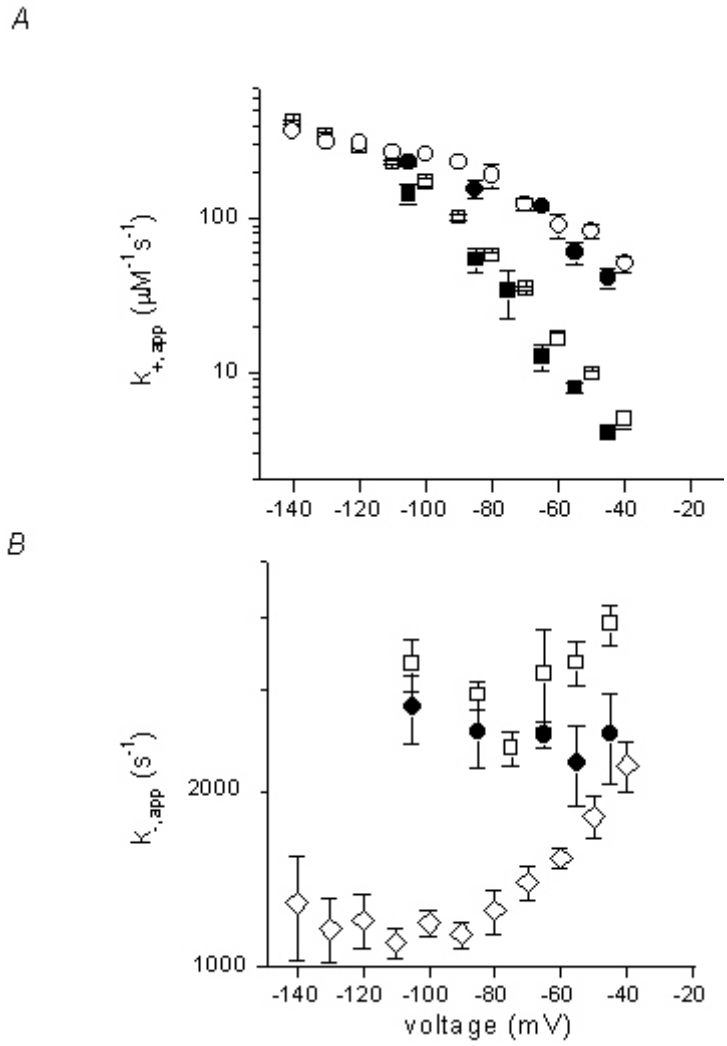

Figure 22. The effects of changing $[Cs^+]_i$ on Mg^{2+}_o $k_{+,app}$ and $k_{-,app}$. The voltage-dependent effects of changing $[Cs^+]_i$ on Mg^{2+}_o $k_{+,app}$ (A) and $k_{-,app}$ (B) of NR1/2D and cortical receptors are shown here. Symbols, receptor types, and ionic conditions are: (A), ■, NR1/2D,140 Na^+_o / 125 Cs^+_i; ●, NR1/2D, 140 Na^+_o / 8 Cs^+_i; □, Cortical, 140 Na^+_o / 125 Cs^+_i; ○, Cortical, 140 Na^+_o / 8 Cs^+_i. (B) □, NR1/2D,140 Na^+_o / 125 Cs^+_i; ●, NR1/2D, 140 Na^+_o / 8 Cs^+_i; ◊, Cortical, 140 Na^+_o / various $[Cs^+]_i$s (130, 25, 8 mM). Since Cs^+_i has no effect on $k_{-,app}$ (Antonov & Johnson, 1999), I plotted the average values of $k_{-,app}$ in multiple $[Cs^+]_i$s. Data from cortical receptors are from a previous study (Antonov and Johnson 1999); NR1/2D data in 140 Na^+_o / 125 Cs^+_i are replotted from Figure 16.

3. Effect of changing $[Na^+]_o$ on Mg^{2+}_o $k_{+,app}$ and $k_{-,app}$

Previous studies (Antonov & Johnson, 1999; Zhu & Auerbach, 2001a, b) have demonstrated the powerful effect of changing external permeant ions on Mg^{2+}_o $k_{+,app}$ and $k_{-,app}$. For examples, Antonov and Johnson (1999) observed that decreasing $[Na^+]_o$ from 140 mM to 70 mM decreased $k_{+,app}$ and increased $k_{-,app}$ with no apparent voltage dependence in cortical receptors (Figure 23). I investigated if changing $[Na^+]_o$ has a similar effect on Mg^{2+}_o $k_{+,app}$ and $k_{-,app}$ in NR1/2D receptors.

In the single-channel experiments, three sets of ionic solutions were used: 140 Na^+_o / 125 Cs^+_i, 140 Na^+_o / 8 Cs^+_i, and 70 Na^+_o / 25 Cs^+_i. I chose these experimental conditions to facilitate comparison with previous single-channel experiments (Antonov & Johnson, 1999) and to minimize data collection, which was very demanding for NR1/2D receptors. The disadvantage was that I could not directly examine the effect of changing $[Na^+]_o$ on Mg^{2+}_o $k_{+,app}$ and $k_{-,app}$ since $[Cs^+]_i$ was not constant. Mg^{2+}_o $k_{+,app}$ in 70 Na^+_o / 25 Cs^+_i solution was comparable in NR1/2D and cortical receptors at depolarized voltages but was lower in NR1/2D than cortical receptors at hyperpolarized voltages (Figure 23A). Mg^{2+}_o $k_{-,app}$ was lower in NR1/2D than cortical receptors (Figure 23B). Data of $k_{-,app}$ of cortical receptors in 70 Na^+_o / 25 Cs^+_i was from a single patch and therefore may not be very accurate. Also shown in Figure 23 were predictions of Mg^{2+}_o $k_{+,app}$ and $k_{-,app}$ in 140 Na^+_o / 25 Cs^+_i using a kinetic model, the details of which will be discussed in the section below.

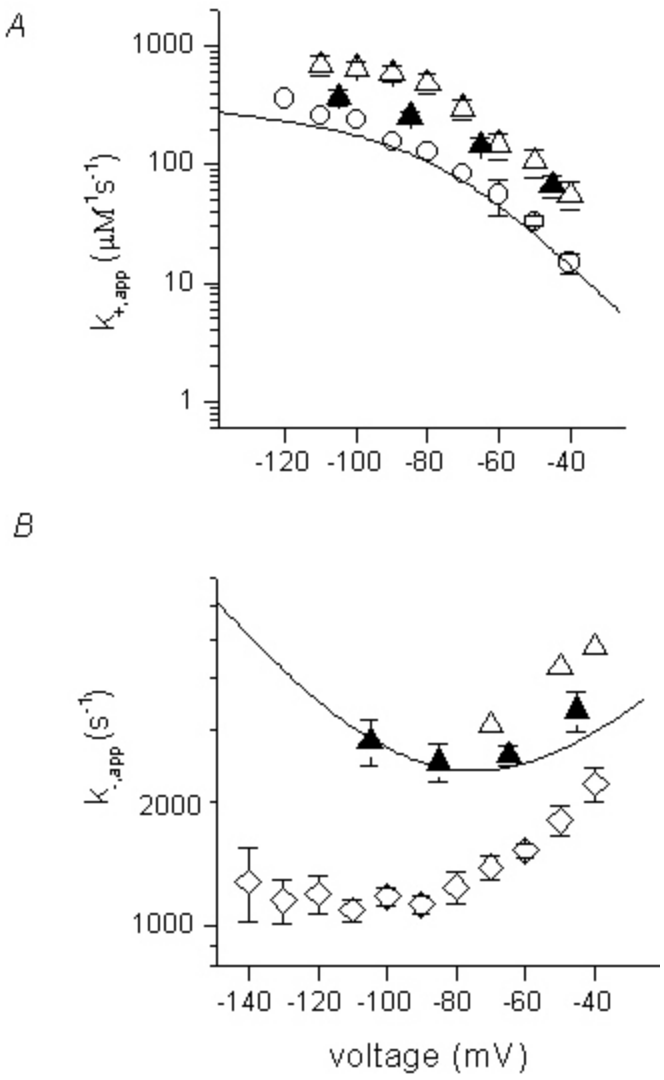

Figure 23. The effects of changing $[Na^+]_o$ on $Mg^{2+}{}_o$ $k_{+,app}$ and $k_{-,app}$. The effects of $Na^+{}_o$ on $Mg^{2+}{}_o$ $k_{+,app}$ (A) and $k_{-,app}$ (B) of NR1/2D and cortical receptors are shown here. Symbols, receptor types, and ionic conditions are: (A) ▲, NR1/2D,70 $Na^+{}_o$ / 25 $Cs^+{}_i$; line, NR1/2D, model predictions for 140 $Na^+{}_o$ / 25 $Cs^+{}_i$ (see IV. D. 6.); △, cortical, 70 $Na^+{}_o$ / 25 $Cs^+{}_i$; ○, cortical, 140 $Na^+{}_o$ / 25 $Cs^+{}_i$. (B) ▲, NR1/2D,70 $Na^+{}_o$ / 25 $Cs^+{}_i$; line, NR1/2D, model predictions for 140 $Na^+{}_o$ / 25 $Cs^+{}_i$ (see IV. D. 6.); △, cortical, 70 $Na^+{}_o$ / 25 $Cs^+{}_i$; ◇, cortical, 140 $Na^+{}_o$ / multiple $[Cs^+]_i$s (see Figure 23 legend). Data from cortical receptors are from a previous study (Antonov and Johnson 1999).

Visual inspection of NR1/2D receptors Mg^{2+}_o $k_{+,app}$ and $k_{-,app}$ in different ionic conditions offers clues of the effects of changing $[Na^+]_o$ (Figure 25A): $k_{+,app}$ in140 Na^+_o / 25 $Cs^+_{i,}$ which should fall between values of 140 Na^+_o / 125 Cs^+_i and 140 Na^+_o / 8 Cs^+_i, is likely to be lower than values in 70 Na^+_o / 25 Cs^+_i, suggesting that the effect of changing $[Na^+]_o$ on $k_{+,app}$ may be similar between NR1/2D and cortical receptors; changing $[Na^+]_o$ only has a weak effect on $k_{-,app}$, since $k_{-,app}$ in 70 Na^+_o / 25 Cs^+_i falls between values from 140 Na^+_o / 125 Cs^+_i and 140 Na^+_o / 8 Cs^+_i.

4. Development of a kinetic model

In order to understand the mechanism of permeant ion effects on Mg^{2+}_o block in NR1/2D receptors, I developed a quantitative model to account for whole-cell and single-channel data.

<u>Cs^+_i effect</u>

The data showed that lowering $[Cs^+]_i$ dramatically increased $k_{+,app}$ and this effect was much stronger at depolarized voltages (Figure 22A). This could readily be explained by previously proposed model (Antonov & Johnson, 1999; also see Figure 3) which incorporates an external Cs^+_i binding site, occupancy of which prevents Mg^{2+}_o blocking. The voltage dependence of this effect originates from the fact that occupancy of an external ion binding site by an internal permeant ion is voltage-dependent.

Changing $[Cs^+]_i$ also affected Mg^{2+}_o $k_{-,app}$ in NR1/2D receptors: decreasing $[Cs^+]_i$ reduced $k_{-,app}$, especially at depolarized voltages (Figure 22B). This is different from what was observed with

the cortical receptors, in which changing $[Cs^+]_i$ had no effect on $k_{-,app}$ (Antonov & Johnson, 1999). To explain the effect of changing $[Cs^+]_i$ on $k_{-,app}$ in NR1/2D receptors, I propose an internal binding site for Cs^+_i. Cs^+_i binding to this internal site prevents Mg^{2+}_o permeation but at the same time greatly accelerates Mg^{2+}_o unblocking to the external site, possibly through electrostatic repulsions. The voltage dependence of the effect of changing $[Cs^+]_i$ on $k_{-,app}$ can be explained if the internal Cs^+ site is located part way into the voltage field. Cs^+_i binding at the internal site must not have much impact on Mg^{2+}_o $k_{+,app}$, because if Cs^+_i binding at this site slows down Mg^{2+}_o entering the channel, I would expect that the difference in $k_{+,app}$ between NR1/2D and cortical receptors would be greater in normal than in low $[Cs^+]_i$s, especially at depolarized voltages. This was not observed (Figure 22A).

Na^+_o effect

As discussed earlier, the effects of changing $[Na^+]_o$ on Mg^{2+}_o $k_{+,app}$ and $k_{-,app}$ in NR1/2D receptors could not be directly examined from data since changing $[Na^+]_o$ was accompanied by changing $[Cs^+]_i$. However, comparison of Mg^{2+}_o $k_{+,app}$ and $k_{-,app}$ in different ionic conditions suggests that the effect of changing $[Na^+]_o$ on $k_{+,app}$ may be similar between NR1/2D and cortical receptors while the effect of changing $[Na^+]_o$ on $k_{-,app}$ is likely to be weaker in NR1/2D than cortical receptors. Based on these observations, I propose that, just like for the cortical receptors (Anotonov & Johnson, 1999; also see Figure 3), Na^+_o binding to one or two external ion binding sites prevents Mg^{2+}_o block; Na^+_o binding to the external sites must not be significant to have strong effects on $k_{-,app}$.

Description of the kinetic model

The features of a kinetic model (Model 1) are illustrated in Figure 24. This model accounts for the effects of changing permeant ion concentrations on Mg^{2+}_o $k_{+,app}$ and $k_{-,app}$ in NR1/2D receptors. (1) There are two external and one internal permeant ion binding sites. Cs^+_i can occupy the internal site and one of the external sites; Na^+_o can occupy either one of the external sites. Permeant ion binding to one site does not affect the affinity of ions for other site(s). (2) Mg^{2+}_o can only enter and block the channel when the external sites are empty (through States 1 and 9). (3) Mg^{2+}_o can exit to the external side, or permeate the channel. When the external site(s) are occupied by Na^+_o, Mg^{2+}_o unblock to the external side is prevented but Mg^{2+}_o permeation can still take place. When the internal site is occupied by Cs^+_i, Mg^{2+}_o permeation is prevented but its unblocking to the external site is greatly enhanced (State10).

Model 1, which was developed to explain the data in NR1/2D receptors, is distinct from previous proposed model (Antonov & Johnson, 1999) for cortical receptors (Figure 3) in that Model 1 introduces an additional internal Cs^+_i binding site, occupancy of which greatly accelerates Mg^{2+}_o $k_{-,app}$.

Figure 24. Model of Mg^{2+}_o block of NR1/2D receptors. Model 1, which is based on single-channel experiments, is illustrated here. ●, Cs^+_i; ●, Na^+_o; ●, Mg^{2+}_o; ↔, transitions at equilibrium or psudo-equilibrium; →, transitions which can only go one direction; ⇋, Mg^{2+}_o blocking and unblocking steps. States 1-8 are states with the intracellular Cs^+_i site unoccupied: states 1 and 2 schematize Mg^{2+}_o blocks and unblocks a channel with no permeant ion bound; states 3-6 illustrate states in which the external permeant ion sites are occupied and Mg^{2+}_o blocking is prevented. States 7-8 are states in which Mg^{2+}_o cannot unblock due to lock-in effect by Na^+_o. States 9-16 correspond to states 1-8, except a Cs^+_i bound to the intracellular site. Dashed boxes highlight states which are occupied rarely.

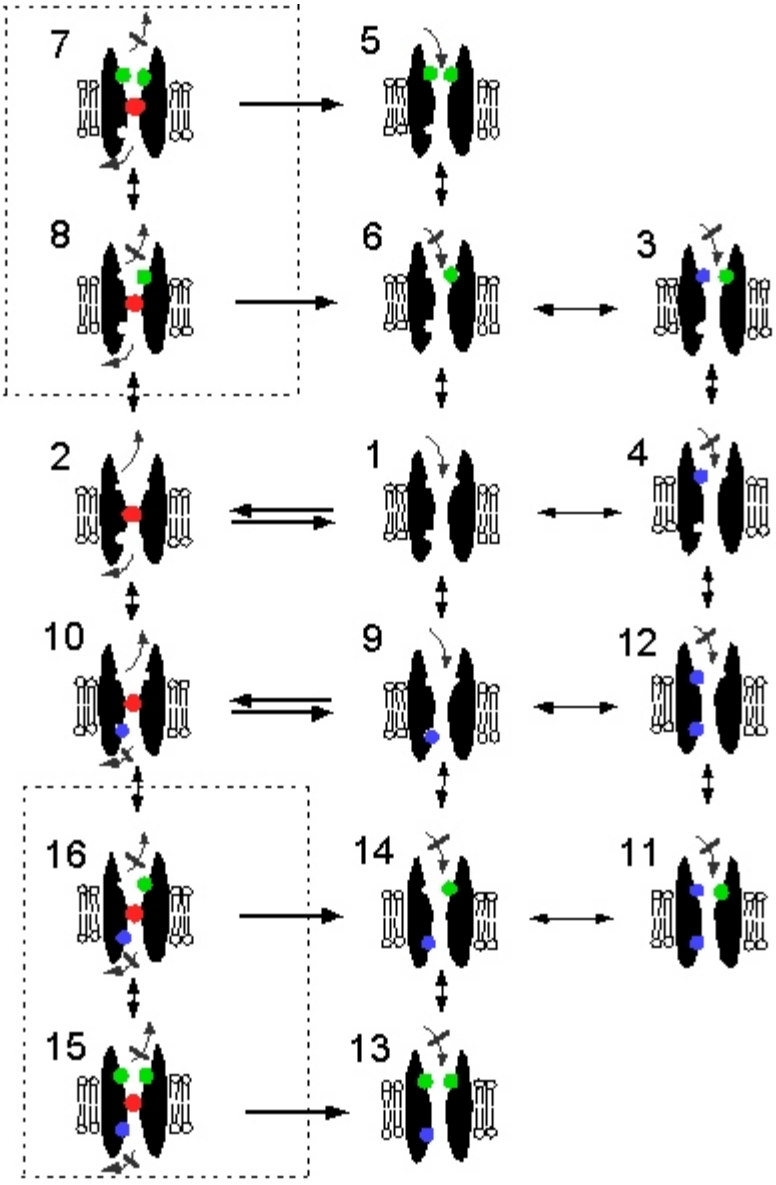
7
5
8
6
3
2
1
4
10
9
12
16
14
11
15
13

5. Fitting equations and procedures

The equations used in fitting of Model 1 are listed below:

(1) $k_{+,app} = k_{+} * (1+ [Na^{+}]_o /K_{Na1})^{-1} * (1+ [Na^{+}]_o /K_{Na1}+ [Cs^{+}]_i / K_{Cs1})^{-1}$

$k_{+} = k_{+}(0) * \exp(-V_m / V_1)$

$K_{Cs1}= K_{Cs1}(0) * \exp(-V_m / V_{Cs1})$

(2) $k_{-,app} = k_{-,o} * (1+ [Cs^{+}]_i / K_{Cs2})^{-1} *(1+ [Na^{+}]_o / K_{Na2})^{-2} + k_{-,o}' (1+ K_{Cs2} / [Cs^{+}]_i)^{-1} *(1+ [Na^{+}]_o / K_{Na2})^{-2} + k_{-,i} * (1+ [Cs^{+}]_i / K_{Cs2})^{-1}$

$k_{-,o} = k_{-,o}(0) * \exp(V_m/V_2)$

$k_{-,o}' = k_{-,o}(0)' * \exp(V_m/V_2)$

$k_{-,i} = k_{-,i}(0) * \exp(-V_m/V_3)$

$K_{Cs2}= K_{Cs2}(0) * \exp(-V_m/ V_{Cs2})$

The meaning of the parameters is listed below. The adjustable parameters used in fitting are shown in bold (see text below).

K_{Na1} Na^{+}_o equilibrium dissociation constant to the external site(s) with no Mg^{2+}_o bound

K_{Na2} Na^{+}_o equilibrium dissociation constant to the external site(s) with Mg^{2+}_o binding

K_{Cs1} Cs^{+}_i pseudo equilibrium dissociation constant for the external site

$K_{Cs1}(0)$ K_{Cs1} at 0 mV

V_{Cs1} voltage-dependence of K_{Cs1}

K_{Cs2}	Cs^+_i pseudo equilibrium dissociation constant for the internal site with Mg^{2+}_o bound
$\mathbf{K_{Cs2}(0)}$	K_{Cs2} at 0 mV
$\mathbf{V_{Cs2}}$	voltage-dependence of K_{Cs2}
$k_{+,app}$	apparent Mg^{2+}_o blocking rate constant
k_+	true Mg^{2+}_o blocking rate constant
$\mathbf{k_+(0)}$	k_+ at 0 mV
$\mathbf{V_1}$	voltage-dependence of k_+
$k_{-,app}$	apparent Mg^{2+}_o unblocking rate
$k_{-,o}$	Mg^{2+}_o unblocking to the outside without Cs^+_i bound at the internal site
$\mathbf{k_{-,o}(0)}$	$k_{-,o}$ at 0 mV
$\mathbf{V_2}$	voltage-dependence of $k_{-,o}$ and $k_{-,o}'$
$k_{-,o}'$	Mg^{2+}_o unblocking to the outside with Cs^+_i bound at the internal site
$\mathbf{k_{-,o}(0)'}$	$k_{-,o}'$ at 0 mV
$k_{-,i}$	true rate of Mg^{2+}_o permeation
$\mathbf{k_{-,i}(0)}$	$k_{-,i}$ at 0 mV
$\mathbf{V_3}$	voltage-dependence of $k_{-,i}$

Eight data sets were used for model fitting: (1) $k_{+,app}$ in 140 Na^+_o / 125 Cs^+_i; (2) $k_{+,app}$ in 140 Na^+_o / 8 Cs^+_i; (3) $k_{+,app}$ in 70 Na^+_o / 25 Cs^+_i; (4) $k_{-,app}$ in 140 Na^+_o / 125 Cs^+_i; (5) $k_{-,app}$ in 140 Na^+_o / 8 Cs^+_i; (6) $k_{-,app}$ in 70 Na^+_o / 25 Cs^+_i; (7) whole-cell measured IC_{50} values in 140 Na^+_o / 125 Cs^+_i; (8) whole-cell measured IC_{50} value in 140 Na^+_o / 8 Cs^+_i. Since IC_{50} values are in good agreement with the ratios of $k_{-,app}$ to $k_{+,app}$ measured from single-channel experiments (Figure 17 for 140 Na^+_o / 125 Cs^+_i; data not shown for 140 Na^+_o / 8 Cs^+_i), data sets (7) and (8) gave the values of ratio of $k_{-,app}$ to

$k_{+,app}$ in 140 Na^+_o / 125 Cs^+_i and 140 Na^+_o / 8 Cs^+_i solutions. Data sets (7) and (8) are related to, but independent of data sets (1), (2), (4) and (5) since the experiments were performed independently and under different conditions (whole-cell vs. single-channel). Including whole-cell data has considerable advantages because (1) whole-cell experiments were carried out over a wider ranges of voltages; (2) whole-cell estimates of IC_{50} were based on many data points that were measured with low noise, so errors of IC_{50} are very small, and thus they improve the confidence of the fitting results. Whole-cell data collected in70 Na^+_o / 8 Cs^+_i, however, were not used in fitting, since single-channel data under the same ionic condition were not available to assess if IC_{50} values agree with the ratios of $k_{-,app}$ and $k_{+,app}$; this agreement is a prerequisite for fitting of whole-cell and single channel data together.

Adjustable parameters used in fitting of $k_{+,app}$ were K_{Na1}, $K_{Cs1}(0)$, $V_{Cs1,}$ $k_+(0)$ and V_1. Adjustable parameters used in fitting of $k_{-,app}$ were K_{Na2}, $K_{Cs2}(0)$, V_{Cs2}, $k_{-,o}(0)$, $V_{2,}$ $k_{-,o}(0)'$, $k_{-,i}(0)$ and $V_{3.}$. All the adjustable parameters were used in fitting of IC_{50}. Fitting of the eight data sets were performed simultaneously so that a single set of parameter values derived from fitting applied to all eight data sets.

6. Fitting results

The results from simultaneous fitting of whole-cell and single-channel data are shown in Figure 25 and the parameter values are listed in Table 3 (under Model 1). All adjustable parameters were left free during fitting, without constraining them to any predetermined values. In general, Model 1 provides satisfactory fits to both whole-cell and single-channel data.

The parameter values provide additional insights into permeant ion binding and Mg^{2+}_o block. The equilibrium dissociation constant of Na^+_o and Cs^+_i for the external binding sites suggest that, at a resting potential of -70mV, Mg^{2+}_o can access the channel of NR1/2D receptors only about 1% of the time. The voltage-dependence of Mg^{2+}_o block suggests that the energy barrier for Mg^{2+}_o block is about 9% into the voltage field, and the Mg^{2+}_o binding site about 42% into the voltage-field (from the external side). The model suggests that Mg^{2+}_o unblocking to the external side is greatly accelerated (230-fold) by the presence of Cs^+_i at the internal site. It might be surprising that Cs^+_i can exert such a great influence on Mg^{2+}_o $k_{-,app}$ when its equilibrium dissociation constant (K_{Cs2}, with Mg^{2+}_o bound)is as high as 15.5 M. This is indeed the case due to much faster $k_{-,o}$' than $k_{-,o}$: much faster Mg^{2+}_o unblock rate from State 10 than State 2 compensates for the fact that State 10 is only rarely occupied (because of high K_{Cs2}), comparing to State 2. As expected from the data, the affinity of Na^+_o for the external site(s) with Mg^{2+}_o is in the channel is very low; the equilibrium dissociation constant is 452 mM. Parameter values from Model 1 (Table 3) were also used to predict $k_{-,app}$ and $k_{+,app}$ in 140 Na^+_o / 25 Cs^+_i (Figure 23). The effect of reducing $[Na^+]_o$ on $k_{+,app}$ is similar in NR1/2D and cortical receptors (Figure 23A). The effect of reducing $[Na^+]_o$ on $k_{-,app}$ in NR1/2D receptors is clearly distinct from that in cortical receptors (Figure 23B).

I also used an alternative model to fit the data. This model (Model 2) has all the states in Model 1, except States 7,8, 15 and 16. Thus, Model 2 explicitly prevents Na^+_o binding when Mg^{2+}_o is in the channel. When free fits were attempted initially, although the model fit data very well, parameter V_{Cs2} did not yield a value which was physically possible – it placed the internal site all the way to the external side. Zhu and Auerbach (2001a) also reported a permeant ion site internal to the

Mg^{2+}_o binding site in NR1/2A or NR1/2B receptors. Although it is possible that the relative positions of ion binding sites are different between NR1/2D and NR1/2A or NR1/2B receptors, I nevertheless used their value to constrain the position of the internal site to test the feasibility of the model. Parameter values from Model 2 are listed in Table 3. Model 2 also gave excellent fits to the data (results not shown). Model 1 gave slightly better fit statistically.

I also used the kinetic models discussed above to predict the ratio of Mg^{2+}_o $k_{-,app}$ to $k_{+,app}$ in 70 Na^+_o / 8 Cs^+_i (using parameter values listed in Table 3) and results are shown in Figure 25C (only results from Model 1 are shown; Model 2 gave comparable results). Although the predictions of $k_{-,app}$ and $k_{+,app}$ ratios do not agree with Mg^{2+}_o IC_{50} values very well, the deviation between model predictions and data is small and the model does predict the difference in voltage dependence of IC_{50} between 140 Na^+_o / 8 Cs^+_i and 70 Na^+_o / 8 Cs^+_i. What is the origin of this difference, when the effects of Na^+_o on Mg^{2+}_o $k_{+,app}$ (or $k_{-,app}$) are voltage-independent? The difference in voltage dependence likely originates from the competition between Na^+_o and Cs^+_i for the external site, since at depolarized voltages Cs^+_i occupation of one of the external sites is high and Na^+_o binding has little additional effect on $k_{+,app}$, while at hyperpolarized voltage Cs^+_i occupies the external site less frequently and Na^+_o binding can have a greater effect on $k_{+,app}$.

The reason for the discrepancy between data (Mg^{2+}_o IC_{50}) and model predictions (K_D) in 70 Na^+_o / 8 Cs^+_i is unclear. It is worth noting that in cortical receptors (Qian *et al.*, 2002), the model also fails to provide very accurate predictions for the data in 70 Na^+_o / 8 Cs^+_i. It might be the case that under very low permeant ion concentrations, channel gating or receptor conformation is altered and

Figure 25. Model fitting of the effects of Cs^+_i and Na^+_o on Mg^{2+}_o block of NR1/2D receptors. (A) Mg^{2+}_o $k_{+,app}$ measured in 140 Na^+_o / 125 Cs^+_i (■), 140 Na^+_o / 8 Cs^+_i (●), and 70 Na^+_o / 25 Cs^+_i (●) are plotted as a function of voltage. Predictions of Model 1 using parameter values shown in Table 3 are plotted as lines; line colors have the same meaning as symbol colors . (B) Voltage-dependence of Mg^{2+}_o $k_{-,app}$ measured in 140 Na^+_o / 125 Cs^+_i (■), 140 Na^+_o / 8 Cs^+_i (●), and 70 Na^+_o / 25 Cs^+_i (●) are plotted as a function of voltage. Predictions of Model 1 using parameter values shown in Table 3 are plotted as lines (line colors have the same meaning as symbol colors). (C) The voltage-dependence of Mg^{2+}_o IC_{50} values measured in 140 Na^+_o / 125 Cs^+_i (■), 140 Na^+_o / 8 Cs^+_i (●), and 70 Na^+_o / 8 Cs^+_i (■) are plotted as a function of voltage. Lines are predictions of Model 1 for Mg^{2+}_o IC_{50} in 140 Na^+_o / 125 Cs^+_i, 140 Na^+_o / 8 Cs^+_i and 70 Na^+_o / 8 Cs^+_i (line colors have the same meaning as symbol colors). Whole-cell data collected in 70 Na^+_o / 8 Cs^+_I were not used in fitting (see text).

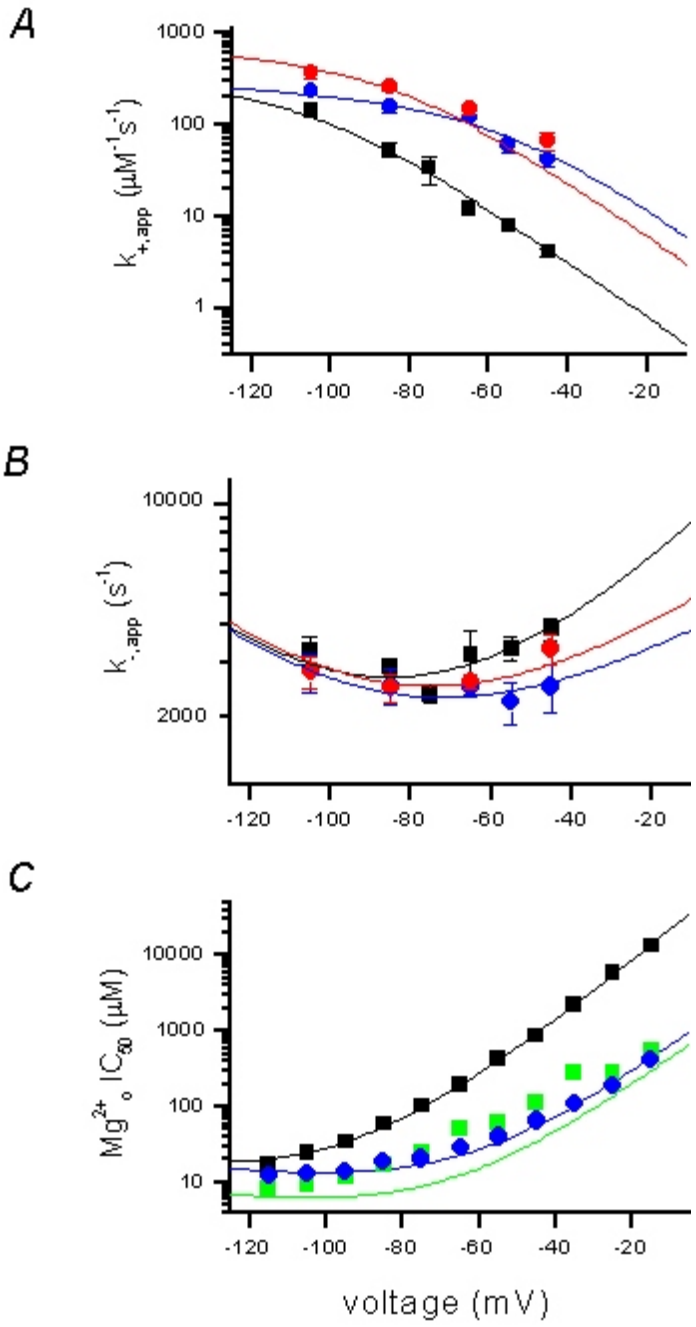
A
1000
100
10
1
$k_{+,app}$ ($\mu M^{-1}s^{-1}$)
-120
-100
-80
-60
-40
-20
B
10000
2000
$k_{-,app}$ (s^{-1})
-120
-100
-80
-60
-40
-20
C
10000
1000
100
10
Mg^{2+}_{o} IC_{50} (μM)
-120
-100
-80
-60
-40
-20
voltage (mV)

Table 3 Parameter values from model fitting

Parameter	Model 1	Model 2
K_{Na1}	59.7 mM	59.2 mM
$k_{+}(0)$	1170 μM^{-1} s^{-1}	1420 μM^{-1} s^{-1}
V_1	137 mV	180 mV
$K_{Cs1}(0)$	79.0 μM	67.9 μM
V_{Cs1}	16.9 mV	16.5 mV
$k_{-,o}(0)$	7420 s^{-1}	4920 s^{-1}
V_2	38.7 mV	33.7 mV
$k_{-,o}(0)'$	1710000 s^{-1}	186000 s^{-1}
$k_{-,i}(0)$	556 s^{-1}	707 s^{-1}
V_3	68.7 mV	78.8 mV
$K_{Cs2}(0)$	15.5 M	2.86 M
V_{Cs2}	94 mV	158 mV *
K_{Na2}	452 M	—
$K_{Cs3}(0)$**	66.7 mM	75.3 mM

These parameter values gave best fit as determined by sum of squared errors in SigmaPlot 2001.

* Parameter was constrained to this value (Zhu & Auerbach, 2001a).

** $K_{Cs}3(0)$, the pseudo equilibrium dissociation constant of Cs^{+}_{i} for the internal site with no Mg^{2+}_{o} bound at 0 mV, is not incorporated in the equations (IV. D. 5.). Its value was calculated in each model assuming that microreversibility is conserved in the closed loop of States 1, 2, 9 and 10.

consequently a common set of parameter values can not account for Mg^{2+}_o block under both relatively normal and extreme ionic conditions.

E. DISCUSSION

To understand the mechanism of the permeant ion effects on Mg^{2+}_o block in NR1/2D receptors, it was instructive to compare the results with work on cortical receptors from published work (Antonov & Johnson, 1999), which was conducted using comparable experimental protocols as those described in the current study. Cortical receptors contain either NR2A or NR2B NR2 subunits. This is supported by previous biochemical and biophysical findings (Monyer *et al.*, 1994; Zhong *et al.*, 1994; Kirson & Yaari, 1996; Antonov & Johnson, 1999). When Mg^{2+}_o IC_{50} values from cortical and NR1/2A receptors were compared, the results from both receptors were in general comparable. This was true for both Mg^{2+}_o IC_{50} values measured (Figure 13), as well as the effects of changing $[Na^+]_o$ and $[Cs^+]_i$ on Mg^{2+}_o inhibition. In both receptors, the prominent and voltage-dependent effects produced by changing $[Cs^+]_i$ are evident (compare Figures 8 and 20); the effects of changing $[Na^+]_o$ are moderate and voltage-independent in both receptors ($p = 0.068$ for NR1/2A; $p = 0.157$ for cortical receptors). Therefore, the mechanism proposed for cortical receptors (Antonov & Johnson, 1999) can be used as a reasonable model for NR1/2A receptors as well.

There were, however, some small but noticeable differences between Mg^{2+}_o IC_{50} values measured from the two receptor types (compare Figures 8 and 20). Since IC_{50} values at each voltage were single fits to a population data, statistical tests could not be used to assess the significance of the differences. These differences in Mg^{2+}_o IC_{50} between the two receptors, if significant, are

surprising since the experimental protocol was exactly the same and cortical receptors almost certainly contained only NR2A and NR2B NR2 types, which are comparable in Mg^{2+}_o inhibition. It is possible that in neurons there was inadequate exchange between cytoplasm and pipette solution and consequently poor control of $[Cs^+]_i$. This was not very likely since (1) whole-cell recording started at least five minutes after breaking into whole-cell; (2) for cortical receptors, whole-cell measured IC_{50} and single-channel measured K_D values were very similar, suggesting that measurements of IC_{50} for cortical receptors were accurate. Thus, the origin of the small differences between cortical receptors and NR1/2A receptors expressed in expression system is unclear at this point.

Comparison between NR1/2D and cortical receptors

The results presented here provide mechanistic explanations for the differences in the effects of permeant ions on Mg^{2+}_o block of NR1/2D and cortical receptors. Although the effects of Na^+_o and Cs^+_i on Mg^{2+}_o blocking rates were qualitatively similar in the two receptors, there are significant differences between them in terms of how Na^+_o and Cs^+_i affect Mg^{2+}_o unblocking rates. In NR1/2D receptors, lowering $[Cs^+]_i$ reduced Mg^{2+}_o $k_{-,app}$ in a voltage-dependent manner while changing $[Cs^+]_i$ had no effect on $k_{-,app}$ in cortical receptors. This explains the observed differences between cortical and NR1/2D in Mg^{2+}_o IC_{50} ratios in normal and low $[Cs^+]_i$s shown in Figure 20A. The ratios of Mg^{2+}_o IC_{50} in normal and low $[Cs^+]_i$s are higher in NR1/2D than cortical receptors due to two processes: (1) Cs^+_i binding affinity to the external site is higher in NR1/2D receptors and changing $[Cs^+]_i$ has greater effects on $k_{+,app}$ in NR1/2D than cortical receptors. (2) Cs^+_i binding to the internal site greatly enhance Mg^{2+}_o unblocking to the outside and the voltage dependence of this process

further exaggerates the already steep voltage dependence of Cs^+_i effect. Since the effect of Cs^+_i binding to internal site on enhancing Mg^{2+}_o unblocking is absent in cortical receptors, their ratio of Mg^{2+}_o IC_{50} in normal and low $[Cs^+]_i$ are not as steeply voltage-dependent as in NR1/2D receptors.

Changing $[Na^+]_o$ had similar effects on $k_{+,app}$ in NR1/2D and cortical receptors (Figure 23A). The effect of changing $[Na^+]_o$ on $k_{-,app}$ is, however, different between the two receptors (Figure 23B): in cortical receptors, Na^+_o has a lock-in effect on Mg^{2+}_o $k_{-,app}$ but this is nearly absent in NR1/2D receptors. Thus, based on models, the ratios of Mg^{2+}_o IC_{50} in140 Na^+_o / 8 Cs^+_i and 70 Na^+_o / 8 Cs^+_i solutions should be different between the two receptors (Figure 20B): decreasing $[Na^+]_o$ in NR1/2D decreases IC_{50} since $k_{+,app}$ was increased but $k_{-,app}$ was not affected; decreasing $[Na^+]_o$ only has a weak effect on IC_{50}, since increasing in both $k_{-,app}$ and $k_{+,app}$ would cancel out each other.

Despite the differences in the mechanisms of Na^+_o and Cs^+_i interaction with Mg^{2+}_o block of NR1/2D and cortical receptors, the present study suggests that both receptors follow a common design in the overall arrangements of permeant ion binding sites: two external ion binding sites and one internal ion binding site. A model, which was based on work done on the effects of changing $[K^+]$ on Mg^{2+}_o $k_{+,app}$ and $k_{-,app}$ in NR1/2A or NR1/2B receptors (Zhu & Auerbach, 2001a), included permeant ion binding sites very similar to what is proposed here. Although Antonov and Johnson (1999) did not see evidence for an internal ion binding site, it could simply be because the binding affinity of the internal site is very different among permeant ions. Consistent with this idea, Na^+ did not appear to bind to the internal site either (Zhu & Auerbach, 2001b). Interestingly, Antonov *et al.* (1998) reported an internal Cs^+ binding site which affected how the organic channel blocker IEM-

1754 interacts with NMDA receptors. This site, which is located outside the voltage field, may be distinct from the internal ion site discussed earlier.

In addition to the differences in permeant ion effects on Mg^{2+}_o $k_{+,app}$ and $k_{-,app}$, the true properties of Mg^{2+}_o block (value and voltage-dependence of blocking and unblocking rates in the absence of permeant ions) are also likely to be different between NR1/2D and cortical receptors (see Table 3; Antonov & Johnson, 1999). For example, the barrier site for Mg^{2+}_o blocking is much shallower in NR1/2D than in cortical receptors; Mg^{2+}_o permeation is also likely to be faster in NR1/2D receptors. These properties will be further discussed in Chapter V.

V. GENERAL DISCUSSIONS

NMDA receptors are critically involved in functions of the vertebrate CNS. The research presented in this Dissertation was designed to advance our understanding of a fundamental property of NMDA receptor: the voltage-dependent block by Mg^{2+}_o. Mg^{2+}_o block not only serves crucial physiological functions, it also provides an opportunity to explore fundamental biophysical issues, including the mechanism of gating, the properties of the ion channel, and the structure of the channel. I focused my research on the permeant ion and NR2 subunit dependence of Mg^{2+}_o block. The broader implications of this research are discussed in this chapter.

A. CHANNEL GATING STATES AND INTERACTION WITH BLOCKERS

An ion channel can exist in multiple gating states, including closed, open at different conductance levels, or desensitized states. Whether a channel is open or closed can influence the effectiveness of a channel blocker. To demonstrate that Mg^{2+}_o preferably binds to the open vs. the closed channel is a challenging task. Since Mg^{2+}_o blocking and unblocking kinetics are much faster than the gating transitions, even if Mg^{2+}_o could block the closed channel, it may unblock before the channel opens. Although many studies, including both work presented here and elsewhere (Nowak *et al.*, 1984; Ascher & Nowak, 1988; Sobolevsky & Yelshansky, 2000), have demonstrated that Mg^{2+}_o can occupy a site in the channel when it is open, the possibility remains that Mg^{2+}_o can readily bind to the closed channel. At present, there is no direct way to put this issue to rest. Amar *et al.*

(2001) reported the high affinity Zn^{2+} block of a mutant NMDA receptor. Zn^{2+} blocks the channel with slow kinetics and it blocks preferably to the open channels. Zn^{2+}_o, whose blocking site is very near that of Mg^{2+}_o, is also more similar to Mg^{2+}_o in size than larger organic molecules. Notwithstanding the imperfect analogy (mutant vs. wild type receptors; Zn^{2+}_o vs. Mg^{2+}_o), it lends support to Mg^{2+}_o blocking only open channels.

Channel blockers can affect gating transitions. This effect ranges from completely preventing channel closures (e.g., as do sequential blockers) to having no effect on gating. In both cortical and NR1/2D receptors, whole-cell measured Mg^{2+}_o IC_{50} and microscopic K_D values are very similar under various voltage and ionic conditions. For other channel blockers that affect gating transitions, the ratio of IC_{50} to K_D could be as high as 60 (Sobolevsky, 2003). The most parsimonious explanation for the ratio of IC_{50} to K_D being 1 is that Mg^{2+}_o block has no effect on gating movements, or, to put it differently, conformational changes that occur during gating have no impact on the Mg^{2+}_o binding site. This observation has implications for the location of the gate – it is likely to be somewhere other than near the Mg^{2+}_o blocking site. An external gate is supported by studies characterizing organic channel blockers of NMDA receptors (Qian & Johnson, 2002), while a deeper gate is suggested by SCAM experiments in combination with channel blocker studies (Sobolevsky *et al.*, 2002a).

In contrast to the active research on NR1/2A or NR1/2B receptors, NR1/2D receptors have not been rigorously investigated. Many intriguing aspects of NR1/2D receptor gating have been reported: (1) the deactivation of NMDA receptors after glutamate application is extremely slow

(Monyer *et al.*, 1992; Vicini *et al.*, 1998; Wyllie *et al.*, 1998), (2) there is a prominent subconductance state (Wyllie *et al.*, 1996; Misra *et al.*, 2000), and (3) the transitions from the main conductance to the subconductance state is nearly twice as frequent as the reverse transition (Wyllie *et al.*, 1996; Misra *et al.*, 2000).

The origin of subconductance states is not well understood. In some cases, different conductance states are correlated with various liganded states; subconductance states predominate for partially liganded-channels, while main conductance states are more prevalent for fully liganded channels (Ruiz & Karpen, 1997; Rosenmund *et al.*, 1998). Whether a correlation between receptor activation and conductance states exists for NR1/2D receptors is unknown at present. Ion selectivity may differ among various receptor activation states (for example, Hackos & Korenbrot, 1999). Schneggenburger and Ascher (1997) reported a mutant NMDA receptor which exhibits differential ion selectivity for difference conductance states. It would be very interesting to determine whether Mg^{2+}_{o} blocks the main and subconductance states with similar properties. Unfortunately, the short duration of channel open events makes it impossible at present to reliably address this question.

Direct transitions between two conductance states often occur with equal frequency in each direction (for example, Stern *et al.*, 1992). Even NR1/2C receptors, which have similar main and subconductance states as in NR1/2D receptors, do not exhibit unequal frequency of transitions that NR1/2D receptors do (Wyllie *et al.*, 1996). The unbalance in the transition frequency in NR1/2D receptors could be the result of permeant ion interaction with gating (Lauger, 1985). Incidentally, permeant ion interaction with gating might be taken as indirect evidence that the gate is near the

selectivity filter, if the receptor can only hold a single ion at a time. The fact that NR1/2D receptors alone shows the unbalance in the transition frequency raises the possibility that the gate location, or gating mechanism, of NR1/2D receptors is fundamentally different from other NMDA receptors. Further work is needed to explore these differences.

B. ION INTERACTIONS IN THE CHANNEL

1. Voltage-dependence of channel block

Channel block often exhibits voltage dependence. Charged blockers may experience voltage dependence if the blocking site is part way into the voltage-field (Woodhull, 1973). Even when the blocking site is outside the voltage-field, voltage-dependence of channel block could be achieved if the block is coupled to permeant ion movements, which are themselves voltage-sensitive (for examples, Hille & Schwarz, 1978; Spassova & Lu, 1998; Guo *et al.*, 2003). Blockers of multi-ion channels often exhibit very steep voltage-dependence since ion movements are highly coupled within such channels. Previous works (Antonov & Johnson, 1999; Zhu & Auerbach, 2001a, b; Qian *et al.*, 2002), as well as research presented here, have demonstrated that Mg^{2+}_o block of NMDA receptors derives its voltage-dependence from both the presence of its binding site in the voltage field, and voltage-dependent permeant ion effects.

The model presented in Figure 24 allows the true Mg^{2+}_o blocking and unblocking rates, in the absence of permeant ion effects, to be predicted. Table 4 lists the true rate constants and the voltage dependence for these values of Mg^{2+}_o block of NR1/2D receptors. I also listed previously published values for Mg^{2+}_o block of cortical receptors (Antonov & Johnson, 1999) for comparison.

The true Mg^{2+}_o blocking and unblocking properties differ between the two receptors. For example, Mg^{2+}_o $k_{-,o}(0)$ is about 15-fold higher in cortical than NR1/2D receptors, while Mg^{2+}_o $k_{-,i}(0)$ is 9-fold higher in NR1/2D than cortical receptors. Mg^{2+}_o in the channel of NMDA receptors experiences a series of energy barriers and wells. The location of these barriers and wells within the voltage field can be inferred from the voltage-dependence of rate constants by using the following equation (Woodhull, 1973):

$$\delta = RT/VzF$$

where R, T, z and F have their usual meanings. $\delta 1$, the fraction of voltage field Mg^{2+}_o needs to cross to reach the energy barrier, is calculated from V_1, the voltage dependence of $k_+(0)$; $\delta 2$, the fraction of voltage field Mg^{2+}_o needs to travel to reach the energy barrier from the point of its binding site, is calculated from V_2, the voltage dependence of $k_{-,o}(0)$; $\delta 1$ plus $\delta 2$ gives the electrical depth of the Mg^{2+}_o binding site; $\delta 3$, the fraction of voltage-field between the Mg^{2+}_o binding site and the permeation barrier, can be calculated from V_3, the voltage dependence of $k_{-,i}(0)$. The location of the Mg^{2+}_o binding site is comparable in the two receptors, 0.42 and 0.47 for NR1/2D and cortical receptors. Mg^{2+}_o $k_{+,o}(0)$ is also comparable between the two receptors.

2. Permeant ion effects on Mg^{2+}_o block of NMDA receptors

Permeant ions shape the characteristics of Mg^{2+}_o block in cortical and NR1/2D receptors. Voltage-dependent Mg^{2+}_o blocking and unblocking rates in normal (140 Na^+_o / 125 Cs^+_i) and zero ionic (0 Na^+_o / 0 Cs^+_i) conditions are predicted and plotted for cortical and NR1/2D receptors (Figure

Table 4 True Mg^{2+}_{o} blocking and unblocking rates

parameters	NR1/2D	cortical
$k_{+}(0)$	1170 $\mu M^{-1}s^{-1}$	1100 $\mu M^{-1}s^{-1}$
v1	137 mV	55.0 mV
$\delta 1$	0.09	0.23
$k_{-,o}(0)$	7420 $\mu M^{-1}s^{-1}$	110000 $\mu M^{-1}s^{-1}$
v2	38.7 mV	52.7 mV
$\delta 2$	0.33	0.24
$k_{-,i}(0)$	556 s^{-1}	61.8 s^{-1}
v3	68.7 mV	50.0 mV
$\delta 3$	0.18	0.25

See text for meanings of letters.

26). The purpose of these plots is to demonstrate the powerful effects of permeant ions on k_+ and k_-; the plots do not have any physiological meaning. I also assume that under zero ion condition (or very low permeant ion concentrations), the mechanism of Mg^{2+}_o block is the same as in normal ionic conditions. This assumption may not be accurate (for example, Stout *et al.*, 1996). Predictions for NR1/2D receptors were made using the model depicted in Figure 24 and values listed in Table 3; predictions for cortical receptors were made using the model in Figure 3 and values from previous work (Antonov and Johnson, 1999). Both k_+ and k_-, the true Mg^{2+}_o blocking and unblocking rates, are dramatically affected by the presence of permeant ions. For NR1/2D receptors, the voltage-dependence of k_+ is very weak; under normal ionic conditions, $k_{+,\,app}$ values are reduced and the reduction is especially striking at depolarized voltages. The difference between Mg^{2+}_o blocking rate under zero and normal ionic conditions at hyperpolarized voltages is mostly due to the effect of Na^+_o binding to the external sites and preventing Mg^{2+}_o from blocking. Cs^+_i binding to the external site also prevents Mg^{2+}_o from blocking. As voltage depolarizes, Cs^+_i binding to the external site becomes more frequent and, consequently, the effect of Cs^+_i on reducing $k_{+,\,app}$ is greater at depolarized than hyperpolarized voltages. The basic phenomena of permeant ion effects on Mg^{2+}_o k_+ are qualitatively similar between cortical and NR1/2D receptors.

The Mg^{2+}_o k_- is voltage-dependent in NR1/2D receptors (Figure 26B). At voltage more positive than -80 mV, k_- decreases with hyperpolarization, reflecting Mg^{2+}_o exiting predominantly to the outside. At voltage negative than -80 mV, k_- increases with hyperpolarization, reflecting Mg^{2+}_o permeation dominating Mg^{2+}_o unblock. In the presence of permeant ions, Mg^{2+}_o $k_{-,\,app}$ is higher than in zero ionic conditions at depolarized voltages due to Cs^+_i binding to the internal site, which has the

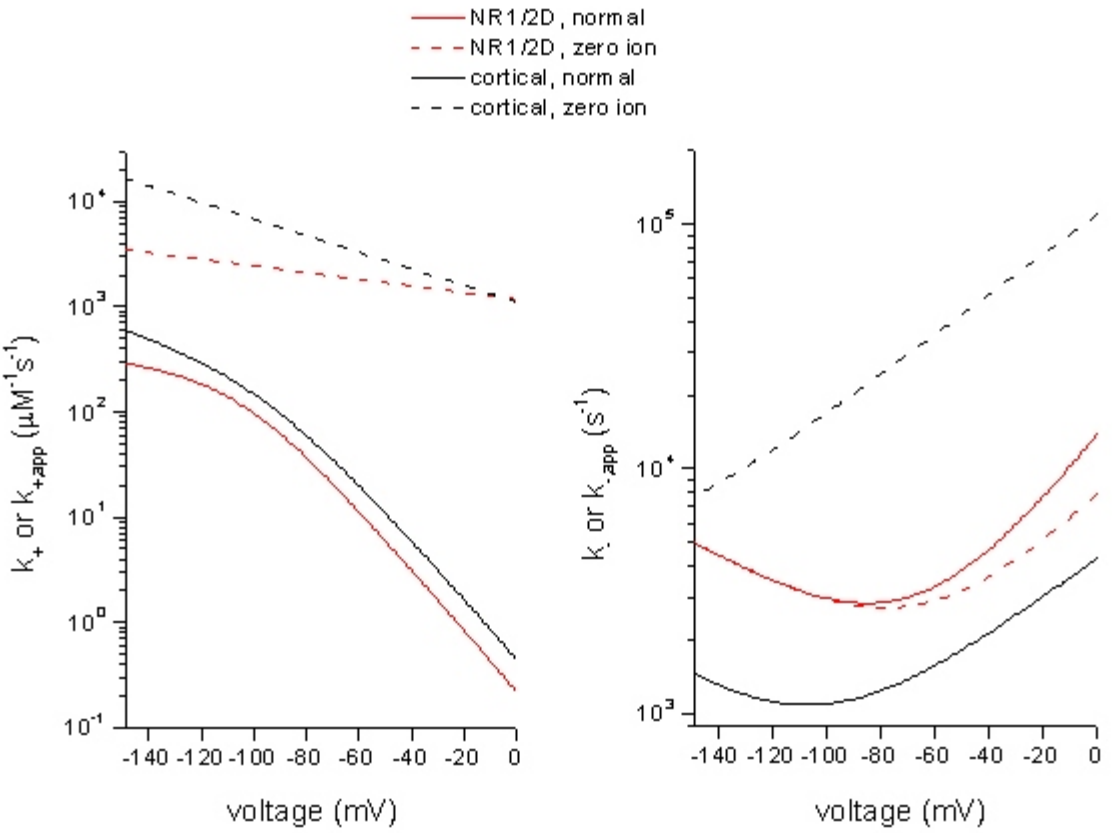

Figure 26 Mg^{2+}_o blocking and unblocking rates under two different ionic conditions. Mg^{2+}_o blocking rates (A) and unblocking rates (B) under normal and zero ionic conditions are plotted for NR1/2D and cortical receptors. Mg^{2+}_o k_+ and k_- were calculated from Model 1 (Figure 24) and Table 3 for NR1/2D receptors; the model shown in Figure 3 and values published previously (Antonov and Johnson, 1999) were used to predict k_+ and k_- of the cortical receptors. k_- is sum of the unblocking rate to the outside and the permeation rate.

net effect of increasing Mg^{2+}_o unblock to the outside. Increasing permeant ion concentrations has minimal effect on $k_{-, app}$ at voltages more negative than -110 mV, since the probability of Cs^+_i occupying the site is low. The effect of Na^+_o on Mg^{2+}_o unblocking is likely weak in NR1/2D receptors. The contrast between Mg^{2+}_o unblocking rates in cortical and NR1/2D receptor is very striking. Mg^{2+}_o k_- is much higher in cortical than NR1/2D receptors. The presence of Na^+_o greatly reduces unblocking rates (due to the lock-in effect) only in cortical receptors while the presence of Cs^+_i speeds up unblocking rates only in NR1/2D receptors. Consequently, $k_{-, app}$ is much faster in NR1/2D than cortical under normal ionic conditions. Although Mg^{2+}_o can permeate the channel in both receptors, permeation is more prominent in NR1/2D than cortical receptors.

From k_+ and k_- values in zero ionic condition, I calculated the equilibrium dissociation constant of Mg^{2+}_o at 0 mV is 6.8 μM for NR1/2D receptors and 100 μM for cortical receptors. This is an unexpected finding, considering that Mg^{2+}_o IC_{50} values are much higher in NR1/2D than cortical receptors under normal ionic conditions. The presence of permeant ions decreases Mg^{2+}_o blocking rates in a comparable manner in NR1/2D and cortical receptors. While the presence of permeant ions increases Mg^{2+}_o unblocking rates in NR1/2D receptors, it greatly decreases the unblocking rates in cortical receptors.

3. Other ion interactions in the channel of NMDA receptors

The research described in this Dissertation focuses on the effects of Na^+_o and Cs^+_i on Mg^{2+}_o block. Questions remain concerning how other monovalent ions affect Mg^{2+}_o block. A particularly important ion is K^+, which is one of the main charge carriers of NMDA receptors under physiological

conditions. Previous studies suggest that monovalent ions may have very different affinities for the internal permeant ion binding site of NR1/2A or NR2B receptors (Zhu & Auerbach, 2001a, b), even though the selectivity filter does not distinguish among monovalent ion species (Tsuzuki *et al.*, 1994). There are differences in how Cs^+_i and internal K^+ affect Mg^{2+}_o unblock in NR1/2A or NR1/2B receptors: increasing internal K^+ increases Mg^{2+}_o unblocking to the outside and decreasing Mg^{2+}_o permeation (Zhu & Auerbach, 2001a) while changing $[Cs^+]_i$ has no observable effects on Mg^{2+}_o unblock (Antonov & Johnson, 1999). It is possible that Cs^+_i interaction with the internal site is so weak that it does not appear to have any effect on Mg^{2+}_o unblock; an alternative scenario is that Cs^+_i has very high affinity for the internal side and the site is almost always occupied, even at very low $[Cs^+]_i$. A third possibility, as proposed by Zhu and Auerbach (2001a), is that in cortical receptors, the effect of Cs^+_i binding to the internal site on Mg^{2+}_o unblock would be hard to detect, if $[Na^+]_o$ is high: the effect of Na^+_o (the lock-in effect) would partly cancel out the effect of Cs^+_i binding to the internal site. Antonov and colleagues (1998) also proposed an internal Cs^+_i binding site, which can affect an organic blocker's movement in the channel and is located deep in the channel, outside the voltage field. This location is distinct from the internal binding site discussed in this study and the works by Zhu and Auerbach (2001 a and b).

Ca^{2+} is a particularly interesting permeant ion of NMDA receptors. Although I have examined the concentration- and voltage-dependent effects of Ca^{2+} on Mg^{2+}_o inhibition of cortical receptor-mediated currents (Chapter II), the role of Ca^{2+} on Mg^{2+}_o block in NR1/2D receptors is still unknown. Furthermore, a model is not yet available to describe the effects of Ca^{2+} on Mg^{2+}_o inhibition of NMDA receptors of any subunit combination. A working hypothesis can be postulated

based the whole-cell data: Ca^{2+} binding to an external site in the channel affects Mg^{2+}_o blocking and unblocking. An external Ca^{2+} binding site has been suggested by previous works (Premkumar & Auerbach, 1996; Sharma & Stevens, 1996a; Wollmuth & Sakmann, 1998; Watanabe *et al.*, 2002). Formulation of a detailed kinetic model requires information on the voltage-dependent microscopic Mg^{2+}_o blocking and unblocking rates under various ionic conditions.

Permeant ion effects on Mg^{2+}_o inhibition of NMDA receptors may also have physiological relevance. During normal synaptic transmission and in pathological states, ion concentrations may fluctuate significantly from resting values (Grisar, 1984; Lux *et al.*, 1986; Kager *et al.*, 2000; Rose & Konnerth, 2001). Computation of dynamic changes in Mg^{2+}_o block due to fluctuations in permeant ion concentrations during normal neuronal firing or under pathological conditions will aid our understanding of the physiological regulation of NMDA receptor by Mg^{2+}_o.

4. Single- ion vs. multi-ion pore

Whether a channel is a single-ion or multi-ion pore is a basic biophysical question which has significant consequences for the permeation and blocking characteristics of the channel. For example, in Ca^{2+} channels, occupancy of channel by more than one Ca^{2+} ion allows the channel to be both selective and highly conductive (Hess & Tsien, 1984; Dang & McCleskey, 1998). Ion interactions in the channel can also shape the characteristics of channel block, as demonstrated by the work presented here.

In NR1/2A receptors, there is evidence suggesting when only monovalent ions are present, the channel behaves like a single-ion pore (Zarei & Dani, 1994). When divalent ions are present, the channel can clearly contain two or more ions (Antonov *et al.*, 1998; Wollmuth & Sakmann, 1998; Antonov & Johnson, 1999; Zhu & Auerbach, 2001a, b). Whether NR1/2D receptors have a single-ion or multi-ion pore has not been explored. The work presented here suggests that NR1/2D receptors can hold more than one ion, at least under some circumstance. However, the observation that Na^{+}_{o} and Cs^{+}_{i} binding to the external and internal binding sites are very weak when Mg^{2+}_{o} is in the channel raises the possibility that NR1/2D receptor predominantly acts as a single-ion pore. It is interesting to note that the single-channel conductance is lower in NR1/2D or 2C receptors than in NR1/2A or 2B receptors, even though the selectivity filter are conserved among different NMDA receptors. Differential occupancy of the pore may provide an explanation for the difference in single-channel conductance.

C. STRUCTURE OF CHANNEL

Kuner and Schoepfer (1996) reported that various regions of NMDA receptors underlie the subunit-dependence of Mg^{2+}_{o} inhibition. These regions include a region near the N - terminus of M1, the linker between M2 and M3, and the region near M4. This finding is puzzling since it suggests that areas in the external and internal vestibules are involved in Mg^{2+}_{o} inhibition. To what do these structural components correspond?

It appears that the permeant monovalent ion effect on Mg^{2+}_{o} blocking rate is similar in cortical and NR1/2D receptors, suggesting that the external ion binding sites are not very different. Since

the true Mg^{2+}_o unblocking rate to the outside at 0 mV of the two receptor subtypes is very different (Table 4), the residues in the external vestibule (the N - terminus of M1 and around M4 region) may influence the energy profile for Mg^{2+}_o unblock. There is evidence suggesting that a hydrophobic region exists in the external vestibule of NMDA receptors (Subramaniam *et al.*, 1994). The property and position of this hydrophobic region may influence the height of the energy barrier Mg^{2+}_o must overcome in order to exit the channel. The linker between the M2 and M3 regions may correspond to either the permeation barrier, or the internal permeant ion binding site, both of which appear to be differ strongly between cortical and NR1/2D receptors (Table 4 and Chapter IV).

It is possible to have subunit dependence of permeant ion effects on Mg^{2+}_o block, even if the ion binding sites are identical; the effects of permeant ions can be different if the distance between permeant ion binding sites and Mg^{2+}_o blocking sites differ between the two receptors. For example, the observation that Na^{+}_o can bind readily with Mg^{2+}_o in the channel in cortical but not in NR1/2D receptors can be explained if the binding sites for Na^{+}_o and Mg^{2+}_o are very close to each other in NR1/2D receptors and therefore cannot be simultaneously occupied.

The models developed for cortical (Figure 3) and NR1/2D receptors (Figure 24) contain a pair of external permeant ion binding sites (also see Zhu & Auerbach, 2001a, b). An internal permeant ion binding site is also suggested for NR1/2D (Figure 24) and NR1/2A or NR1/2B receptors (Antonov *et al.*, 1998; Zhu & Auerbach, 2001a). Therefore, it seems plausible that the basic architecture of the two receptor subtypes is not very different. To substantiate our knowledge of the structure of NMDA receptors, it is necessary to identify the molecular constituents of the

permeant ion binding sites. Mutagenesis approach can be employed to identify the amino acid residues of NR1 or NR2 subunits which are involved in permeant ion effects.

D. GENERAL CONCLUSIONS

Permeant ion and subunit dependence of Mg^{2+}_o block of NMDA receptors are investigated in this Dissertation. The principal findings are:

(1) Mg^{2+}_o inhibition of whole-cell currents in cortical receptors is dependent on $[Cs^+]_i$ and $[Na^+]_o$. Decreasing $[Cs^+]_i$ greatly increased Mg^{2+}_o inhibition, especially at depolarized voltages. Decreasing $[Na^+]_o$ increased Mg^{2+}_o inhibition weakly in a voltage-independent manner.

(2) The effects of Na^+_o and Cs^+_i on Mg^{2+}_o inhibition in cortical receptors can be explained by a model which suggests that Na^+_o and Cs^+_i binding to external vestibule prevents Mg^{2+}_o from blocking and unblocking.

(3) In cortical receptors, changing $[Ca^{2+}]_o$ over low concentration range (0.1 - 1 mM) had no effect on Mg^{2+}_o inhibition; increasing $[Ca^{2+}]_o$ to a higher concentration range (2 - 20 mM) greatly decreased Mg^{2+}_o inhibition, especially at hyperpolarized voltages.

(4) In NR1/2D receptors, decreasing $[Cs^+]_i$ also greatly increased Mg^{2+}_o inhibition, especially at depolarized voltages; this was due to increased Mg^{2+}_o $k_{+,\,app}$ and decreased $k_{-,\,app}$ at depolarized voltages in lower $[Cs^+]_i$.

(5) In NR1/2D receptors, decreasing $[Na^+]_o$ weakly decreased Mg^{2+}_o inhibition at depolarized voltages but increased Mg^{2+}_o inhibition at hyperpolarized voltages. Lowering $[Na^+]_o$ increased Mg^{2+}_o $k_{+, app}$ in a voltage-independent manner but had no effect on $k_{-, app}$.

(6) In NR1/2D receptors, the effects of Na^+_o on Mg^{2+}_o $k_{+, app}$ can be explained using a model in which binding of Na^+_o to external site(s) in the channel prevents Mg^{2+}_o from blocking; Na^+_o has little effect on Mg^{2+}_o $k_{-, app}$; in cortical receptors, Na^+_o binding to the channel prevents Mg^{2+}_o from blocking and unblocking. In both NR1/2D and cortical receptors, Cs^+_i binding to a site in the external vestibule of the channel prevents Mg^{2+}_o from blocking; in NR1/2D receptors but not in cortical receptors, Cs^+_i can bind to an internal site and subsequently affect Mg^{2+}_o unblocking.

(7) Under physiological ionic conditions, Mg^{2+}_o inhibition is much weaker in NR1/2D than cortical receptors due much faster Mg^{2+}_o $k_{-, app}$. Mg^{2+}_o $k_{-, app}$ is greatly influenced by the presence of permeant ions in both receptors: in cortical receptors, Na^+_o binding to the external sites reduces Mg^{2+}_o unblocking while in NR1/2D receptors, Cs^+_i binding to the internal site has the net effect of greatly increasing Mg^{2+}_o unblocking.

(8) There is agreement between Mg^{2+}_o K_D and IC_{50} values in both cortical and NR1/2D receptors, consistent with Mg^{2+}_o block having no influence on gating transitions. It further suggests that the Mg^{2+}_o blocking site in either receptor subtype is isolated from gating induced conformational change.

The research included in this Dissertation has deepened our understanding of the mechanism of Mg^{2+}_{o} block . The work also provides insights into NMDA receptor structure and gating. Future work can further advance the knowledge of NMDA receptors by, for example, developing kinetic models for Ca^{2+} effects on channel block, identifying the molecular constituents of the various ion binding sites, and investigating the structural differences between the two receptor types.

BIBLIOGRAPHY

Bibliography

ADAMS, P. R. (1977). Voltage jump analysis of procaine action at frog end-plate. *J Physiol* **268,** 291-318.

AIZENMAN, E, SINOR, J.D., BRIMECOMBE, J. C. & HERIN, G. A. (2000). Alterations of –methyl-D-aspartate receptor properties after chemical ischemia. *J Pharmacol Exp Ther* **295**, 572-577

AKAZAWA, C., SHIGEMOTO, R., BESSHO, Y., NAKANISHI, S. & MIZUNO, N. (1994). Differential expression of five N-methyl-D-aspartate receptor subunit mRNAs in the cerebellum of developing and adult rats. *J Comp Neurol* **347,** 150-160.

AMAR, M., PERIN-DUREAU, F. & NEYTON, J. (2001). High-affinity Zn block in recombinant N-methyl-D-aspartate receptors with cysteine substitutions at the Q/R/N site. *Biophys J* **81,** 107-116.

ANSON, L. C., CHEN, P. E., WYLLIE, D. J., COLQUHOUN, D. & SCHOEPFER, R. (1998). Identification of amino acid residues of the NR2A subunit that control glutamate potency in recombinant NR1/NR2A NMDA receptors. *J Neurosci* **18,** 581-589.

ANTONOV, S. M., GMIRO, V. E. & JOHNSON, J. W. (1998). Binding sites for permeant ions in the channel of NMDA receptors and their effects on channel block. *Nat Neurosci* **1,** 451-461.

ANTONOV, S. M. & JOHNSON, J. W. (1996). Voltage-dependent interaction of open-channel blocking molecules with gating of NMDA receptors in rat cortical neurons. *J Physiol* **493 (Pt 2),** 425-445.

ANTONOV, S. M. & JOHNSON, J. W. (1999). Permeant ion regulation of N-methyl-D-aspartate receptor channel block by Mg(2+). *Proc Natl Acad Sci U S A* **96,** 14571-14576.

ARMSTRONG, C. M. (1966). Time course of TEA(+)-induced anomalous rectification in squid giant axons. *J Gen Physiol* **50,** 491-503.

ARMSTRONG, C. M. (1971). Interaction of tetraethylammonium ion derivatives with the potassium channels of giant axons. *J Gen Physiol* **58,** 413-437.

ARMSTRONG, N. & GOUAUX, E. (2000). Mechanisms for activation and antagonism of an AMPA-sensitive glutamate receptor: crystal structures of the GluR2 ligand binding core. *Neuron* **28,** 165-181.

ARMSTRONG, N., SUN, Y., CHEN, G. Q. & GOUAUX, E. (1998). Structure of a glutamate-receptor ligand-binding core in complex with kainate. *Nature* **395,** 913-917.

ASCHER, P. & NOWAK, L. (1988). The role of divalent cations in the N-methyl-D-aspartate responses of mouse central neurones in culture. *J Physiol* **399,** 247-266.

BEAR, M. F., KLEINSCHMIDT, A., GU, Q. A. & SINGER, W. (1990). Disruption of experience-dependent synaptic modifications in striate cortex by infusion of an NMDA receptor antagonist. *J Neurosci* **10,** 909-925.

BECK, C., WOLLMUTH, L. P., SEEBURG, P. H., SAKMANN, B. & KUNER, T. (1999). NMDAR channel segments forming the extracellular vestibule inferred from the accessibility of substituted cysteines. *Neuron* **22,** 559-570.

BEHE, P., STERN, P., WYLLIE, D. J., NASSAR, M., SCHOEPFER, R. & COLQUHOUN, D. (1995). Determination of NMDA NR1 subunit copy number in recombinant NMDA receptors. *Proc R Soc Lond B Biol Sci* **262,** 205-213.

BENGZON, J., OKABE, S., LINDVALL, O. & MCKAY, R. D. (1999). Suppression of epileptogenesis by modification of N-methyl-D-aspartate receptor subunit composition. *Eur J Neurosci* **11,** 916-922.

BENVENISTE, M. & MAYER, M. L. (1995). Trapping of glutamate and glycine during open channel block of rat hippocampal neuron NMDA receptors by 9-aminoacridine. *J Physiol* **483 (Pt 2),** 367-384.

BLANPIED, T. A., BOECKMAN, F. A., AIZENMAN, E. & JOHNSON, J. W. (1997). Trapping channel block of NMDA-activated responses by amantadine and memantine. *J Neurophysiol* **77,** 309-323.

BLISS, T. V. & COLLINGRIDGE, G. L. (1993). A synaptic model of memory: long-term potentiation in the hippocampus. *Nature* **361,** 31-39.

BOWIE, D. & LANGE, G. D. (2002). Functional stoichiometry of glutamate receptor desensitization. *J Neurosci* **22,** 3392-3403.

BRICKLEY, S. G., MISRA, C., MOK, M. H., MISHINA, M. & CULL-CANDY, S. G. (2003). NR2B and NR2D subunits coassemble in cerebellar Golgi cells to form a distinct NMDA receptor subtype restricted to extrasynaptic sites. *J Neurosci* **23,** 4958-4966.

BRIMECOMBE, J. C., BOECKMAN, F. A. & AIZENMAN, E. (1997). Functional consequences of NR2 subunit composition in single recombinant N-methyl-D-aspartate receptors. *Proc Natl Acad Sci U S A* **94,** 11019-11024.

BRUENING-WRIGHT, A., SCHUMACHER, M. A., ADELMAN, J. P. & MAYLIE, J. (2002). Localization of the activation gate for small conductance Ca2+-activated K+ channels. *J Neurosci* **22,** 6499-6506.

BURNASHEV, N., SCHOEPFER, R., MONYER, H., RUPPERSBERG, J. P., GUNTHER, W., SEEBURG, P. H. & SAKMANN, B. (1992). Control by asparagine residues of calcium permeability and magnesium blockade in the NMDA receptor. *Science* **257,** 1415-1419.

BURNASHEV, N., ZHOU, Z., NEHER, E. & SAKMANN, B. (1995). Fractional calcium currents through recombinant GluR channels of the NMDA, AMPA and kainate receptor subtypes. *J Physiol* **485 (Pt 2),** 403-418.

CATHALA, L., MISRA, C. & CULL-CANDY, S. (2000). Developmental profile of the changing properties of NMDA receptors at cerebellar mossy fiber-granule cell synapses. *J Neurosci* **20,** 5899-5905.

CHAPMAN, A. G. (2000). Glutamate and epilepsy. *J Nutr* **130,** 1043S-1045S.

CHATTERTON, J. E., AWOBULUYI, M., PREMKUMAR, L. S., TAKAHASHI, H., TALANTOVA, M., SHIN, Y., CUI, J., TU, S., SEVARINO, K. A., NAKANISHI, N., TONG, G., LIPTON, S. A. & ZHANG, D. (2002). Excitatory glycine receptors containing the NR3 family of NMDA receptor subunits. *Nature* **415,** 793-798.

CHAZOT, P. L. & STEPHENSON, F. A. (1997). Molecular dissection of native mammalian forebrain NMDA receptors containing the NR1 C2 exon: direct demonstration of NMDA receptors

comprising NR1, NR2A, and NR2B subunits within the same complex. *J Neurochem* **69,** 2138-2144.

CHEFFINGS, C. M. & COLQUHOUN, D. (2000). Single channel analysis of a novel NMDA channel from Xenopus oocytes expressing recombinant NR1a, NR2A and NR2D subunits. *J Physiol* **526 Pt 3,** 481-491.

CHEN, C. & OKAYAMA, H. (1987). High-efficiency transformation of mammalian cells by plasmid DNA. *Mol Cell Biol* **7,** 2745-2752.

CHEN, G. Q., CUI, C., MAYER, M. L. & GOUAUX, E. (1999). Functional characterization of a potassium-selective prokaryotic glutamate receptor. *Nature* **402,** 817-821.

CHEN, H. S. & LIPTON, S. A. (1997). Mechanism of memantine block of NMDA-activated channels in rat retinal ganglion cells: uncompetitive antagonism. *J Physiol* **499 (Pt 1),** 27-46.

CHEN, L. & HUANG, L. Y. (1992). Protein kinase C reduces Mg2+ block of NMDA-receptor channels as a mechanism of modulation. *Nature* **356,** 521-523.

CIABARRA, A. M., SULLIVAN, J. M., GAHN, L. G., PECHT, G., HEINEMANN, S. & SEVARINO, K. A. (1995). Cloning and characterization of chi-1: a developmentally regulated member of a novel class of the ionotropic glutamate receptor family. *J Neurosci* **15,** 6498-6508.

CLEMENTS, J. D. & WESTBROOK, G. L. (1991). Activation kinetics reveal the number of glutamate and glycine binding sites on the N-methyl-D-aspartate receptor. *Neuron* **7,** 605-613.

CLINE, H. T., DEBSKI, E. A. & CONSTANTINE-PATON, M. (1990). The role of the NMDA receptor in the development of the frog visual system. *Adv Exp Med Biol* **268,** 197-203.

COLQUHOUN, D. & SIGWORTH, F. J. (1995). Fitting and statistical analysis of single-channel records. In *Single-Channel Recording*. ed. SAKMANN, B. & NEHER, E., pp. 483-587. Plenum Press, New York.

COSTA, A. C. & ALBUQUERQUE, E. X. (1994). Dynamics of the actions of tetrahydro-9-aminoacridine and 9-aminoacridine on glutamatergic currents: concentration-jump studies in cultured rat hippocampal neurons. *J Pharmacol Exp Ther* **268,** 503-514.

CULL-CANDY, S., BRICKLEY, S. & FARRANT, M. (2001). NMDA receptor subunits: diversity, development and disease. *Curr Opin Neurobiol* **11,** 327-335.

DANG, T. X. & MCCLESKEY, E. W. (1998). Ion channel selectivity through stepwise changes in binding affinity. *J Gen Physiol* **111,** 185-193.

DAS, S., SASAKI, Y. F., ROTHE, T., PREMKUMAR, L. S., TAKASU, M., CRANDALL, J. E., DIKKES, P., CONNER, D. A., RAYUDU, P. V., CHEUNG, W., CHEN, H. S., LIPTON, S. A. & NAKANISHI, N. (1998). Increased NMDA current and spine density in mice lacking the NMDA receptor subunit NR3A. *Nature* **393,** 377-381.

DEL CAMINO, D. & YELLEN, G. (2001). Tight steric closure at the intracellular activation gate of a voltage-gated K(+) channel. *Neuron* **32,** 649-656.

DINGLEDINE, R., BORGES, K., BOWIE, D. & TRAYNELIS, S. F. (1999). The glutamate receptor ion channels. *Pharmacol Rev* **51,** 7-61.

DUNAH, A. W., LUO, J., WANG, Y. H., YASUDA, R. P. & WOLFE, B. B. (1998). Subunit composition of N-methyl-D-aspartate receptors in the central nervous system that contain the NR2D subunit. *Mol Pharmacol* **53,** 429-437.

EHLERS, M. D., FUNG, E. T., O'BRIEN, R. J. & HUGANIR, R. L. (1998). Splice variant-specific interaction of the NMDA receptor subunit NR1 with neuronal intermediate filaments. *J Neurosci* **18,** 720-730.

EHLERS, M. D., TINGLEY, W. G. & HUGANIR, R. L. (1995). Regulated subcellular distribution of the NR1 subunit of the NMDA receptor. *Science* **269,** 1734-1737.

EHLERS, M. D., ZHANG, S., BERNHADT, J. P. & HUGANIR, R. L. (1996). Inactivation of NMDA receptors by direct interaction of calmodulin with the NR1 subunit. *Cell* **84,** 745-755.

ERISIR, A. & HARRIS, J. L. (2003). Decline of the critical period of visual plasticity is concurrent with the reduction of NR2B subunit of the synaptic NMDA receptor in layer 4. *J Neurosci* **23,** 5208-5218.

FAYYAZUDDIN, A., VILLARROEL, A., LE GOFF, A., LERMA, J. & NEYTON, J. (2000). Four residues of the extracellular N-terminal domain of the NR2A subunit control high-affinity Zn2+ binding to NMDA receptors. *Neuron* **25,** 683-694.

FELDMAN, D. E., NICOLL, R. A. & MALENKA, R. C. (1999). Synaptic plasticity at thalamocortical synapses in developing rat somatosensory cortex: LTP, LTD, and silent synapses. *J Neurobiol* **41,** 92-101.

FLYNN, G. E., JOHNSON, J. P., JR. & ZAGOTTA, W. N. (2001). Cyclic nucleotide-gated channels: shedding light on the opening of a channel pore. *Nat Rev Neurosci* **2,** 643-651.

FODOR, A. A., GORDON, S. E. & ZAGOTTA, W. N. (1997). Mechanism of tetracaine block of cyclic nucleotide-gated channels. *J Gen Physiol* **109,** 3-14.

FURUKAWA, H. & GOUAUX, E. (2003). Mechanisms of activation, inhibition and specificity: crystal

structures of the NMDA receptor NR1 ligand-binding core. *Embo J* **22,** 2873-2885.

FURUKAWA, Y., OKADA, M., AKAIKE, N., HAYASHI, T. & NABEKURA, J. (2000). Reduction of voltage-dependent magnesium block of N-methyl-D-aspartate receptor-mediated current by in vivo axonal injury. *Neuroscience* **96,** 385-392.

Gardoni, F., Pagliardini, S., Setola, V., Bassanini, S., Cattabeni, F., Battaglia, G. & Di Luca,M.(2003). The NMDA receptor complex is altered in an animal model of human cerebral heterotopia. *J Neuropathol Exp Neurol* **62**, 662-675

Grisar, T. (1984). Glial and neuronal Na+-K+ pump in epilepsy. *Ann Neurol* **16 Suppl,** S128-134.

GROOT-KORMELINK, P. J., BEATO, M., FINOTTI, C., HARVEY, R. J. & SIVILOTTI, L. G. (2002). Achieving optimal expression for single channel recording: a plasmid ratio approach to the expression of alpha 1 glycine receptors in HEK293 cells. *J Neurosci Methods* **113,** 207-214.

GUO, D., RAMU, Y., KLEM, A. M. & LU, Z. (2003). Mechanism of Rectification in Inward-rectifier K+ Channels. *J Gen Physiol* **121,** 261-276.

GUO, H. & HUANG, L. Y. (2001). Alteration in the voltage dependence of NMDA receptor channels in rat dorsal horn neurones following peripheral inflammation. *J Physiol* **537,** 115-123.

HACKOS, D. H. & KORENBROT, J. I. (1999). Divalent cation selectivity is a function of gating in native and recombinant cyclic nucleotide-gated ion channels from retinal photoreceptors. *J Gen Physiol* **113,** 799-818.

HAMILL, O. P., MARTY, A., NEHER, E., SAKMANN, B. & SIGWORTH, F. J. (1981). Improved patch-clamp techniques for high-resolution current recording from cells and cell-free membrane patches. *Pflugers Arch* **391,** 85-100.

HATTON, C. J., SHELLEY, C., BRYDSON, M., BEESON, D. & COLQUHOUN, D. (2003). Properties of the human muscle nicotinic receptor, and of the slow-channel myasthenic syndrome mutant epsilonL221F, inferred from maximum likelihood fits. *J Physiol* **547,** 729-760.

HESS, P. & TSIEN, R. W. (1984). Mechanism of ion permeation through calcium channels. *Nature* **309,** 453-456.

HILLE, B. (2001). *Ion Channels of Excitable Membranes*. Sinauer Associates, Inc., Sunderland, Massachusetts.

HILLE, B. & SCHWARZ, W. (1978). Potassium channels as multi-ion single-file pores. *J Gen Physiol* **72,** 409-442.

HIRAI, H., KIRSCH, J., LAUBE, B., BETZ, H. & KUHSE, J. (1996). The glycine binding site of the N-methyl-D-aspartate receptor subunit NR1: identification of novel determinants of co-agonist potentiation in the extracellular M3-M4 loop region. *Proc Natl Acad Sci U S A* **93,** 6031-6036.

HORI, N. & CARPENTER, D. O. (1994). Transient ischemia causes a reduction of Mg2+ blockade of NMDA receptors. *Neurosci Lett* **173,** 75-78.

HORN, R. (1987). Statistical methods for model discrimination. Applications to gating kinetics and permeation of the acetylcholine receptor channel. *Biophys J* **51,** 255-263.

HRABETOVA, S., SERRANO, P., BLACE, N., TSE, H. W., SKIFTER, D. A., JANE, D. E., MONAGHAN,

D. T. & SACKTOR, T. C. (2000). Distinct NMDA receptor subpopulations contribute to long-term potentiation and long-term depression induction. *J Neurosci* **20,** RC81.

HUETTNER, J. E. & BEAN, B. P. (1988). Block of N-methyl-D-aspartate-activated current by the anticonvulsant MK-801: selective binding to open channels. *Proc Natl Acad Sci U S A* **85,** 1307-1311.

IINO, M., OZAWA, S. & TSUZUKI, K. (1990). Permeation of calcium through excitatory amino acid receptor channels in cultured rat hippocampal neurones. *J Physiol* **424,** 151-165.

IKEDA, K., ARAKI, K., TAKAYAMA, C., INOUE, Y., YAGI, T., AIZAWA, S. & MISHINA, M. (1995). Reduced spontaneous activity of mice defective in the epsilon 4 subunit of the NMDA receptor channel. *Brain Res Mol Brain Res* **33,** 61-71.

IKEDA, K., NAGASAWA, M., MORI, H., ARAKI, K., SAKIMURA, K., WATANABE, M., INOUE, Y. & MISHINA, M. (1992). Cloning and expression of the epsilon 4 subunit of the NMDA receptor channel. *FEBS Lett* **313,** 34-38.

IMMKE, D., WOOD, M., KISS, L. & KORN, S. J. (1999). Potassium-dependent changes in the conformation of the Kv2.1 potassium channel pore. *J Gen Physiol* **113,** 819-836.

ISHII, T., MORIYOSHI, K., SUGIHARA, H., SAKURADA, K., KADOTANI, H., YOKOI, M., AKAZAWA, C., SHIGEMOTO, R., MIZUNO, N., MASU, M. & ET AL. (1993). Molecular characterization of the family of the N-methyl-D-aspartate receptor subunits. *J Biol Chem* **268,** 2836-2843.

IWASATO, T., DATWANI, A., WOLF, A. M., NISHIYAMA, H., TAGUCHI, Y., TONEGAWA, S., KNOPFEL, T., ERZURUMLU, R. S. & ITOHARA, S. (2000). Cortex-restricted disruption of NMDAR1 impairs neuronal patterns in the barrel cortex. *Nature* **406,** 726-731.

JAHR, C. E. & STEVENS, C. F. (1990a). A quantitative description of NMDA receptor-channel kinetic behavior. *J Neurosci* **10,** 1830-1837.

JAHR, C. E. & STEVENS, C. F. (1990b). Voltage dependence of NMDA-activated macroscopic conductances predicted by single-channel kinetics. *J Neurosci* **10,** 3178-3182.

JAHR, C. E. & STEVENS, C. F. (1993). Calcium permeability of the N-methyl-D-aspartate receptor channel in hippocampal neurons in culture. *Proc Natl Acad Sci U S A* **90,** 11573-11577.

JIANG, Y., LEE, A., CHEN, J., CADENE, M., CHAIT, B. T. & MACKINNON, R. (2002a). Crystal structure and mechanism of a calcium-gated potassium channel. *Nature* **417,** 515-522.

JIANG, Y., LEE, A., CHEN, J., CADENE, M., CHAIT, B. T. & MACKINNON, R. (2002b). The open pore conformation of potassium channels. *Nature* **417,** 523-526.

JIANG, Y. & MACKINNON, R. (2000). The barium site in a potassium channel by x-ray crystallography. *J Gen Physiol* **115,** 269-272.

JOHNSON, J. W. & ASCHER, P. (1990). Voltage-dependent block by intracellular Mg2+ of N-methyl-D-aspartate-activated channels. *Biophys J* **57,** 1085-1090.

JOHNSON, J. W. & QIAN, A. (2002). Interaction between channel blockers and channel gating of NMDA receptors. *Membrane and Cell Biology* **19,** 110-115.

JONES, K. S., VANDONGEN, H. M. & VANDONGEN, A. M. (2002). The NMDA receptor M3 segment is a conserved transduction element coupling ligand binding to channel opening. *J Neurosci* **22,** 2044-2053.

KAGER, H., WADMAN, W. J. & SOMJEN, G. G. (2000). Simulated seizures and spreading

depression in a neuron model incorporating interstitial space and ion concentrations. *J Neurophysiol* **84,** 495-512.

KAKIZAWA, S., YAMASAKI, M., WATANABE, M. & KANO, M. (2000). Critical period for activity-dependent synapse elimination in developing cerebellum. *J Neurosci* **20,** 4954-4961.

KASHIWAGI, K., MASUKO, T., NGUYEN, C. D., KUNO, T., TANAKA, I., IGARASHI, K. & WILLIAMS, K. (2002). Channel blockers acting at N-methyl-D-aspartate receptors: differential effects of mutations in the vestibule and ion channel pore. *Mol Pharmacol* **61,** 533-545.

KIM, E., CHO, K. O., ROTHSCHILD, A. & SHENG, M. (1996). Heteromultimerization and NMDA receptor-clustering activity of Chapsyn-110, a member of the PSD-95 family of proteins. *Neuron* **17,** 103-113.

KIRSON, E. D. & YAARI, Y. (1996). Synaptic NMDA receptors in developing mouse hippocampal neurones: functional properties and sensitivity to ifenprodil. *J Physiol* **497 (Pt 2),** 437-455.

KLECKNER, N. W. & DINGLEDINE, R. (1991). Regulation of hippocampal NMDA receptors by magnesium and glycine during development. *Brain Res Mol Brain Res* **11,** 151-159.

KOHDA, K., WANG, Y. & YUZAKI, M. (2000). Mutation of a glutamate receptor motif reveals its role in gating and delta2 receptor channel properties. *Nat Neurosci* **3,** 315-322.

KOHR, G. & SEEBURG, P. H. (1996). Subtype-specific regulation of recombinant NMDA receptor-channels by protein tyrosine kinases of the src family. *J Physiol* **492 (Pt 2),** 445-452.

KRUPP, J. J., VISSEL, B., HEINEMANN, S. F. & WESTBROOK, G. L. (1996). Calcium-dependent

inactivation of recombinant N-methyl-D-aspartate receptors is NR2 subunit specific. *Mol Pharmacol* **50,** 1680-1688.

KRUPP, J. J., VISSEL, B., HEINEMANN, S. F. & WESTBROOK, G. L. (1998). N-terminal domains in the NR2 subunit control desensitization of NMDA receptors. *Neuron* **20,** 317-327.

KRUPP, J. J., VISSEL, B., THOMAS, C. G., HEINEMANN, S. F. & WESTBROOK, G. L. (1999). Interactions of calmodulin and alpha-actinin with the NR1 subunit modulate Ca2+-dependent inactivation of NMDA receptors. *J Neurosci* **19,** 1165-1178.

KUNER, T. & SCHOEPFER, R. (1996). Multiple structural elements determine subunit specificity of Mg2+ block in NMDA receptor channels. *J Neurosci* **16,** 3549-3558.

KUNER, T., WOLLMUTH, L. P., KARLIN, A., SEEBURG, P. H. & SAKMANN, B. (1996). Structure of the NMDA receptor channel M2 segment inferred from the accessibility of substituted cysteines. *Neuron* **17,** 343-352.

KUPPER, J., ASCHER, P. & NEYTON, J. (1996). Probing the pore region of recombinant N-methyl-D-aspartate channels using external and internal magnesium block. *Proc Natl Acad Sci U S A* **93,** 8648-8653.

KURYATOV, A., LAUBE, B., BETZ, H. & KUHSE, J. (1994). Mutational analysis of the glycine-binding site of the NMDA receptor: structural similarity with bacterial amino acid-binding proteins. *Neuron* **12,** 1291-1300.

KUTSUWADA, T., KASHIWABUCHI, N., MORI, H., SAKIMURA, K., KUSHIYA, E., ARAKI, K., MEGURO, H., MASAKI, H., KUMANISHI, T., ARAKAWA, M. & ET AL. (1992). Molecular diversity of the NMDA receptor channel. *Nature* **358,** 36-41.

LAU, L. F., MAMMEN, A., EHLERS, M. D., KINDLER, S., CHUNG, W. J., GARNER, C. C. & HUGANIR, R. L. (1996). Interaction of the N-methyl-D-aspartate receptor complex with a novel synapse-associated protein, SAP102. *J Biol Chem* **271,** 21622-21628.

LAUBE, B., HIRAI, H., STURGESS, M., BETZ, H. & KUHSE, J. (1997). Molecular determinants of agonist discrimination by NMDA receptor subunits: analysis of the glutamate binding site on the NR2B subunit. *Neuron* **18,** 493-503.

LAUBE, B., KUHSE, J. & BETZ, H. (1998). Evidence for a tetrameric structure of recombinant NMDA receptors. *J Neurosci* **18,** 2954-2961.

LAUGER, P. (1985). Ionic channels with conformational substates. *Biophys J* **47,** 581-590.

LEI, S., CZERWINSKA, E., CZERWINSKI, W., WALSH, M. P. & MACDONALD, J. F. (2001). Regulation of NMDA receptor activity by F-actin and myosin light chain kinase. *J Neurosci* **21,** 8464-8472.

LIN, J. W., WYSZYNSKI, M., MADHAVAN, R., SEALOCK, R., KIM, J. U. & SHENG, M. (1998). Yotiao, a novel protein of neuromuscular junction and brain that interacts with specific splice variants of NMDA receptor subunit NR1. *J Neurosci* **18,** 2017-2027.

LISMAN, J. E. & MCINTYRE, C. C. (2001). Synaptic plasticity: a molecular memory switch. *Curr Biol* **11,** R788-791.

LI-SMERIN, Y. & JOHNSON, J. W. (1996). Kinetics of the block by intracellular Mg2+ of the NMDA-activated channel in cultured rat neurons. *J Physiol* **491 (Pt 1),** 121-135.

LI-SMERIN, Y., LEVITAN, E. S. & JOHNSON, J. W. (2001). Free intracellular Mg(2+) concentration and inhibition of NMDA responses in cultured rat neurons. *J Physiol* **533,** 729-743.

LOW, C. M., ZHENG, F., LYUBOSLAVSKY, P. & TRAYNELIS, S. F. (2000). Molecular determinants of coordinated proton and zinc inhibition of N-methyl-D-aspartate NR1/NR2A receptors. *Proc Natl Acad Sci U S A* **97,** 11062-11067.

LUMMIS, S. C., FLETCHER, E. J. & GREEN, T. (2002). Identification of a new site in the S1 ligand binding region of the NMDA receptor NR2A subunit involved in receptor activation by glutamate. *Neuropharmacology* **42,** 437-443.

LUX, H. D., HEINEMANN, U. & DIETZEL, I. (1986). Ionic changes and alterations in the size of the extracellular space during epileptic activity. *Adv Neurol* **44,** 619-639.

MACDERMOTT, A. B., MAYER, M. L., WESTBROOK, G. L., SMITH, S. J. & BARKER, J. L. (1986). NMDA-receptor activation increases cytoplasmic calcium concentration in cultured spinal cord neurones. *Nature* **321,** 519-522.

MACDONALD, J. F., MILJKOVIC, Z. & PENNEFATHER, P. (1987). Use-dependent block of excitatory amino acid currents in cultured neurons by ketamine. *J Neurophysiol* **58,** 251-266.

MACKINNON, R. (1995). Pore loops: an emerging theme in ion channel structure. *Neuron* **14,** 889-892.

MAREN, S. (1999). Long-term potentiation in the amygdala: a mechanism for emotional learning and memory. *Trends Neurosci* **22,** 561-567.

MAYER, M. L., VYKLICKY, L., JR. & CLEMENTS, J. (1989). Regulation of NMDA receptor desensitization in mouse hippocampal neurons by glycine. *Nature* **338,** 425-427.

MAYER, M. L. & WESTBROOK, G. L. (1987). Permeation and block of N-methyl-D-aspartic acid

receptor channels by divalent cations in mouse cultured central neurones. *J Physiol* **394,** 501-527.

MAYER, M. L., WESTBROOK, G. L. & GUTHRIE, P. B. (1984). Voltage-dependent block by Mg2+ of NMDA responses in spinal cord neurones. *Nature* **309,** 261-263.

MCBAIN, C. J. & MAYER, M. L. (1994). N-methyl-D-aspartic acid receptor structure and function. *Physiol Rev* **74,** 723-760.

MEGURO, H., MORI, H., ARAKI, K., KUSHIYA, E., KUTSUWADA, T., YAMAZAKI, M., KUMANISHI, T., ARAKAWA, M., SAKIMURA, K. & MISHINA, M. (1992). Functional characterization of a heteromeric NMDA receptor channel expressed from cloned cDNAs. *Nature* **357,** 70-74.

MELDRUM, B. S. (1992). Excitatory amino acid receptors and disease. *Curr Opin Neurol Neurosurg* **5,** 508-513.

MISRA, C., BRICKLEY, S. G., WYLLIE, D. J. & CULL-CANDY, S. G. (2000). Slow deactivation kinetics of NMDA receptors containing NR1 and NR2D subunits in rat cerebellar Purkinje cells. *J Physiol* **525 Pt 2,** 299-305.

MIYAMOTO, Y., YAMADA, K., NODA, Y., MORI, H., MISHINA, M. & NABESHIMA, T. (2002). Lower sensitivity to stress and altered monoaminergic neuronal function in mice lacking the NMDA receptor epsilon 4 subunit. *J Neurosci* **22,** 2335-2342.

MOHN, A. R., GAINETDINOV, R. R., CARON, M. G. & KOLLER, B. H. (1999). Mice with reduced NMDA receptor expression display behaviors related to schizophrenia. *Cell* **98,** 427-436.

MOMIYAMA, A., FELDMEYER, D. & CULL-CANDY, S. G. (1996). Identification of a native low-

conductance NMDA channel with reduced sensitivity to Mg2+ in rat central neurones. *J Physiol* **494 (Pt 2),** 479-492.

MONAGHAN, D. T. & COTMAN, C. W. (1985). Distribution of N-methyl-D-aspartate-sensitive L-[3H]glutamate-binding sites in rat brain. *J Neurosci* **5,** 2909-2919.

MONYER, H., BURNASHEV, N., LAURIE, D. J., SAKMANN, B. & SEEBURG, P. H. (1994). Developmental and regional expression in the rat brain and functional properties of four NMDA receptors. *Neuron* **12,** 529-540.

MONYER, H., SPRENGEL, R., SCHOEPFER, R., HERB, A., HIGUCHI, M., LOMELI, H., BURNASHEV, N., SAKMANN, B. & SEEBURG, P. H. (1992). Heteromeric NMDA receptors: molecular and functional distinction of subtypes. *Science* **256,** 1217-1221.

MORI, H., MASAKI, H., YAMAKURA, T. & MISHINA, M. (1992). Identification by mutagenesis of a Mg(2+)-block site of the NMDA receptor channel. *Nature* **358,** 673-675.

MORIYOSHI, K., MASU, M., ISHII, T., SHIGEMOTO, R., MIZUNO, N. & NAKANISHI, S. (1991). Molecular cloning and characterization of the rat NMDA receptor. *Nature* **354,** 31-37.

MULLER, B. M., KISTNER, U., KINDLER, S., CHUNG, W. J., KUHLENDAHL, S., FENSTER, S. D., LAU, L. F., VEH, R. W., HUGANIR, R. L., GUNDELFINGER, E. D. & GARNER, C. C. (1996). SAP102, a novel postsynaptic protein that interacts with NMDA receptor complexes in vivo. *Neuron* **17,** 255-265.

NAKAZAWA, K., QUIRK, M. C., CHITWOOD, R. A., WATANABE, M., YECKEL, M. F., SUN, L. D., KATO, A., CARR, C. A., JOHNSTON, D., WILSON, M. A. & TONEGAWA, S. (2002). Requirement for hippocampal CA3 NMDA receptors in associative memory recall. *Science* **297,** 211-218.

NEHER, E. & STEINBACH, J. H. (1978). Local anaesthetics transiently block currents through single acetylcholine-receptor channels. *J Physiol* **277,** 153-176.

NEYTON, J. & MILLER, C. (1988a). Discrete Ba2+ block as a probe of ion occupancy and pore structure in the high-conductance Ca2+ -activated K+ channel. *J Gen Physiol* **92,** 569-586.

NEYTON, J. & MILLER, C. (1988b). Potassium blocks barium permeation through a calcium-activated potassium channel. *J Gen Physiol* **92,** 549-567.

NIETHAMMER, M., KIM, E. & SHENG, M. (1996). Interaction between the C terminus of NMDA receptor subunits and multiple members of the PSD-95 family of membrane-associated guanylate kinases. *J Neurosci* **16,** 2157-2163.

NOWAK, L., BREGESTOVSKI, P., ASCHER, P., HERBET, A. & PROCHIANTZ, A. (1984). Magnesium gates glutamate-activated channels in mouse central neurones. *Nature* **307,** 462-465.

OH, B. H., KANG, C. H., DE BONDT, H., KIM, S. H., NIKAIDO, K., JOSHI, A. K. & AMES, G. F. (1994). The bacterial periplasmic histidine-binding protein. structure/function analysis of the ligand-binding site and comparison with related proteins. *J Biol Chem* **269,** 4135-4143.

OH, B. H., PANDIT, J., KANG, C. H., NIKAIDO, K., GOKCEN, S., AMES, G. F. & KIM, S. H. (1993). Three-dimensional structures of the periplasmic lysine/arginine/ornithine-binding protein with and without a ligand. *J Biol Chem* **268,** 11348-11355.

OKABE, S., COLLIN, C., AUERBACH, J. M., MEIRI, N., BENGZON, J., KENNEDY, M. B., SEGAL, M. & MCKAY, R. D. (1998). Hippocampal synaptic plasticity in mice overexpressing an embryonic subunit of the NMDA receptor. *J Neurosci* **18,** 4177-4188.

PANCHENKO, V. A., GLASSER, C. R. & MAYER, M. L. (2001). Structural similarities between glutamate receptor channels and K(+) channels examined by scanning mutagenesis. *J Gen Physiol* **117,** 345-360.

PAOLETTI, P., NEYTON, J. & ASCHER, P. (1995). Glycine-independent and subunit-specific potentiation of NMDA responses by extracellular Mg2+. *Neuron* **15,** 1109-1120.

PAOLETTI, P., PERIN-DUREAU, F., FAYYAZUDDIN, A., LE GOFF, A., CALLEBAUT, I. & NEYTON, J. (2000). Molecular organization of a zinc binding n-terminal modulatory domain in a NMDA receptor subunit. *Neuron* **28,** 911-925.

PATNEAU, D. K. & MAYER, M. L. (1990). Structure-activity relationships for amino acid transmitter candidates acting at N-methyl-D-aspartate and quisqualate receptors. *J Neurosci* **10,** 2385-2399.

PREMKUMAR, L. S. & AUERBACH, A. (1996). Identification of a high affinity divalent cation binding site near the entrance of the NMDA receptor channel. *Neuron* **16,** 869-880.

PREMKUMAR, L. S. & AUERBACH, A. (1997). Stoichiometry of recombinant N-methyl-D-aspartate receptor channels inferred from single-channel current patterns. *J Gen Physiol* **110,** 485-502.

QIAN, A., ANTONOV, S. M. & JOHNSON, J. W. (2002). Modulation by permeant ions of Mg(2+) inhibition of NMDA-activated whole-cell currents in rat cortical neurons. *J Physiol* **538,** 65-77.

QIAN, A. & JOHNSON, J. W. (2002). Channel gating of NMDA receptors. *Physiol Behav* **77,** 577-582.

RAMOA, A. S., MOWER, A. F., LIAO, D. & JAFRI, S. I. (2001). Suppression of cortical NMDA receptor function prevents development of orientation selectivity in the primary visual cortex. *J Neurosci* **21,** 4299-4309.

REGALADO, M. P., VILLARROEL, A. & LERMA, J. (2001). Intersubunit cooperativity in the NMDA receptor. *Neuron* **32,** 1085-1096.

ROCHE, K. W., STANDLEY, S., MCCALLUM, J., DUNE LY, C., EHLERS, M. D. & WENTHOLD, R. J. (2001). Molecular determinants of NMDA receptor internalization. *Nat Neurosci* **4,** 794-802.

ROSE, C. R. & KONNERTH, A. (2001). NMDA receptor-mediated Na+ signals in spines and dendrites. *J Neurosci* **21,** 4207-4214.

ROSENMUND, C., STERN-BACH, Y. & STEVENS, C. F. (1998). The tetrameric structure of a glutamate receptor channel. *Science* **280,** 1596-1599.

RUIZ, M. L. & KARPEN, J. W. (1997). Single cyclic nucleotide-gated channels locked in different ligand-bound states. *Nature* **389,** 389-392.

RUPPERSBERG, J. P., KITZING, E. & SCHOEPFER, R. (1994). The mechanism of magnesium block of NMDA receptors. *Seminars in The Neurosciences* **6,** 87-96.

SAKURADA, K., MASU, M. & NAKANISHI, S. (1993). Alteration of Ca2+ permeability and sensitivity to Mg2+ and channel blockers by a single amino acid substitution in the N-methyl-D-aspartate receptor. *J Biol Chem* **268,** 410-415.

SCHELL, M. J., MOLLIVER, M. E. & SNYDER, S. H. (1995). D-serine, an endogenous synaptic modulator: localization to astrocytes and glutamate-stimulated release. *Proc Natl Acad*

Sci U S A **92,** 3948-3952.

SCHNEGGENBURGER, R. (1996). Simultaneous measurement of Ca2+ influx and reversal potentials in recombinant N-methyl-D-aspartate receptor channels. *Biophys J* **70,** 2165-2174.

SCHNEGGENBURGER, R. & ASCHER, P. (1997). Coupling of permeation and gating in an NMDA-channel pore mutant. *Neuron* **18,** 167-177.

SCHNEGGENBURGER, R., ZHOU, Z., KONNERTH, A. & NEHER, E. (1993). Fractional contribution of calcium to the cation current through glutamate receptor channels. *Neuron* **11,** 133-143.

SCHORGE, S. & COLQUHOUN, D. (2003). Studies of NMDA receptor function and stoichiometry with truncated and tandem subunits. *J Neurosci* **23,** 1151-1158.

SCOTT, D. B., BLANPIED, T. A., SWANSON, G. T., ZHANG, C. & EHLERS, M. D. (2001). An NMDA receptor ER retention signal regulated by phosphorylation and alternative splicing. *J Neurosci* **21,** 3063-3072.

SHARMA, G. & STEVENS, C. F. (1996a). Interactions between two divalent ion binding sites in N-methyl-D-aspartate receptor channels. *Proc Natl Acad Sci U S A* **93,** 14170-14175.

SHARMA, G. & STEVENS, C. F. (1996b). A mutation that alters magnesium block of N-methyl-D-aspartate receptor channels. *Proc Natl Acad Sci U S A* **93,** 9259-9263.

SHENG, M., CUMMINGS, J., ROLDAN, L. A., JAN, Y. N. & JAN, L. Y. (1994). Changing subunit composition of heteromeric NMDA receptors during development of rat cortex. *Nature* **368,** 144-147.

SIGWORTH, F. J. & SINE, S. M. (1987). Data transformations for improved display and fitting of single-channel dwell time histograms. *Biophys J* **52,** 1047-1054.

SOBOLEVSKY, A. I. (2003). Channel block of glutamate receptors. *Recent Res. Devel. Phyisol.* **1,** 1-38.

SOBOLEVSKY, A. I., BECK, C. & WOLLMUTH, L. P. (2002a). Molecular rearrangements of the extracellular vestibule in NMDAR channels during gating. *Neuron* **33,** 75-85.

SOBOLEVSKY, A. I., KOSHELEV, S. G. & KHODOROV, B. I. (1999). Probing of NMDA channels with fast blockers. *J Neurosci* **19,** 10611-10626.

SOBOLEVSKY, A. I., ROONEY, L. & WOLLMUTH, L. P. (2002b). Staggering of subunits in NMDAR channels. *Biophys J* **83,** 3304-3314.

SOBOLEVSKY, A. I. & YELSHANSKY, M. V. (2000). The trapping block of NMDA receptor channels in acutely isolated rat hippocampal neurones. *J Physiol* **526 Pt 3,** 493-506.

SOBOLEVSKY, A. I., YELSHANSKY, M. V. & WOLLMUTH, L. P. (2003). Different gating mechanisms in glutamate receptor and K+ channels. *J Neurosci* **23,** 7559-7568.

SPASSOVA, M. & LU, Z. (1998). Coupled ion movement underlies rectification in an inward-rectifier K+ channel. *J Gen Physiol* **112,** 211-221.

SPRENGEL, R., SUCHANEK, B., AMICO, C., BRUSA, R., BURNASHEV, N., ROZOV, A., HVALBY, O., JENSEN, V., PAULSEN, O., ANDERSEN, P., KIM, J. J., THOMPSON, R. F., SUN, W., WEBSTER, L. C., GRANT, S. G., EILERS, J., KONNERTH, A., LI, J., MCNAMARA, J. O. & SEEBURG, P. H. (1998). Importance of the intracellular domain of NR2 subunits for NMDA receptor function in vivo. *Cell* **92,** 279-289.

STANDLEY, S., ROCHE, K. W., MCCALLUM, J., SANS, N. & WENTHOLD, R. J. (2000). PDZ domain suppression of an ER retention signal in NMDA receptor NR1 splice variants. *Neuron* **28,** 887-898.

STEPHENSON, F. A. (2001). Subunit characterization of NMDA receptors. *Curr Drug Targets* **2,** 233-239.

STERN, P., BEHE, P., SCHOEPFER, R. & COLQUHOUN, D. (1992). Single-channel conductances of NMDA receptors expressed from cloned cDNAs: comparison with native receptors. *Proc R Soc Lond B Biol Sci* **250,** 271-277.

STERN, P., CIK, M., COLQUHOUN, D. & STEPHENSON, F. A. (1994). Single channel properties of cloned NMDA receptors in a human cell line: comparison with results from Xenopus oocytes. *J Physiol* **476,** 391-397.

STOUT, A. K., LI-SMERIN, Y., JOHNSON, J. W. & REYNOLDS, I. J. (1996). Mechanisms of glutamate-stimulated Mg2+ influx and subsequent Mg2+ efflux in rat forebrain neurones in culture. *J Physiol* **492 (Pt 3),** 641-657.

SUBRAMANIAM, S., DONEVAN, S. D. & ROGAWSKI, M. A. (1994). Hydrophobic interactions of n-alkyl diamines with the N-methyl-D-aspartate receptor: voltage-dependent and -independent blocking sites. *Mol Pharmacol* **45,** 117-124.

SUCHER, N. J., AKBARIAN, S., CHI, C. L., LECLERC, C. L., AWOBULUYI, M., DEITCHER, D. L., WU, M. K., YUAN, J. P., JONES, E. G. & LIPTON, S. A. (1995). Developmental and regional expression pattern of a novel NMDA receptor-like subunit (NMDAR-L) in the rodent brain. *J Neurosci* **15,** 6509-6520.

SUN, Y., OLSON, R., HORNING, M., ARMSTRONG, N., MAYER, M. & GOUAUX, E. (2002).

Mechanism of glutamate receptor desensitization. *Nature* **417,** 245-253.

TANG, Y. P., SHIMIZU, E., DUBE, G. R., RAMPON, C., KERCHNER, G. A., ZHUO, M., LIU, G. & TSIEN, J. Z. (1999). Genetic enhancement of learning and memory in mice. *Nature* **401,** 63-69.

TINGLEY, W. G., EHLERS, M. D., KAMEYAMA, K., DOHERTY, C., PTAK, J. B., RILEY, C. T. & HUGANIR, R. L. (1997). Characterization of protein kinase A and protein kinase C phosphorylation of the N-methyl-D-aspartate receptor NR1 subunit using phosphorylation site-specific antibodies. *J Biol Chem* **272,** 5157-5166.

TOVAR, K. R. & WESTBROOK, G. L. (1999). The incorporation of NMDA receptors with a distinct subunit composition at nascent hippocampal synapses in vitro. *J Neurosci* **19,** 4180-4188.

TSAI, G. & COYLE, J. T. (2002). Glutamatergic mechanisms in schizophrenia. *Annu Rev Pharmacol Toxicol* **42,** 165-179.

TSUZUKI, K., MOCHIZUKI, S., IINO, M., MORI, H., MISHINA, M. & OZAWA, S. (1994). Ion permeation properties of the cloned mouse epsilon 2/zeta 1 NMDA receptor channel. *Brain Res Mol Brain Res* **26,** 37-46.

VICINI, S., WANG, J. F., LI, J. H., ZHU, W. J., WANG, Y. H., LUO, J. H., WOLFE, B. B. & GRAYSON, D. R. (1998). Functional and pharmacological differences between recombinant N-methyl-D-aspartate receptors. *J Neurophysiol* **79,** 555-566.

VILLARROEL, A., BURNASHEV, N. & SAKMANN, B. (1995). Dimensions of the narrow portion of a recombinant NMDA receptor channel. *Biophys J* **68,** 866-875.

VILLARROEL, A., REGALADO, M. P. & LERMA, J. (1998). Glycine-independent NMDA receptor desensitization: localization of structural determinants. *Neuron* **20,** 329-339.

VYKLICKY, L., JR., BENVENISTE, M. & MAYER, M. L. (1990). Modulation of N-methyl-D-aspartic acid receptor desensitization by glycine in mouse cultured hippocampal neurones. *J Physiol* **428,** 313-331.

WAFFORD, K. A., BAIN, C. J., LE BOURDELLES, B., WHITING, P. J. & KEMP, J. A. (1993). Preferential co-assembly of recombinant NMDA receptors composed of three different subunits. *Neuroreport* **4,** 1347-1349.

WAGNER, D. A. & LEONARD, J. P. (1996). Effect of protein kinase-C activation on the Mg(2+)-sensitivity of cloned NMDA receptors. *Neuropharmacology* **35,** 29-36.

WANG, L. Y. & MACDONALD, J. F. (1995). Modulation by magnesium of the affinity of NMDA receptors for glycine in murine hippocampal neurones. *J Physiol* **486 (Pt 1),** 83-95.

WATANABE, J., BECK, C., KUNER, T., PREMKUMAR, L. S. & WOLLMUTH, L. P. (2002). DRPEER: a motif in the extracellular vestibule conferring high Ca2+ flux rates in NMDA receptor channels. *J Neurosci* **22,** 10209-10216.

WILLIAMS, K., PAHK, A. J., KASHIWAGI, K., MASUKO, T., NGUYEN, N. D. & IGARASHI, K. (1998). The selectivity filter of the N-methyl-D-aspartate receptor: a tryptophan residue controls block and permeation of Mg2+. *Mol Pharmacol* **53,** 933-941.

WOLLMUTH, L. P., KUNER, T. & SAKMANN, B. (1998a). Adjacent asparagines in the NR2-subunit of the NMDA receptor channel control the voltage-dependent block by extracellular Mg2+. *J Physiol* **506 (Pt 1),** 13-32.

WOLLMUTH, L. P., KUNER, T. & SAKMANN, B. (1998b). Intracellular Mg2+ interacts with structural determinants of the narrow constriction contributed by the NR1-subunit in the NMDA receptor channel. *J Physiol* **506 (Pt 1),** 33-52.

WOLLMUTH, L. P., KUNER, T., SEEBURG, P. H. & SAKMANN, B. (1996). Differential contribution of the NR1- and NR2A-subunits to the selectivity filter of recombinant NMDA receptor channels. *J Physiol* **491 (Pt 3),** 779-797.

WOLLMUTH, L. P. & SAKMANN, B. (1998). Different mechanisms of Ca2+ transport in NMDA and Ca2+-permeable AMPA glutamate receptor channels. *J Gen Physiol* **112,** 623-636.

WOOD, M. W., VANDONGEN, H. M. & VANDONGEN, A. M. (1995). Structural conservation of ion conduction pathways in K channels and glutamate receptors. *Proc Natl Acad Sci U S A* **92,** 4882-4886.

WOOD, M. W., VANDONGEN, H. M. & VANDONGEN, A. M. (1997). An alanine residue in the M3-M4 linker lines the glycine binding pocket of the N-methyl-D-aspartate receptor. *J Biol Chem* **272,** 3532-3537.

WOODHULL, A. M. (1973). Ionic blockage of sodium channels in nerve. *J Gen Physiol* **61,** 687-708.

WYLLIE, D. J., BEHE, P. & COLQUHOUN, D. (1998). Single-channel activations and concentration jumps: comparison of recombinant NR1a/NR2A and NR1a/NR2D NMDA receptors. *J Physiol* **510 (Pt 1),** 1-18.

WYLLIE, D. J., BEHE, P., NASSAR, M., SCHOEPFER, R. & COLQUHOUN, D. (1996). Single-channel currents from recombinant NMDA NR1a/NR2D receptors expressed in Xenopus oocytes. *Proc R Soc Lond B Biol Sci* **263,** 1079-1086.

WYSZYNSKI, M., LIN, J., RAO, A., NIGH, E., BEGGS, A. H., CRAIG, A. M. & SHENG, M. (1997). Competitive binding of alpha-actinin and calmodulin to the NMDA receptor. *Nature* **385,** 439-442.

YAMAZAKI, M., MORI, H., ARAKI, K., MORI, K. J. & MISHINA, M. (1992). Cloning, expression and modulation of a mouse NMDA receptor subunit. *FEBS Lett* **300,** 39-45.

YELLEN, G. (1998). The moving parts of voltage-gated ion channels. *Q Rev Biophys* **31,** 239-295.

ZAREI, M. M. & DANI, J. A. (1994). Ionic permeability characteristics of the N-methyl-D-aspartate receptor channel. *J Gen Physiol* **103,** 231-248.

ZAREI, M. M. & DANI, J. A. (1995). Structural basis for explaining open-channel blockade of the NMDA receptor. *J Neurosci* **15,** 1446-1454.

ZERON, M. M., HANSSON, O., CHEN, N., WELLINGTON, C. L., LEAVITT, B. R., BRUNDIN, P., HAYDEN, M. R. & RAYMOND, L. A. (2002). Increased sensitivity to N-methyl-D-aspartate receptor-mediated excitotoxicity in a mouse model of Huntington's disease. *Neuron* **33,** 849-860.

ZHANG, L., RZIGALINSKI, B. A., ELLIS, E. F. & SATIN, L. S. (1996). Reduction of voltage-dependent Mg2+ blockade of NMDA current in mechanically injured neurons. *Science* **274,** 1921-1923.

ZHANG, S., EHLERS, M. D., BERNHARDT, J. P., SU, C. T. & HUGANIR, R. L. (1998). Calmodulin mediates calcium-dependent inactivation of N-methyl-D-aspartate receptors. *Neuron* **21,** 443-453.

ZHENG, F., ERREGER, K., LOW, C. M., BANKE, T., LEE, C. J., CONN, P. J. & TRAYNELIS, S. F.

(2001). Allosteric interaction between the amino terminal domain and the ligand binding domain of NR2A. *Nat Neurosci* **4,** 894-901.

ZHONG, J., RUSSELL, S. L., PRITCHETT, D. B., MOLINOFF, P. B. & WILLIAMS, K. (1994). Expression of mRNAs encoding subunits of the N-methyl-D-aspartate receptor in cultured cortical neurons. *Mol Pharmacol* **45,** 846-853.

ZHOU, M., MORAIS-CABRAL, J. H., MANN, S. & MACKINNON, R. (2001). Potassium channel receptor site for the inactivation gate and quaternary amine inhibitors. *Nature* **411,** 657-661.

ZHU, Y. & AUERBACH, A. (2001a). K(+) occupancy of the N-methyl-d-aspartate receptor channel probed by Mg(2+) block. *J Gen Physiol* **117,** 287-298.

ZHU, Y. & AUERBACH, A. (2001b). Na(+) occupancy and Mg(2+) block of the n-methyl-d-aspartate receptor channel. *J Gen Physiol* **117,** 275-286.